



# The nature of compact radio sources: the case of FR 0 radio galaxies

Ranieri D. Baldi<sup>1</sup> 

Received: 14 February 2023 / Accepted: 14 July 2023 / Published online: 30 August 2023  
© The Author(s) 2023

## Abstract

Radio-loud compact radio sources (CRSs) are characterised by morphological *compactness* of the jet structure centred on the active nucleus of the galaxy. Most of the local elliptical galaxies are found to host a CRS with nuclear luminosities lower than those of typical quasars,  $\lesssim 10^{42}$  erg s<sup>-1</sup>. Recently, low-luminosity CRSs with a LINER-like optical spectrum have been named Fanaroff–Riley (FR) type 0 to highlight their lack of substantially extended radio emission at kpc scales, in contrast with the other Fanaroff–Riley classes, full-fledged FR Is and FR II radio galaxies. FR 0s are the most abundant class of radio galaxies in the local Universe, and characterised by a higher core dominance, poorer Mpc-scale environment and smaller (sub-kpc scale, if resolved) jets than FR Is. However, FR 0s share similar host and nuclear properties with FR Is. A different accretion–ejection paradigm from that in place in FR Is is invoked to account for the parsec-scale FR 0 jets. This review revises the state-of-the-art knowledge about FR 0s, their nature, and which open issues the next generation of radio telescopes can solve in this context.

**Keywords** Galaxies: active · Galaxies: jets · Radio continuum: galaxies

---

✉ Ranieri D. Baldi  
ranieri.baldi@inaf.it

<sup>1</sup> INAF-Istituto di Radioastronomia, Via Piero Gobetti 101, 40129 Bologna, Italy

## Contents

1	Introduction.....	2
2	Compact radio sources .....	7
3	Low-luminosity CRSs: the FR 0s .....	9
3.1	Selection of FR 0s .....	12
3.2	Host properties .....	15
4	Radio luminosity function .....	17
5	Radio properties.....	17
5.1	Low resolution .....	19
5.1.1	GHz-band: sub/arcsec-scale with VLA.....	19
5.1.2	High-frequency up to mm-band.....	20
5.1.3	Low frequency.....	21
5.2	High resolution.....	22
5.3	Radio SED .....	24
6	Optical and infrared properties.....	25
7	High-energy properties .....	27
7.1	X-ray.....	27
7.2	Gamma-ray.....	28
8	Accretion and ejection.....	30
9	Environment.....	36
10	Feedback .....	37
11	Comparison with FR II LERGs .....	40
12	Models for FR 0s.....	41
12.1	Static scenarios.....	41
12.2	Dynamic scenarios .....	44
13	Conclusions and future perspective.....	49
	References .....	51

## 1 Introduction

A minority of the Active Galactic Nuclei (AGN), named radio-loud AGN (RLAGN)<sup>1</sup> ( $\sim 10\text{--}20\%$ , e.g. Urry and Padovani 1995; Kratzer and Richards 2015; Macfarlane et al. 2021), is known to launch relativistic collimated jets from parsec (pc) to Mpc scales, which connect the active supermassive black hole (BH) with the interstellar medium (ISM) to the furthest intra-cluster medium (ICM) (e.g. Blandford et al. 2019; Hardcastle and Croston 2020; Saikia 2022). A significant excess of radio emission over that expected from star formation (SF) processes is attributed to non-thermal jet emission in RLAGN (e.g. Condon 1992; Bonzini et al. 2013; Padovani et al. 2015). However, a fraction of radio-quiet (RQ) AGN can also produce non-thermal emission from jets, which are, though, uncollimated and sub-relativistic (e.g. Padovani 2016; Panessa et al. 2019). Jets, whether relativistic or not, are found to play a key role in galaxy evolution and in the maintenance of massive galaxies in the present-day Universe (e.g. Croton et al. 2006; Kharb and Silpa 2023), by releasing a large amount of energy to their surrounding environment (the so-called radio-mode feedback)

<sup>1</sup> Radio loudness,  $R$ , is defined as ratio between the flux densities in the radio (6 cm, 5 GHz) and in the optical band ( $\sim 4400 \text{ \AA}$ ) (Kellermann et al. 1989): RLAGN have  $R \geq 10$ , whereas radio-quiet AGN have  $R < 10$ . See also Terashima and Wilson (2003) for a radio loudness definition based on radio and X-ray (2–10 keV) luminosity ratio.

(Fabian 2012). In fact, RLAGN are typically associated with the most evolved systems, i.e. massive early-type galaxies (ETGs, and mostly ellipticals) and the most massive BHs (e.g. Heckman and Best 2014), although a small number of exceptions have been found (e.g. Hota et al. 2011; Singh et al. 2015a; Kaviraj et al. 2015; Kotilainen et al. 2016; Mao et al. 2018; Webster et al. 2021b; Davis et al. 2022).

One of the most historically important classifications of RLAGN was introduced by Fanaroff and Riley (1974), based on the extended radio structure: edge-darkened sources were classified as Fanaroff–Riley type I (FR Is), while edge-brightened as type II (FR IIs): the latter generally more radio luminous ( $> 2 \times 10^{25} \text{ W Hz}^{-1}$  at 178 MHz) than the former. Extended plumes, lobes, and tails account for typically 90% of their total radio emission (Miley 1980). Other than the radio linear size and morphology, the jet orientation with respect to the line of sight is another important variable to characterise RLAGN: extended sources inclined at small angles may appear compact due to projection effects and their radio emission can be boosted due to relativistic beaming of the nuclear jets moving at relativistic velocities. A further crucial aspect of RLAGN is the radio spectrum (flux density  $S_\nu$ , varies with frequency  $\nu$  as  $\nu^{-\alpha}$  and  $\alpha$  is the spectral index): steep-spectrum sources ( $\alpha > 0.5$ ) are typically associated with optically-thin emission from extended jets, while flat/inverted-spectrum sources ( $\alpha < 0.5$ ) are largely due to (synchrotron-self or free-free) absorption process involved in compact cores and jet knots. While misaligned (type-2) RLAGN (with respect to the line of sight, e.g. FR I/II), commonly named as radio galaxies (RGs), are typically dominated by their extended emission with steep spectra, aligned (type-1) RLAGN, named blazars,<sup>2</sup> show flat, inverted or complex radio spectra of the dominant cores.

Traditionally, compact radio sources (CRSs) associated with misaligned RLAGN are believed to represent the early stages of evolution of full-fledged RLAGN (FR I/ IIs, O’Dea 1998) and are characterised by a peaked radio spectrum (see Sect. 2). Recently, Baldi et al. (2015) introduced a new class of *low-power CRSs* ( $\lesssim 10^{24} \text{ W Hz}^{-1}$ ), named *FR 0* RGs, whose compact radio emission is dominated by the core and pc-scale jets and not related to a juvenile radio activity. The characteristic property of such an abundant class of RGs is the substantial lack of kpc-scale jet emission, that has changed the classical view on the kpc/Mpc-scale RLAGN phenomenology, particularly at low luminosities, where jets are scarcely studied. An increasingly incomplete list of RLAGN classes is given in Table 1.

The complex radio taxonomy of RLAGN needs to find a correspondence with the optical classification schemes to modes of accretion onto the BHs (e.g. Jackson and Rawlings 1997; Heckman and Best 2014; Hardcastle and Worrall 2000). Based on their optical spectra, RGs have been classified into Low Excitation Radio Galaxies (LERGs) and High Excitation Radio Galaxies (HERGs) (Table 1), which basically reflect two BH-accretion states (Buttiglione et al. 2010; Tadhunter 2016a) with distinct distributions of Eddington ratios.<sup>3</sup> LERGs are typically accreting below 1%

<sup>2</sup> The blazar population consists in two sub-classes, the flat-spectrum radio quasars and BL Lacs, generally at high and low luminosities, respectively.

<sup>3</sup> The Eddington ratio  $\dot{L}_E$  gauges the BH-accretion properties and is defined by the ratio between the bolometric AGN luminosity and the Eddington luminosity given its BH mass.

**Table 1** Radio-optical AGN taxonomy

Acronyms	Main properties	Reference
Quasar	Quasi-stellar radio source	1
RLAGN	Radio-loud AGN (relativistic collimated jets)	2
RQAGN	Radio-quiet AGN (thermal/non-thermal emission, uncollimated sub-relativistic jet)	2, 3
CRS	RL or RQ radio compact source	4
FR I	Fanaroff–Riley class I radio source; radio core-brightened	5
FR II	Fanaroff–Riley class II radio source; radio edge-brightened	5
FR 0	Fanaroff–Riley class 0 radio source; RL CRS lacking kpc-scale extended emission	6
RG	Radio galaxy, misaligned RL AGN	7
Blazar	Aligned RL AGN	7
REAF	Radiatively efficient accretion disc	8
RIAF	Radiatively inefficient accretion disc	9
LERG	Low-excitation radio galaxies	10
HERG	High-excitation radio galaxies	10
LLAGN	Low-luminosity AGN	11
CSS	Compact steep spectrum radio source; young RG	12
GPS	Gigahertz-peaked radio source; young RG	12
HPF	High frequency peakers; young RG	12
CSO	Compact symmetric object; young RG	12
MSO	Medium-sized symmetric object; young RG	12
Seyfert	High-ionisation nuclear emission-line regions, RQ AGN	13
LINER	Low-ionisation nuclear emission-line regions, RQ or RL AGN	13, 14
CoreG	Core galaxies, nearby low-luminosity FR 0-like RGs	15

The complex radio-optical AGN taxonomy includes several acronyms. Here a partial but helpful list of labels for AGN, their properties and references (first/key papers or recent papers, which give up-to-date details). References: 1. Schmidt (1963), 2. Padovani (2016), 3. Panessa et al. (2019), 4. Kellermann and Pauliny-Toth (1981), 5. Fanaroff and Riley (1974), 6. Baldi et al. (2015), 7. Urry and Padovani (1995), 8. Shakura and Sunyaev (1973) 9. Yuan and Narayan (2014), 10. Heckman and Best (2014), 11. Ho (2008), 12. O'Dea and Saikia (2021), 13. Kewley et al. (2006), 14. Heckman (1980), 15. Balmaverde and Capetti (2006)

of their Eddington accretion rate limit, while HERGs have typical accretion rates between 1 and 10% (or even higher) (Heckman and Best 2014). HERGs, accretion-dominated RLAGN, are characterised by radiatively efficient accretion flows (REAF), i.e. standard optically thick, geometrically thin discs (Shakura and Sunyaev 1973). LERGs, jet-dominated RLAGN, are powered by radiatively inefficient accretion flows (RIAF), which include the disc solutions of geometrically thick advection-dominated accretion flows (ADAF) (e.g. Narayan and Yi 1994, 1995; Narayan et al. 2000; Yuan and Narayan 2014). LERGs prefer redder, gas-poorer, more massive ETGs with lower star-formation rates, which inhabit richer and more dynamically relaxed environment and feed more massive BHs than HERGs (Baldi

and Capetti 2008; Heckman and Best 2014). LERGs are generally thought to be fuelled by the cooling of hot gas from haloes present in their massive host galaxies, whereas the HERGs generally tend to accrete cold gas efficiently, from processes external or internal to the galaxy (Hardcastle et al. 2007). Several radio-optical studies of RGs concluded that the two FR radio morphologies are not representative of two distinct accretion states, but can co-exist in the same optical class (e.g. Gendre et al. 2013; Mingo et al. 2019, 2022). In fact, local LERGs are associated with a FR I or FR II morphology, whereas HERGs, which are on average of higher luminosity, are generally FR IIs. The new low-power FR 0 class has thus further entangled, although already complex, the radio-optical classification scheme (Table 1).

Other than radio and optical bands, decades of observations of accreting BHs at different wavelengths have shed new light on specific aspects of the accretion-jet phenomena (e.g. X-ray, broad/narrow optical lines, IR excess), collecting evidence for an anisotropic AGN emission. The attempt to unify all the AGN classes in one single picture concluded with the Unification Model (UM, e.g. Barthel 1989; Antonucci 1993; Urry and Padovani 1995), which states that, despite their differences, RLAGN have the same basic structure (attested for powerful sources): optically thick circumnuclear matter (torus) obscuring the accretion disc in an edge-on view, perpendicular to a relativistic jet, Doppler boosted when seen at small angles to the line of sight. This orientation-based scheme represents the most courageous way to characterise the fact that the nuclear continuum and emission-line radiation from all types of AGN are simply a function of wavelength, inclination to the line of sight and source luminosity. However, the advent of modern sensitive and survey-mode telescopes has unveiled new regions in the space parameters of RLAGN phenomenology (see, e.g. in time domain astronomy, radio/optical/X-ray spectroscopy and polarimetry, jet/wind structure, disc and dust properties, Padovani 2016; Padovani et al. 2017; Spinoglio and Fernández-Ontiveros 2021), which have defined specific accretion–ejection states of AGN and relative transitions, which the simplistic UM cannot explain. Although the UM is still generally valid, the most logical way to relieve the tension is the inclusion of the time variable in the UM, i.e. the parameters can evolve across time. An evolutionary scheme of RLAGN offers a more adaptable method to fine-tune the AGN parameters observed in distinct and transitioning states of accretion and ejections (Antonucci 2012; Netzer 2015; Tadhunter 2016a).

The dynamic evolution of the accretion–ejection coupling in RLAGN is traditionally explained as a progression of the radio power with the linear size of the radio structure (see An and Baan 2012 and references therein). Figure 1 shows the radio power  $P$  versus the total extent of the source,  $D$  (the so-called “ $P$ – $D$ ” diagram, Baldwin 1982): different populations of radio-emitting AGN (quiet and loud) span over a very wide range in radio luminosities (nearly ten orders of magnitude) and source sizes (six orders of magnitude) (Hardcastle et al. 2019; Hardcastle and Croston 2020). For RLAGN, in Fig. 1, two representative evolutionary tracks within the  $P$ – $D$  diagram are shown and predict RL CRSs to evolve into traditional  $\sim 100$ -kpc double RGs (FR Is or FR IIs, e.g. Kunert-Bajraszewska et al. 2010; An and Baan 2012; Kunert-Bajraszewska 2016). However, there is an important caveat. All the evolutionary models and our current knowledge

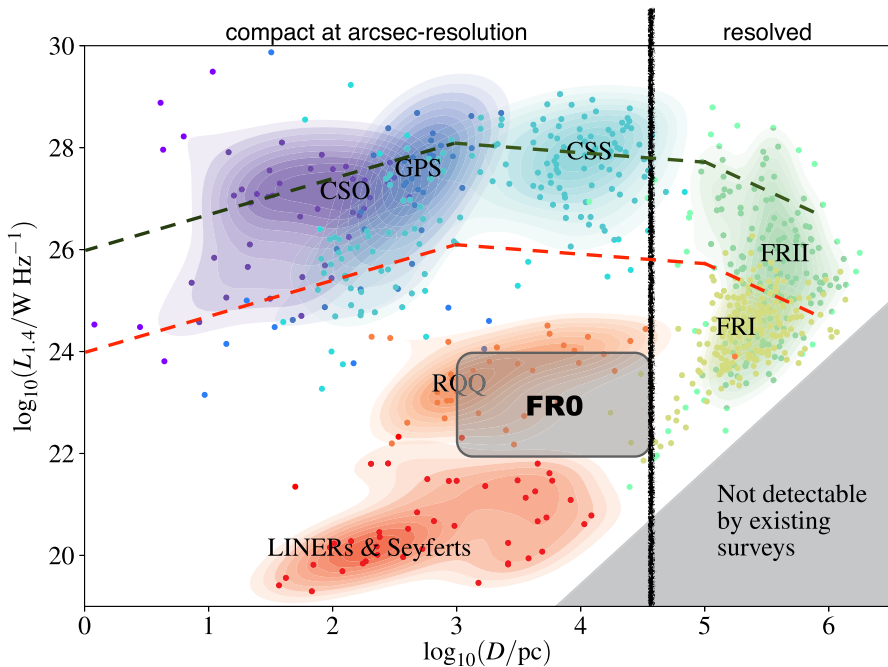


**Fig. 1** Radio power/linear-size plot ( $P$ – $D$  diagram) for different types of RL and RQ AGN, adapted from plots presented by An and Baan (2012), Jarvis et al. (2019) and Hardcastle and Croston (2020). Points show individual objects and coloured contours represent a smoothed estimator of source density. The different categories of source shown are: CSO, GPS, CSS, FR I, FR II, RQ quasars, Seyferts and LINERS, and FR 0s (see Sects. 1 and 2 for the definition of the classes). Red and dark-green dashed lines represent the classical evolutionary tracks of FR Is and FR IIs (e.g. An and Baan 2012). The shaded bottom-right corner shows the effect of surface-brightness limitations by existing radio surveys: very recently, deep LOFAR and MeerKAT surveys are starting to explore this region of the  $P$ – $D$  diagram (Whittam et al. 2022; Best et al. 2023). The vertical line roughly represents the separation between resolved and unresolved/compact sources based on arcsec angular resolution, generally provided by the VLA array. The black box depicts the VLA detected FR 0s and represents an upper limit on their actual radio physical size. This figure is a modified version of Fig. 2 from Hardcastle and Croston (2020)

on RG populations have long been based on samples of powerful sources, mostly above  $10^{24} \text{ W Hz}^{-1}$ , selected from high-flux low-frequency radio surveys such as the Third Cambridge (3C) catalogue (Bennett 1962). In opposition to the past, recent large-area sensitive surveys have revealed that the local RG population is dominated by sources with radio power below  $10^{24} \text{ W Hz}^{-1}$  (Best and Heckman 2012), which includes mostly compact FR 0-type RGs. The UM model is not able to successfully reproduce such an abundant population of ‘low-luminosity’ RLAGN.

A milestone in the comprehension of the RLAGN phenomenon is the work by Best et al. (2005b), which selected the largest complete sample of low-luminosity RGs ( $\lesssim 10^{41} \text{ erg s}^{-1}$ ) by cross-matching Sloan Digital Sky Survey (SDSS, York et al. 2000), National Radio Astronomy Observatory (NRAO) Very Large Array (VLA) Sky Survey (NVSS, Condon et al. 1998), and the Faint Images of the Radio Sky at Twenty centimetres survey (FIRST, Becker et al. 1995) with flux densities  $> 5 \text{ mJy}$

a 1.4 GHz. This flux-density cut is much below than the selection of, e.g. the 3C catalogue (178 MHz flux density  $> 9$  Jy, Bennett 1962), on which most of our comprehension of the radio-AGN phenomenon is based. The most interesting result from the radio-optical survey is that their radio morphology appears unresolved at the scale of the FIRST radio maps, i.e.  $5''$ , which corresponds to 10–20 kpc with  $z < 0.3$ . These compact RGs, named later *FR 0s*, which belong to a heterogeneous population of LERG-type red massive ellipticals, represent the bulk of the RG population of the local Universe with a space density  $> 100$  times higher than 3C/RGs. The study of the FR 0 population has a relevant role in the modern astrophysics because: (i) since they are the most common RLAGN in the local Universe, their comprehension provides an important insight on the accretion–ejection mechanism for ordinary RGs; (ii) since their radio emission is on galactic scale, their jets can have a tremendous impact on the galaxy evolution in the context of radio-mode feedback.

In this review, we provide an overview of the observational properties and theoretical understanding of this interesting class of compact RGs, FR 0s. We introduce the class of CRSs in Sect. 2 to then focus on the FR 0s (Sect. 3), by discussing their selection (radio and host properties). Then we derive the radio luminosity function of local RGs to demonstrate the abundance of FR 0s with respect to the FR I/IIs (Sect. 4). Then, we review their multi-band properties from radio (Sect. 5), optical and IR (Sect. 6) to high energy bands (Sect. 7) to picture their typical spectral energy distribution (SED). A discussion of the accretion–ejection coupling (Sect. 8), environmental properties (Sect. 9) and their role of compact sources in AGN feedback (Sect. 10) lead to drawing static and dynamic scenarios to account for the multi-band properties of FR 0s in relation to the other FR classes (Sects. 11 and 12). A final chapter on future perspective is also included (Sect. 13).

We adopt in this work  $H_0 = 70 \text{ km s}^{-1} \text{ Mpc}^{-1}$ ,  $\Omega_{m_0} = 0.3$ ,  $\Omega_{A_0} = 0.7$ .

## 2 Compact radio sources

In this review, we consider CRSs, those AGN which appear unresolved at small angular sizes ( $\lesssim$  a few arcseconds). CRSs can be RQ or RL, and here we will focus on the latter. In RL CRSs, the compact component is generally ascribed to the radio core, which is interpreted as non-thermal self-absorbed synchrotron emission from the base of a relativistic jet, that extracts energy from the spinning BH and/or the accretion disc (Blandford and Znajek 1977; Blandford and Payne 1982). The connection between the compact core emission and the pc–kpc–Mpc-scale extended jet emission, has been discussed in previous reviews (e.g. Condon and Dressel 1978; O’Dell 1978; Kellermann 1980; Kellermann and Pauliny-Toth 1981; O’Dea 1998; Falcke et al. 2004; Lobanov 2006; Tadhunter 2016b; O’Dea and Saikia 2021), which all gather increasing evidence of a large population of CRSs in the local Universe.

*What does ‘compact’ mean and what defines the compactness?* The angular size of a compact source can vary from milli-arcsecond (mas) to a few arcseconds depending on the frequency, resolution and depth of observations. There is no a specific limit on the physical scale for a compact source. The morphological compactness can be defined as the ‘unresolved’ structure of a radio source, when the

deconvolved size is smaller or equal to the radio-map beam width and when its visibility function is flat across the entire spatial-frequency plane. Starting with the Rayleigh–Jeans limit for brightness temperature  $T_b$  [K] (Condon and Ransom 2016), the angular dimension  $\theta$  of a compact source with its peak intensity  $S_\nu$  [mJy beam $^{-1}$ ] at the frequency  $\nu$  [GHz] is

$$\theta \sim 35 S_\nu^{1/2} T_b^{-1/2} \nu^{-1} \text{ arcsec.} \quad (1)$$

For brightness temperatures above the threshold to discriminate between an AGN and stellar origin (Falcke et al. 2000),  $T_b \gg 10^7$  K, for a spectral peak frequency between hundreds of MHz to GHz, the angular size varies between a few mas to a few arcseconds. This corresponds to a linear dimension range of several hundreds of pc to kpc in the nearby Universe ( $z < 0.3$ ). However, in the literature, a CRS is trivially classified as a morphologically point-like source based on the corresponding angular resolution.

In theory, a conventional definition of a compact source predicts the presence of a characteristic self-absorption in the radio spectrum at low frequencies (below GHz regime). A varying opacity throughout the source entails a spectral characterisation: a flat, inverted or undulating spectrum over a wide range of frequencies due to the superposition of several radio-emitting partially opaque sources. Both the generally flat-spectrum and the compactness of the source can lead to the interpretation of an unresolved radio-emitting nucleus.

A (flat-spectrum) compact radio core can be observed across all types of galaxies and AGN. Even normal spiral, star-forming galaxies, RQAGN and late-type galaxies (LTG) in general can reveal a compact nucleus, whose radio origin is thermal and non-thermal emission from several physical processes (Condon 1992; Panessa et al. 2019). Since the most radio-loud AGN are preferentially hosted by bulge-dominated evolved galaxies with masses larger than  $10^{11} M_\odot$  and much less signs of morphological disturbance (spirals, bars) and SF than RQAGN (e.g. Best et al. 2005a; Ho 2008; Best and Heckman 2012; Kozieł-Wierzbowska et al. 2017a, b; Magliocchetti 2022), a prior selection of the optical hosts, ETGs rather than LTGs, can help to exclude RQAGN from genuine RL CRS samples at the cost of completeness in the RLAGN population.

The presence of an arcsec-scale compact radio emission at the centre of ETGs has been affirmed since 1970s as the main results of shallow VLA radio surveys up to now (e.g. Rogstad and Ekers 1969; Heeschen 1970; Ekers and Ekers 1973; Kellermann and Pauliny-Toth 1981; Sadler 1984; Fanti et al. 1986, 1987; Wrobel and Heeschen 1991; Slee et al. 1994; Giroletti et al. 2005; Capetti et al. 2009; Nyland et al. 2016; Hardcastle et al. 2019; Roy et al. 2021; Grossová et al. 2022; Wójtowicz et al. 2023; Capetti and Brienza 2023). More massive galaxies and earlier in type appear to be more probably connected to the presence of a RLAGN (e.g. Smith et al. 1986; Best et al. 2005a; Floyd et al. 2010; Kim et al. 2017; Zheng et al. 2020), able to launch from the weakest to the most powerful jets in the Universe (large range of luminosities, morphologies, duty cycles and speeds, e.g. Heckman and Best 2014; Morganti 2017; Morganti et al. 2021a; Saikia 2022).

Hosted in ETGs, RL CRSs have been classified based on radio spectral and morphological properties. Other than blazars which have a large intrinsic radio size but appear compact because of projection effects and are affected by relativistic beaming (one-sidedness, superluminal motions, and high brightness temperatures), misaligned RL CRSs (Readhead et al. 1994; O’Dea 1998; Orienti 2016; O’Dea and Saikia 2021) have been studied mainly at high powers ( $L_{1.4\text{GHz}} > 10^{25} \text{ W Hz}^{-1}$ ) and are characterised by a convex synchrotron radio spectrum: the peak position around 100 MHz in the case of compact-steep-spectrum (CSS) sources (well determined only by LOFAR and MWA observations in the recent years, e.g. Mahony et al. 2016; Callingham et al. 2017; Slob et al. 2022), and at about 1 GHz in the case of GHz-peaked spectrum (GPS) sources, or even up to a few GHz in the sub-population of high frequency peakers (HFP) (Fanti et al. 1985; Spencer et al. 1989; Stanghellini et al. 1998; Snellen et al. 1998; Dallacasa et al. 2000; Kunert et al. 2002; Orienti et al. 2007; Hancock et al. 2010) (Fig. 1). Morphologically, lobes and/or hot spots are typically resolved with very-long baseline interferometry (VLBI) observations and a weak component hosting the core is occasionally present (e.g. Wilkinson et al. 1991; Gugliucci et al. 2005; An et al. 2010, 2012; Wu et al. 2013). Depending on their size, CSS/GPS may be termed as compact symmetric objects (CSO) if they are smaller than 1 kpc, or medium-sized symmetric objects (MSO) if they extend up to 10–15 kpc (Conway 2002; Fanti et al. 2001). The existence of a relation between the rest-frame peak frequency and the projected linear size (e.g. O’Dea and Baum 1997) indicates that the mechanism responsible for the curvature of the spectrum is the youth: these sources are small because they are still in an early stage of their evolution, and will develop into FR I/II sources (e.g. Phillips and Mutel 1982; Fanti et al. 1990; Snellen et al. 2000; An and Baan 2012). The alternative scenarios point to a dense medium which might limit and frustrate the jet growth (van Breugel et al. 1984; Carvalho 1994, 1998; Ghisellini et al. 2004; Giroletti et al. 2005), or to a short or recurrent activity due to occasional BH accretion (Readhead et al. 1994; Gugliucci et al. 2005; Kunert-Bajraszewska et al. 2010, 2011; An and Baan 2012; Kiehlmann et al. 2023).

In conclusion, the CRS category can embrace a large population of radio-emitting sources: RQAGN, star-forming galaxies, blazars, young RGs and the FR 0s. In the next section, we will focus on the properties of this ‘new’ class of compact RGs, FR 0s, in relation to the large-scale RLAGN population.

### 3 Low-luminosity CRSs: the FR 0s

A significant fraction of nearby galaxies shows evidence of weak nuclear activity unrelated to normal stellar processes. Recent high-resolution, multi-wavelength observations indicate that this activity derives from BH accretion with a wide range of accretion rates and is associated with a CRS (e.g. Nagar et al. 2005; Ho 2008; Zuther et al. 2012; Saikia et al. 2018; Williams et al. 2022, 2023). In fact, moving to lower luminosities generally corresponds to selecting AGN with smaller and weaker jet (compact) structures and flatter radio spectra (e.g. Nagar et al. 2005; Sadler et al. 2014; Baldi and Capetti 2010; Gürkan et al. 2018; Sabater et al. 2019; Hardcastle

et al. 2019; Dabhade and Gopal-Krishna 2023), but with an increasing contribution from spurious RQAGN (Mezcua and Prieto 2014; Bonzini et al. 2013; Baldi et al. 2021b). Current radio surveys of the local Universe have unearthed a large population of low-luminosity AGN (LLAGN, with bolometric luminosities  $\lesssim 10^{40} \text{ erg s}^{-1}$ ), which were poorly explored in the past. Best and Heckman (2012), up-dating the sample of Best et al. (2005b), select 18 286 RGs (the SDSS/NVSS sample, hereafter), with low powers ( $L_{1.4 \text{ GHz}} < 10^{24} \text{ W Hz}^{-1}$ ) at low redshifts ( $z < 0.3$ ), whose the majority ( $\sim 80\%$ ) are LLAGN and radio compact ( $5''$ ), with linear sizes  $\lesssim 10\text{--}20 \text{ kpc}$ .

The role of LLAGN and their compact-jet emission in galaxy-BH co-evolution (Ho 2008; Kormendy and Ho 2013) is crucial for several aspects:

(i) since LLAGN outnumber the quasar population by a few orders of magnitudes at  $z < 0.3$  (Nagar et al. 2005; Best et al. 2005a; Saikia et al. 2018), they provide the snapshot of the ordinary relation between an accreting BH and its host. The absence of an outshining AGN at the galaxy centre allows us to better study the co-evolutionary link between host and BH;

(ii) since LLAGN reside in less massive galaxies, the identification of LLAGN would help to constrain the occupation fraction of active BH in galaxies at low stellar masses  $> 10^{9-10} M_{\odot}$  (Greene 2012; Gallo and Sesana 2019), and the BH mass density function at  $M_{\text{BH}} < 10^8 M_{\odot}$ . These quantities are fundamental to calibrate the prescriptions for BH-galaxy growth of semi-analytical and numerical models (e.g. Shankar 2009; Barausse et al. 2017);

(iii) due to the lack of sensitive surveys in the past, the role of LLAGN in galaxy evolution has been always downgraded with respect to powerful quasars, which by definition can offer a larger energetic budget to the host. Yet, recently the advent of deep radio surveys is reversing our view on AGN activity: LLAGN are always switched on at some level at low radio powers ( $L_{150 \text{ MHz}} \gtrsim 10^{21} \text{ W Hz}^{-1}$ , Sabater et al. 2019) and have galactic-scale jets, that can have a tremendous impact on their hosts by continuously injecting energy into the host, a crucial aspect for the jet-mode (or radio-mode) feedback (Fabian 2012).

While in the optical band the role of LLAGN in BH-galaxy co-evolution and their BH-accretion properties have been largely studied (Ho 2008; Fanidakis et al. 2011), their connection with the radio band has recently started to be explored. The past and current optical-radio studies of radio-emitting LLAGN collect observational evidence that three states of accretion–ejection exist: RQ Seyferts, RQ LINERs and RL LINERs (Low-Ionisation Nuclear Emission line Regions, Hine and Longair 1979; Heckman 1980; Kewley et al. 2006), different from the accretion–ejection states at higher luminosities, LERGs and HERGs and RQ quasars.<sup>4</sup> LINERs have lower accretion rates ( $\dot{m}$ ), are usually more radio-loud and reside in earlier type galaxies than Seyferts (Ho 2008). In fact, LINERs tend to host compact cores (Cohen et al. 1969; Falcke et al. 2000; Filho et al. 2002b; Maoz 2007), more radio luminous as the

<sup>4</sup> At low luminosities, the presence of intermediate RL Seyferts is still unclear and a luminosity gap between Seyferts and HERGs seems to exist (e.g. Baldi and Capetti 2010; Pierce et al. 2019, 2020). At high luminosities, the studies on LERG-type REAF-type quasars are still contradictory (see e.g. Younes et al. 2012).

BH mass (or galaxy mass) increases (e.g. Laor 2000; Best et al. 2005b; Mauch and Sadler 2007). RQ LINERs and Seyferts exhibit sub-relativistic and not collimated jets (e.g. Ulvestad et al. 1999; Wrobel 2000; Ulvestad and Ho 2001a; Gallimore et al. 2006; Singh et al. 2015b; Baldi et al. 2021b). Conversely, RL LINERs have been generally interpreted as the scaled-down version of powerful RLAGN in terms of accretion and jet luminosities (Chiaberge et al. 2005; Balmaverde and Capetti 2006). The nuclei of RL LINERs can be described with a model of synchrotron self-absorbed base of a low-power (mildly) relativistic jet coupled with an underluminous RIAF disc (typically an ADAF, Narayan and Yi 1994), analogous to FR I/LERG disc-jet coupling (e.g. Balmaverde and Capetti 2006; Hardcastle et al. 2009). The low-power CRS population selected from the SDSS/NVSS sample (Best and Heckman 2012) in the same luminosity range ( $\lesssim 10^{41} \text{ erg s}^{-1}$ ) of classical 3C/FR Is includes a heterogeneous population of mostly LINER/LERGs<sup>5</sup> with a broad distribution of BH mass and host properties.

Baldi et al. (2010) analysed in detail the photometric and spectroscopic properties of the SDSS/NVSS sample to select the bona-fide RLAGN population (see Sect. 3.1). They found that the majority of the SDSS/NVSS sample ( $\sim 80\%$ ) consists of compact LERGs, that are characterised by a total jet power up to a factor  $\sim 1000$  lower than what expected by RGs with bolometric AGN luminosity similar to those of the 3C/FR Is ( $\sim 10^{40} \text{ erg s}^{-1}$ ). This remarkable result that the local Universe is dominated by low-luminosity CRSs lacking of substantial extended emission, expresses the need to include these sources in the taxonomy of RGs. Ghisellini (2011) for the first time introduced in the literature the name *FR 0* to characterise a population of weak RL CRSs hosted in ellipticals, named Core Galaxies<sup>6</sup> (CoreG), which exhibit radio core and AGN bolometric luminosities similar to the weakest 3C/FR Is (M87), but with an extended radio emission hundreds of times weaker (Baldi and Capetti 2009). CoreG host genuine ‘miniature’ RGs with LINER-like nuclei, which extend the nuclear luminosity correlations reported for 3C/FR Is by a factor of  $\sim 1000$  towards lower luminosities (Balmaverde and Capetti 2006; Kharb et al. 2012): this has been interpreted as a sign of a common central engine (RIAF disc) (Balmaverde and Capetti 2006; Kharb et al. 2012). CoreG are characterised by kpc-scale jets and a deficit of total radio emission in analogy to the SDSS/NVSS sample, but at lower radio luminosities.

In analogy to CoreG, the FR 0 classification (see Sect. 3.1) does not correspond to a pure radio morphological selection of CRSs, but also includes an optical identification (host and AGN properties) to separate the genuine FR 0s which are all RLAGN, from spurious RQAGN and star-forming galaxies (bluer LTGs with emission-line ratios consistent with Seyfert or SF and steeper radio spectra, Baldi et al. 2016).

A closer look at the FR 0s at sub-arcsec/mas scale revealed that the majority still appears radio compact, with a flat spectrum in the GHz band (Baldi et al. 2015, 2019a; Cheng and An 2018; Cheng et al. 2021). However, a small fraction of

<sup>5</sup> LERG and RL LINER are equivalent classes at low luminosities.

<sup>6</sup> The Core Galaxy nomenclature comes from the (core-type) optical flat surface-brightness profile in innermost region of an ETG (e.g. Faber et al. 1997).

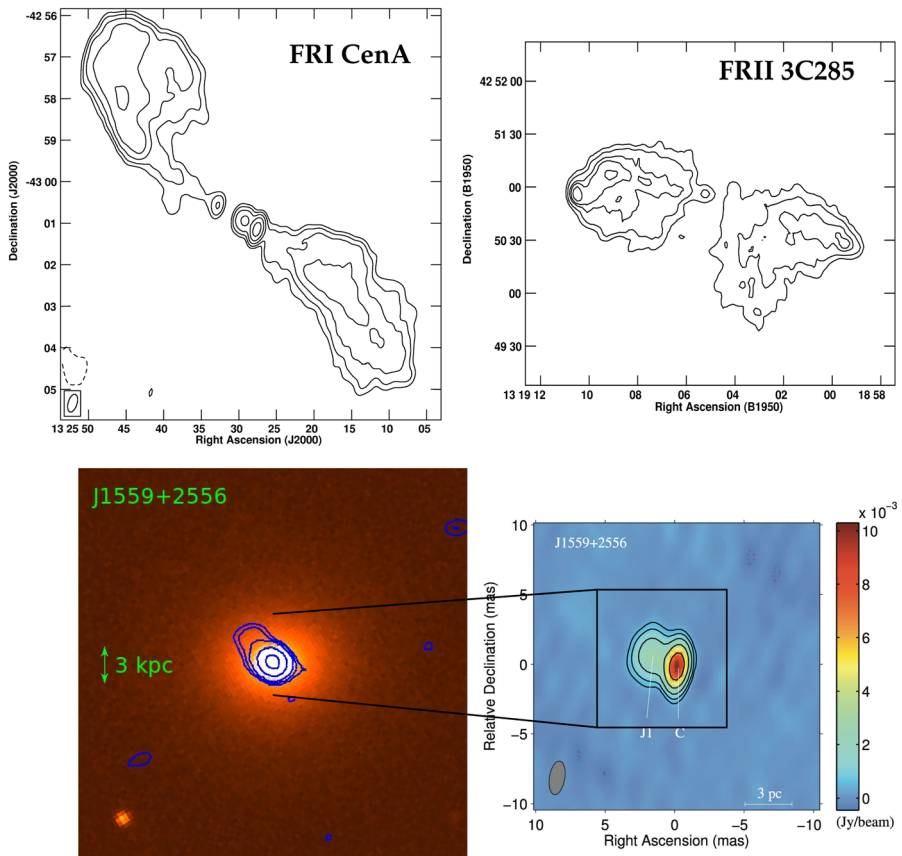


**Fig. 2** Multi-band composite panel of RGs. On the top, two examples of typical radio morphologies of a FR I (Cen A, Burns et al. 1983 at 1.4 GHz) and a FR II (3C 285, Alexander and Leahy 1987 at 1.4 GHz). On the bottom, we show an example of FR 0. The left panel displays the r-band SDSS image of the ETG which hosts the FR 0 with the blue VLA 4.5 GHz radio contours (Baldi et al. 2019a) (3 kpc-scale set by the green arrow). The right panel represents the high-resolution zoom on the radio core (on the scale of 3 pc) provided by the VLBI image from Cheng and An (2018). Image reproduced with permission from Baldi et al. (2019c), copyright by the authors

those exhibits kpc/pc-scale core-brightened jets, suggesting that FR 0s can actually produce collimated structures. The lack of substantially extended radio emission at kpc scale and the spectral flatness for the majority of these CRSs have led to the affirmation of the FR 0 nomenclature as a unique class of genuine compact RGs different from the other RLAGN classes.

In conclusion, in the last decade, different parallel studies have brought to light a revolutionary result, i.e. classical 3C FR I/ IIs do not represent the ordinary picture of the RLAGN phenomenon in the local Universe, but FR 0-like LLAGN represent the bulk of the local RG population (Fig. 2). The paucity of sources with weak extended radio structures in high-flux limited samples (such as in the 3C sample) is due to a selection bias, since the inclusion of such objects is highly disfavored. In fact, in

support to this interpretation, Baldi and Capetti (2009) showed that the lower flux threshold of B2 sample ( $<250$  mJy at 408 MHz, Fanti et al. 1978) drastically reduces the selection bias and allows the inclusion of a larger fraction of core-dominated.<sup>7</sup> galaxies, consistent with being FR 0s.

### 3.1 Selection of FR 0s

Disentangling bona-fide FR 0s from the radio compact impostors (blazars, young RGs, RQAGN, compact star-forming galaxies) represents a multi-band selection process. This can be harder at low luminosities (mJy-level at  $z < 0.3$ ). For example, Best et al. (2005b) used several optical photometric and spectroscopic diagnostics and radio properties to select RLAGN in the SDSS/NVSS sample, however a small fraction ( $\sim 10\%$ ) of a possible RQAGN contribution is still present after the selection. Since aligned and young RGs can be removed from the sample only on the basis of a spectral and temporal radio study which are often not available, the simplest method to select bona-fide FR 0 candidates is based on a shallow optical-radio (largely available) selection process which consists of a few steps to maximise the probabilities that the radio emission is associated with a compact RL active nucleus. Accordingly, Baldi et al. (2018) have compiled a catalogue of 104 FR 0 sources (namely, FR0CAT) from the SDSS/NVSS sample, by adopting the following criteria:

- nearby (redshift  $z \lesssim 0.05$ ) galaxies.
- compact: the sources are unresolved in the NVSS maps at  $45''$  resolution. More stringently, the source must appear unresolved at FIRST resolution,  $5''$ . The FR 0 candidates consist of unresolved sources for which the deconvolved size is smaller than  $4''$ . At  $z = 0.05$ , this corresponds to  $\sim 5$  kpc, that is, to a radius of 2.5 kpc.
- FIRST 1.4 GHz flux density  $> 5$  mJy to increase the possibility of an accurate size and flux measurement. This value corresponds to  $\sim 30$  times the noise level of the FIRST maps.
- LERGs. Selecting LINERs allows the exclusion of AGN with high-Eddington ratios (generally Seyferts/HERGs) and are more probably associated with RLAGN phenomena (Heckman and Best 2014; Panessa et al. 2019).

Follow-up observations at higher angular resolution than that of FIRST maps are needed to confirm whether the FR0CAT sources still remain unresolved at sub-kpc scale.

The resulting FR0CAT sample turns out to be a population of RGs with a core dominance of a factor  $\sim 30$  higher than typical 3C/FR Is (Baldi and Capetti 2009; Baldi et al. 2019a; Whittam et al. 2020), where instead the core typically contributes to 1% to the total radio emission (Morganti et al. 1997). Their 1.4 GHz radio

<sup>7</sup> The ratio of core to total extended emission (which in general includes the core emission for simplicity) is called the core-dominance parameter (generally the total and core emission measured, respectively, at 1.4 GHz and  $\gtrsim 5$  GHz) Core-dominated galaxies have typically a core dominance  $\gtrsim 1/3$ .

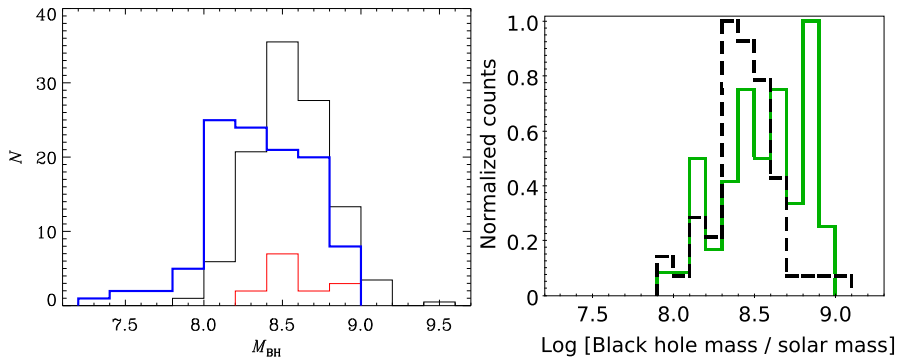


**Fig. 3** Left panel: BH mass distribution (in  $M_{\odot}$ ) of FR0s (FR0CAT, blue line) with respect to FR Is (FRICAT, radio size  $> 30$  kpc, black line) and small FR Is (sFRICAT,  $10 < \text{radio size} < 30$  kpc, red line). Right panel: Compact (black) and extended RGs (green), when matched in radio core luminosities. Images reproduced with permission from [left] Baldi et al. (2018), copyright by ESO; and from [right] Miraghaei and Best (2017), copyright by the author(s)

luminosities are in the range  $10^{38} - 10^{40} \text{ erg s}^{-1}$ . These radio selections turned out to include mostly luminous ( $-21 \gtrsim M_r \gtrsim -23$ ) red ETGs with BH masses  $10^{7.5} \lesssim M_{\text{BH}} \lesssim 10^9 M_{\odot}$ .<sup>8</sup> However, only a minor fraction of the selected FR0s departs from this general behaviour (galaxies with optical photometric and spectroscopic characteristics, typical of blue star-forming spirals and RQAGN, see Sect. 3.2), although a host (ETG) selection was not part of the selection criteria.

As control samples with respect to the FR0CAT, other catalogues of low-luminosity FR Is and FR II have been selected from the SDSS/NVSS sample, a factor  $\sim 10$ – $100$  weaker than 3C/RGs. Capetti et al. (2017a) selected 219 low-luminosity FR Is, named FRICAT, with core-brightened radio morphology, redshift  $\leq 0.15$ , and extending (at the sensitivity of the FIRST images) to a radius ( $r$ ) larger than 30 kpc from the optical centre of the host. The authors also selected an additional sample (sFRICAT) of 14 smaller ( $10 < r < 30$  kpc) FR Is, limiting to  $z < 0.05$ . The distribution of radio luminosity at 1.4 GHz of the FRICAT covers the range  $10^{39} - 10^{41.3} \text{ erg s}^{-1}$  and the sources are all LERGs. The hosts of the FRICAT sources are all luminous ( $-21 \gtrsim M_r \gtrsim -24$ ), red ETGs with BH masses in the range,  $10^8 \lesssim M_{\text{BH}} \lesssim 10^{9.5} M_{\odot}$ , slightly larger than FR0CAT BH masses (Fig. 3). Similarly, Capetti et al. (2017b) selected 122 low-luminosity FR IIs, named FRIICAT, with redshift  $\leq 0.15$ , an edge-brightened radio morphology, and those with at least one of the radio emission peaks located at radius  $r > 30$  kpc from the optical galaxy centre. The radio luminosity at 1.4 GHz of the FRIICAT sources covers the range  $10^{39.5} - 10^{42.5} \text{ erg s}^{-1}$ . The FRIICAT catalog mostly includes LERGs (90%), which are luminous ( $-20 \gtrsim M_r \gtrsim -24$ ), red ETGs with BH masses in the range  $10^8 \lesssim M_{\text{BH}} \lesssim 10^9 M_{\odot}$ .

<sup>8</sup> All the BH masses reported in this work for FR0CAT, FRICAT, sFRICAT and FRIICAT objects are derived from SDSS stellar velocity dispersions  $\sigma$  and considering the  $M_{\text{BH}} - \sigma$  relation of Tremaine et al. (2002).

Other FR 0 samples were selected at lower and higher radio frequencies than the FIRST 1.4 GHz band (see Sect. 5 for details), which instead include a larger contamination from spurious sources than the FR0CAT. At low radio frequencies (hundreds of MHz) which is expected to be dominated by optically-thin emission, the vast majority ( $\sim 70\%$ ) of sources in the wide-area LOFAR (Hardcastle et al. 2019; Sabater et al. 2019; Mingo et al. 2019; Capetti et al. 2020a) and GMRT Survey (Capetti et al. 2019), and in the deep well-studied field (e.g. ELAIS-N1 and BOOTES, Sirothia et al. 2009; Ishwara-Chandra et al. 2020) appear compact with an angular resolution of a few arcsec and have  $\alpha$  between 0 and 0.85, with the flat-spectrum sources more abundant than the steep-spectrum companions.

At higher radio frequencies (tens of GHz) which is expected to be dominated by the optically thick emission, FR 0s have been selected by Sadler et al. (2014) from the AT20G-6dFGS sample and by Whittam et al. (2016) from the Cambridge 10C survey (mostly  $z < 3$ ) based on their radio morphological compactness (a few arcsec). Both the samples selected 70–80% of CRSs, which include FR0-like LERGs and a large fraction of possible GPS/CSS sources.

In conclusion, the selection of flat-spectrum weak CRSs in red massive hosts still remains the safest way to select bona-fide FR 0s in relation with other compact and extended radio galaxies which can exhibit steeper radio spectra and bluer hosts (see next section).

### 3.2 Host properties

The different radio-frequency selections of the FR 0s lead to a heterogeneous distribution of their host properties (e.g. galaxy type, colour, mass,  $M_{\text{BH}}$ ): selecting red massive ETGs represents the most secure criterion of identifying hosts of a FR 0. In fact, a prior host selection through several diagnostics can reduce the probability of inclusion of radio-compact impostors. The concentration index  $C_r$  is defined as the ratio of the galaxy radii including 90% and 50% of the light in the  $r$  band, respectively. ETG have higher values of concentration index than LTG, i.e.  $C_r > 2.6$  (Strateva et al. 2001). The  $\text{Dn}(4000)$  spectroscopic index is defined as the ratio between the flux density measured on two sides of the Ca II break ( $\sim 4000 \text{ \AA}$ ) (Balogh et al. 1999) and high values,  $\text{Dn}(4000) > 1.7$ , are generally associated with old stellar populations ( $\gtrsim 1 \text{ Gyr}$ , Hernán-Caballero et al. 2013) and, hence, with red passive galaxies (Best et al. 2005a; Capetti and Raiteri 2015). Optical and infrared colour can also separate red ellipticals from blue spirals. The combination of these diagnostics with the FR0CAT criteria listed in Sect. 3.1 allows to identify the radio-compact red massive ETGs which have the highest probabilities of hosting a RLAGN.

The vast majority of the FR0CAT, FRICAT and FRIICAT hosts are indistinguishable: red massive ETGs, based on the values of the  $C_r$ , spectroscopic  $\text{Dn}(4000)$  indices and broad-band colour. Their redness is confirmed by the photometric  $u - r$  colour, measured over the whole galaxy. The WISE infrared colours further support the general passive nature of the FRCAT hosts (Fig. 4,  $W1 - W2 < 0.2$ , Wright et al. 2010). Nonetheless, a few galaxies of the FR0CAT extend to redder colours than those from the FRICAT and there is a notable lack of blue host galaxies ( $u - r > 2.5$ ) with respect to the general population of ETGs (Schawinski et al. 2009). In

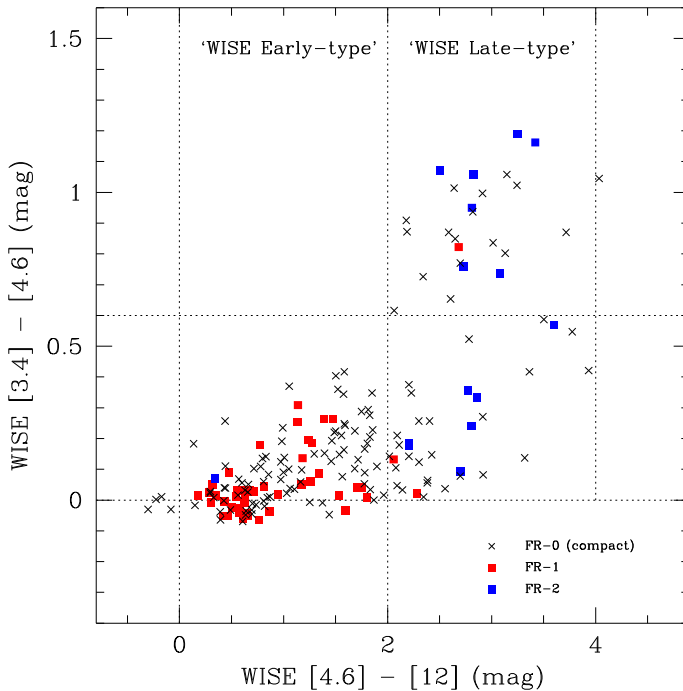


**Fig. 4** WISE colour-colour plot (W2–W3 vs. W1–W2) for the host galaxies of FR I (red squares), FR II (blue squares) and compact (FR 0, black crosses) radio sources in the 20 GHz AT20G-6dFGS sample from Sadler et al. (2014). The horizontal line at a 3.4–4.6  $\mu\text{m}$  colour of 0.6 mag divides the AGN and normal galaxy populations. Objects where radiation from an AGN dominates the galaxy spectrum in the mid-infrared are expected to lie above this line, and objects where starlight dominates should lie below the line. The vertical line  $W2-W3 > 2$  identifies LTGs from ETGs. Image reproduced with permission from Sadler (2016), copyright by Wiley-VCH

addition, the galaxy mass (and BH mass) of FR0CAT sources is on average smaller than those of FRICAT galaxies by a factor  $\sim 1.4$  (Fig. 3), a possible effect of the selection of their lower radio luminosities since radio power and host mass are found to correlate in RL AGN (e.g. Best et al. 2005a; Capetti and Brienza 2023).

At high frequencies, Sadler et al. (2014) did not opt for a host selection and, in fact, found that the host galaxies of FR 0s display heterogeneous properties with a wide range in WISE colours, (33% in LTGs with some ongoing SF, see Fig 4). This implies that the selected FR 0 candidates, which make up the majority of the AT20G-6dFGS sample, probably consists of a mixed bag of genuine FR 0s, young RGs and RQAGN. In fact, the bluer colour of the selected FR 0s is generally attributed to galaxies with a recent SF burst or to young RGs in gas-rich environments.

Since the radio core luminosity has been argued to be a better gauge of jet power than total radio luminosity,<sup>9</sup> Miraghaei and Best (2017) matched a sample of RL CRSs and extended RGs on the basis of the core luminosities. In terms of host

<sup>9</sup> The radio core power is a measure of instantaneous power, rather than the total radio power, that is an averaged value over time and is also influenced by environment.

properties, they found that CRSs and extended RGs differ only in the BH mass (Fig. 3), similar to the result from the FR0CAT (Baldi et al. 2018).

The combination of the following criteria, i.e. the optical red colour, radio compactness and low radio powers (in mJy-level radio surveys), allows to increase the chances to exclude radio-compact impostors and select mostly massive ETGs which harbour compact RL LLAGN,  $< 10^{23} \text{ W Hz}^{-1}$  (Best et al. 2005b; Sabater et al. 2019; Hardcastle et al. 2019), consistent with a FR 0 classification.

## 4 Radio luminosity function

We calculate the radio luminosity functions of the FRCAT sources as object density per unit logarithmic luminosity interval within the maximum volume  $V_{\text{max}}$  in which the objects would be observed (Schmidt 1968; Condon 1989):

$$\Phi(\log L_{\text{NVSS}}) = \frac{4\pi}{\sigma} \sum_{i=1}^{N(\log L_*)} \frac{1}{V_{\text{max}(i)}}, \quad (2)$$

where  $\sigma$  is the area of the sky surveyed,  $N(\log L_*)$  is the number of objects in a given NVSS luminosity bin  $L_*$ , and  $V_{\text{max}(i)}$  is given by the limiting magnitudes/fluxes in both the optical and radio properties of the sample, namely a radio cutoff of 5 mJy and SDSS optical cutoff of  $r < 18$ , as well as any imposed redshift limit for the analysis ( $z < 0.05$  for FR0CAT and sFRICAT and  $z < 0.15$  for FRICAT and FRII-CAT). The sky area of the overlapping region between the SDSS DR7 spectroscopic survey and the FIRST/NVSS radio survey is  $\sigma = 2.17$  steradians. We place detected sources in bins of equal radio luminosities and estimate the uncertainties as in Condon (1989). We use Poisson statistics to estimate uncertainties in luminosity bins with small numbers of sources ( $N < 7$ ). If  $N = 1$ , we set  $1\sigma$  upper limit on the luminosity function in that bin. The 1.4 GHz NVSS luminosities functions are derived for the FR 0s, FR Is and FR IIs from the FRCAT in Fig. 5 and tabulated in Table 2.

Figure 5 shows that, as expected, FR 0s dominate the radio source population at relatively low radio luminosities  $\lesssim 10^{23.5} \text{ W Hz}^{-1}$ , while the FR Is and FR IIs dominate at the highest luminosities. Quantitatively, FR 0s represent the bulk of the RLAGN population of the local Universe ( $z < 0.05$ ) with a space density  $\sim 4.5$  times higher than that of FR Is and  $\sim 100$  than that of FR IIs. In relation to the luminosity function of ETGs, compact sources, consistent with a FR 0 morphology, are found in more than 60% of the giant (K-band magnitude  $\leq -25$ ) ETGs detected by LOFAR with 150 MHz luminosity  $\geq 10^{21} \text{ W Hz}^{-1}$  (Capetti et al. 2022).

## 5 Radio properties

The radio band uniquely characterises the FR 0s as RL CRSs which lack of substantial extended radio emission. In this section, we focus on the radio properties of FR 0s and RL CRSs in general. We provide an overview of the continuum

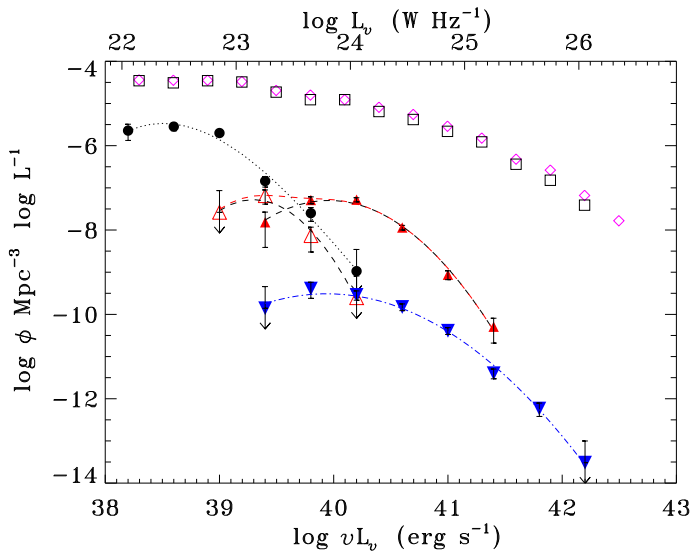


**Fig. 5** The local NVSS luminosity function at 1.4 GHz for RLAGN (pink diamonds) and LERGs (empty squares) from the SDSS/NVSS sample (Best and Heckman 2012). The lower x-axis is expressed in  $\text{erg s}^{-1}$  and the upper one in  $\text{W Hz}^{-1}$ . The other points represent the radio luminosity functions for FR 0s (filled circles), small FR Is (empty red up-ward triangles), FR Is (filled red triangles) and FR IIs (blue filled down-ward triangles) from the FR0CAT (Baldi et al. 2018), sFRICAT/FRICAT (Capetti et al. 2017a) and FRIICAT (Capetti et al. 2017b). The dot, dashed and dot-dashed lines are rough fits of the data-points, respectively, for FR 0s, FR Is, and FR IIs, to better visualise the luminosity functions

**Table 2** The local NVSS radio luminosity functions at 1.4 GHz for FR0CAT, sFRICAT, FRICAT and FRIICAT (LERG) sources

$\log L_{1.4 \text{ GHz}}$ $\text{erg s}^{-1}$	FR0CAT		sFRICAT		FRICAT		FRIICAT	
	$N$	$\log_{10} \rho$	$N$	$\log_{10} \rho$	$N$	$\log_{10} \rho$	$N$	$x \log_{10} \rho$
38.0–38.4	6	$-5.64^{+0.15}_{-0.23}$	0	–	0	–	0	–
38.4–38.8	27	$-5.55^{+0.08}_{-0.10}$	0	–	0	–	0	–
38.8–39.2	48	$-5.70^{+0.06}_{-0.07}$	1	$< -7.58^{+0.51}$	0	–	0	–
39.2–39.6	14	$-6.84^{+0.10}_{-0.14}$	8	$-7.19^{+0.13}_{-0.20}$	3	$-7.82^{+0.24}_{-0.59}$	1	$< -9.86^{+0.51}$
39.6–40.0	8	$-7.60^{+0.13}_{-0.19}$	4	$-8.13^{+0.20}_{-0.39}$	32	$-7.29^{+0.07}_{-0.09}$	7	$-9.39^{+0.15}_{-0.23}$
40.0–40.4	1	$< -9.97^{+0.51}$	1	$< -9.60^{+0.51}$	91	$-7.28^{+0.05}_{-0.05}$	19	$-9.54^{+0.10}_{-0.12}$
40.4–40.8	0	–	0	–	70	$-7.94^{+0.05}_{-0.06}$	36	$-9.82^{+0.07}_{-0.09}$
40.8–41.2	0	–	0	–	19	$-9.06^{+0.09}_{-0.12}$	34	$-10.39^{+0.07}_{-0.09}$
41.2–41.6	0	–	0	–	4	$-10.29^{+0.20}_{-0.39}$	16	$-11.40^{+0.10}_{-0.13}$
41.6–42.0	0	–	0	–	0	–	9	$-12.23^{+0.13}_{-0.19}$
42.0–42.4	0	–	0	–	0	–	1	$< -13.52^{+0.51}$

The first column shows the range of 1.4 GHz radio luminosities ( $\text{erg s}^{-1}$ ) considered in each bin. The  $N$  columns give the total number of radio sources and  $\log_{10} \rho$  their space density (number per  $\log_{10} L$  per  $\text{Mpc}^3$ , see Fig. 5)

observations from different telescopes at different frequencies (from 150 MHz to mm-band) and resolutions (from arcsec to milli-arcsec) to probe the physical mechanism acting at various linear scales along the putative jet. Most studies of CRSs which are reported in the next sub-sections, are related to low- $z$  sources (unless explicated) and typically LERGs.

## 5.1 Low resolution

### 5.1.1 GHz-band: sub/arcsec-scale with VLA

For the large availability of shallow radio data in the band  $\sim 1\text{--}5$  GHz, the VLA has been the first telescope used to select and characterise the properties of FR 0s. In fact, for the large sky coverage, moderately high resolution and sensitivity, FIRST and NVSS 1.4 GHz surveys have been largely exploited to select CRSs and RGs in general in the local Universe, but other than these data the radio information was extremely limited. Later, follow-up VLA observations of 25 FR 0s at 1.4, 4.5, and 7.5 GHz revealed that two third still appear compact at the angular resolution of  $0.3''$  (a few hundreds of parsec) and with a flat radio spectrum in the GHz band (Baldi et al. 2015, 2019a). Only a third of the sample exhibits twin or one-sided jets extended on a scale of  $\sim 2\text{--}14$  kpc (see Fig. 2 as an example). The apparent radio compactness of most FR 0s at kpc scales could be caused by the fact that jet emission is below the surface-brightness limit of most large-scale radio surveys. In fact, Shabala et al. (2017) demonstrated that VLBI-scale compact AGN could have lobes and plumes too faint to be detected by most surveys with the VLA and LOFAR. The absence of substantial extended jet emission, whether due to observational effects (no sufficient sensitivity to detect diffuse jets on larger scales) or to intrinsic reasons (intermittent jet activity, young radio activity, intrinsic jet inefficiency, see Sects. 8 and 12), represents the characteristic feature of the FR 0 class and their uniqueness with respect to the other classes of RGs.

Wide-area GHz-band surveys also revealed a large fraction of low-power CRSs, e.g.  $\sim 93\%$  in the VLA-COSMOS Large Project at 3 GHz (Bondi et al. 2018; Vardoulaki et al. 2021). These FR 0s candidates are associated with less massive hosts  $\sim 10^{10.8} M_{\odot}$ , with lower radio powers ( $\lesssim 10^{22} \text{ W Hz}^{-1}$ ) and at higher redshifts (median  $z \sim 1.0$ ) than the FROCAT sources. In the Very Large Array Sky Survey (VLASS; Lacy et al. 2020) at 3 GHz, Nyland et al. (2020) selected  $\sim 2000$  compact RGs, but the redshift information is not well characterised for the entire sample. The selected CRSs in these surveys consists of a heterogeneous population of AGN with red and blue colours, consistent with genuine FR 0s, star-forming galaxies, RQAGN and blazars. Furthermore, Kozieł-Wierzbowska et al. (2020) found that  $\sim 90\%$  of the optical SDSS galaxies at  $z < 0.5$  with a FIRST counterpart appear compact with  $L_{1.4\text{GHz}} \sim 10^{21}\text{--}10^{26} \text{ W Hz}^{-1}$ , hosted typically by ellipticals, a similar result to the work by Baldi and Capetti (2010).

Other GHz-band studies on core-dominated LINERs with moderate radio-loudness hosted in ETGs (e.g. Nagar et al. 2000; Filho et al. 2000, 2002b; Verdoes Kleijn et al. 2002; Filho et al. 2004; Kharb et al. 2012; Singh et al. 2015b; Dullo et al.

2018; Zajaček et al. 2019; Singh et al. 2019) strengthen the result that nearby elliptical galaxies tend to power RL LLAGN with galactic-scale jet structures, in analogy to FR 0 galaxies.

### 5.1.2 High-frequency up to mm-band

Interferometric observations at  $\nu \gtrsim 5$  GHz have the advantage of isolating better the compact optically thick flat-spectrum core. In fact, at high frequencies the Australia Telescope Compact Array (ATCA) played an important role in the early studies of FR 0s. Sadler et al. (2014) have cross-matched the Australia Telescope 20 GHz (AT20G) Survey with the optical spectroscopic 6dF Galaxy Survey (6dFGS; Jones et al. 2009) to produce a volume-limited sample of 202 high-frequency CRSs associated with local galaxies (at a median  $z \sim 0.06$ ) with 20 GHz flux density limit of 40 mJy. The angular resolution  $10\text{--}15''$  corresponds to a projected linear size of  $10\text{--}15$  kpc. Chhetri et al. (2013) used data from the longest (6 km) ATCA baseline to determine how much of the radio emission seen by the AT20G survey arose in very compact components. They showed that generally almost all their 20 GHz radio emission comes from a central source  $\lesssim 0.2''$  and almost half of the AT20G sources have flat radio spectra at  $1\text{--}20$  GHz. The selected FR 0s represent the dominant population ( $\sim 70\text{--}75\%$ ) of the AT20G-6dFGS catalogue at radio powers between  $\sim 10^{22}$  and  $10^{26}$   $\text{W Hz}^{-1}$  in the local Universe. In addition, the high-frequency selected FR 0s consist of a heterogeneous population in terms of both optical AGN types (75% LERGs, 25% HERGs) and host galaxy types (67% ETGs, 33% LTGs). Further studies of these 20 GHz CRSs confirmed that the flat-spectrum AT20G objects sources tend to preserve a similar spectral shape in polarisation and are hosted in bluer galaxies than standard ETGs (Chhetri et al. 2012, 2020; Massardi et al. 2011).

Whittam et al. (2016, 2020) selected a complete sample of 96 faint ( $> 0.5$  mJy) RGs from the Tenth Cambridge (10C) survey at 15.7 GHz including LERGs and HERGs, mostly, within  $z \sim 3$ . Sixty-five sources are unresolved in the 610 MHz GMRT radio observations, placing an upper limit on their angular size of  $\sim 2''$ . The majority of these sources have flat spectra and are core dominated. The selected FR 0 population is the most abundant in the subset of sources with 15.7 GHz flux densities  $< 1$  mJy, extending the results of Sadler et al. (2014) at higher redshifts,  $z \sim 1$ .

Baldi et al. (in preparation) observed 25 FR0CAT sources at 15 GHz with the Arcminute Microkelvin Imager (AMI) telescope with an angular resolution of  $\sim 30''$ , previously observed with VLA by Baldi et al. (2015, 2019a). The sources appear all unresolved and extend the spectral flatness of the FR0CAT SED at higher frequencies.

Mikhailov and Sotnikova (2021a, 2021b) conducted quasi-simultaneous radio observations of 34 FR 0s up to 22.3 GHz with the single-dish radio telescope RATAN-600 operating in transit mode with resolution varying from  $11$  to  $80''$ . Quasi-simultaneous spectra in the range  $2\text{--}8.2$  GHz are generally flat ( $\alpha < 0.5$ ), but with a larger spread in the spectral index at higher frequencies. The key result is that some FR 0s demonstrate a variability level of up to 25% on a time scale of 1 year.

In the mm-band, a systematic study of FR 0s is still missing. Nevertheless, first studies on mm-band continuum observations of a sample of nearby ETGs and LLAGN found compact nuclear emission (on a scale  $3\text{--}7''$ ), showing flat or inverted spectra consistent with the scenario of small jets powered by RIAF discs (e.g. Doi et al. 2011; Martí-Vidal and Müller 2017; Chen et al. 2023). ALMA continuum observations of bright CRSs (Bonato et al. 2018, 2019; Kawamuro et al. 2022) reveal the presence of a minor population of flat-spectrum radio sources (possibly similar to FR 0s) in opposition to the abundant class of blazars.

### 5.1.3 Low frequency

Low-frequency observations ( $<1$  GHz) have the advantage of probing the synchrotron-aged plasma and the optically thin emission from an extended diffuse jet, crucial to test the duty cycles of FR 0s. Using the data release of the TIFR (Tata Institute of Fundamental Research) GMRT Sky Survey (TGSS), Capetti et al. (2019) studied the low-frequency properties of 43 FR 0 galaxies (FROCAT, with 150 MHz flux densities  $> 17.5$  mJy) at 150 MHz at a resolution of  $\sim 25''$  (corresponding to 10 and 25 kpc). No extended emission has been detected around the detected FR 0s, corresponding to a luminosity limit of  $\lesssim 4 \times 10^{23} \text{ W Hz}^{-1}$  over an area of  $100 \text{ kpc} \times 100 \text{ kpc}$ . The majority of the FR 0s have a flat or inverted SED (150 MHz–1.4 GHz,  $\alpha < 0.5$ ): this spectral behaviour confirms the general paucity of optically thin extended emission within the TGSS beam. By focussing on a sub-sample of FR 0s with 1.4 GHz flux densities  $> 50$  mJy and including 5 GHz data from the Green Bank survey (Gregory et al. 1996), the authors found that  $\sim 75\%$  of them have a slightly convex radio spectrum, with a smaller curvature than powerful GPS sources. The typical FR 0 radio spectrum is better described by a gradual steepening towards high frequencies, rather than a transition from an optically thick to an optically thin regime as seen in young RGs.

Dedicated deep radio surveys on well-studied fields, such as ELIAS-N1, have also detected large numbers of compact RGs: GMRT observations at 610 MHz (Ishwara-Chandra et al. 2020) and 325 MHz (Sirothia et al. 2009) found CRSs with a median spectral index of  $\sim 0.85$  between 610 and 1400 MHz (Ishwara-Chandra et al. 2020). The flat-spectrum sources, which are expected to be core-dominated, represent the FR 0 candidates.

The vast majority,  $\sim 70\%$ , of the radio sources in the LOFAR Two-metre Sky Survey (LoTSS, Shimwell et al. 2017, 2019; Hardcastle et al. 2019) appear compact at 150 MHz with  $6''$  resolution, consistent with a FR 0 classification. Capetti et al. (2020a) explored in details the LOFAR properties of the FROCAT sources. Most of the objects still appear point-like structures with sizes of  $\lesssim 3\text{--}6$  kpc. However,  $\sim 18\%$  of the FR 0s present resolved emission of low surface brightness, usually with a jetted morphology extending between 15 and 50 kpc. No extended emission is detected around the rest of FR 0s, with a typical luminosity limit of  $\sim 5 \times 10^{22} \text{ W Hz}^{-1}$  over an area of  $100 \text{ kpc} \times 100 \text{ kpc}$ . The spectral slopes of FR 0s between 150 MHz and 1.4 GHz span a broad range ( $-0.7 \lesssim \alpha \lesssim 0.8$ ) with a median value of  $\alpha \sim 0.1$ ; only 20% of them have a steep spectrum ( $\alpha \gtrsim 0.5$ ), which is an

indication of the presence of diffuse emission confined within the spatial resolution limit. The fraction of FR 0s showing evidence for the presence of jets, by including both spectral and morphological information, is  $\sim 40\%$ .

In conclusion, the GMRT and LOFAR study of the FR 0s corroborates the result on the absence of extended emission in most of the sources, even in the few hundred MHz regime, where optically thin jet emission is expected to dominate over the core component, as seen in classical large-scale RLAGN.

## 5.2 High resolution

The VLBI technique enables to access to the pc-scale radio emission, a crucial region to study the jet properties of FR 0s closer to the launching site. Cheng and An (2018) and Cheng et al. (2021) studied a sample of FR 0s with world-wide VLBI, the American Very Long Baseline Array (VLBA) and European VLBI Network (EVN) and found resolved jets of a few pc for  $\sim 80\%$  of the sample (Cheng and An 2018; Cheng et al. 2021) (see Fig. 6 as an example). The VLBI multi-epoch data and the symmetry of the radio structures indicate that the jet bulk speeds are mildly relativistic (between  $0.08c$  and  $0.51c$ ) with low bulk Lorentz factors (between 1.7 and 6) and large viewing angles. However, these VLBI-based studies focussed on particularly bright FR 0s (flux densities  $> 50$  mJy, a factor 10 higher than the typical FROCAT flux selection threshold, Baldi et al. 2018) with radio power  $10^{23}$ – $10^{24}$  W Hz $^{-1}$ . Recent VLBI studies also target less luminous FR 0s. Giovannini et al. (2023) studied pc-scale emission of 18 FROCAT objects observed with the VLBA at 1.5 and 5 GHz and/or with the EVN at 1.7 GHz with flux densities a factor several lower than those of the FR 0s studied by Cheng and An (2018) and Cheng et al. (2021). All sources have been detected but one with radio core power down to  $10^{21}$  W Hz $^{-1}$ . Four sources remain unresolved at pc scale, while highly symmetric jets have been detected in all other sources. High-resolution observations carried out with the eMERLIN UK-wide array for a sample of 5 FR 0s at 5 GHz, reaching a

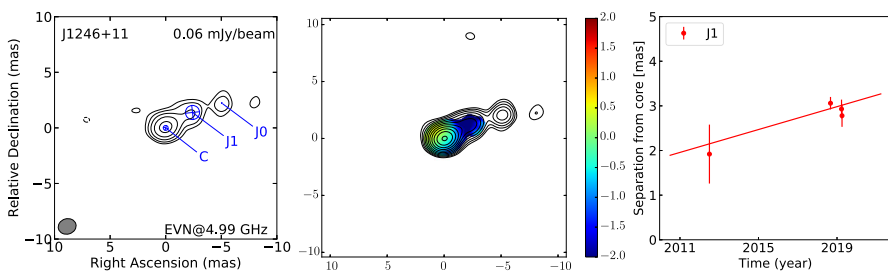


**Fig. 6** EVN image at 5 GHz, spectral index map and jet proper motions of one FR 0 from Cheng et al. (2021) from left to right panel. The grey-coloured ellipse in the bottom-left corner of each panel denotes the restoring beam. The spectral index maps (spectral index colour coded in the left palette) are obtained by using the EVN 5 and 8 GHz data. The proper motions of jet components are determined by the linear fit to the component positions as a function of time. Images reproduced with permission from Cheng et al. (2021), copyright by the author(s)

resolution of  $\sim 40$  mas show sub-mJy core components (Baldi et al. 2021a). The pc-scale core emission contributes, on average, to 3–6% of the total radio emission measured at kpc scale from NVSS maps, although an increasing core contribution for flat/inverted-spectrum sources is evident. VLBI studies of FR 0s clearly demonstrate the jet-to-counter-jet flux ratios of FR 0s are significantly smaller than those of 3C/FR Is (Baldi et al. 2021a; Giovannini et al. 2023), supporting the picture that jet bulk velocities in the FR 0s are lower (see Sect. 8 for further discussion).

Apart from the cases ( $\sim 30\%$ ) where the VLBI core emission is higher than previous low-resolution data, possibly due to source variability and/or an inverted/peculiar radio spectrum, mas-scale radio emission is typically up to half of arcsec-scale core emission unresolved with VLA (Cheng and An 2018; Cheng et al. 2021; Baldi et al. 2021a; Giovannini et al. 2023). This suggests that a large fraction of emission is missed by moving from kpc to pc scale emission. Baldi et al. (2021a) combined, for the first time, the visibility datasets of the eMERLIN and VLA in the same band for five low-power FR 0s (Baldi et al. 2015) in order to probe the intermediate scales of the jet length. This procedure turned out to be successful in detecting pc-scale jets for 4 objects, which were missing in the two original datasets (see Fig. 7 for an example) because unresolved in VLA maps and resolved out in the eMERLIN maps. We can thus conclude that FR 0s, although apparently lacking extended emissions, are effectively able to emanate pc-scale jets, whose both small size and low brightness make them hard to isolate and detect. The combination of long and short baselines represents a powerful tool to study the jet properties of the FR 0 population.

In conclusion, VLBI studies of FR 0s reveal the presence of pc-scale jets, generally more symmetric than those of FR Is, flowing with mildly relativistic jet bulk speeds. These results are in line with VLBI observations of nearby low-power LINERs (e.g. Ulvestad and Ho 2001b; Falcke et al. 2000; Filho et al. 2002a; Nagar et al. 2002a).

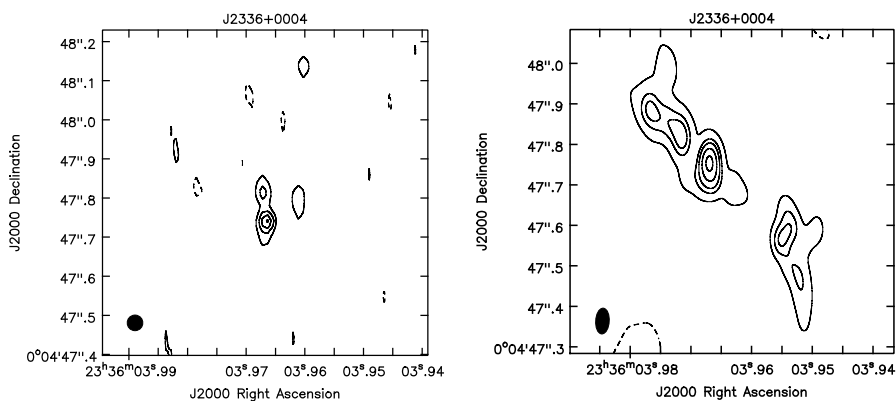


**Fig. 7** The 5 GHz map of the one FR 0 (J2336+0004) observed with the eMERLIN array (resolution  $\sim 40$  mas) and its 4.9 GHz map (resolution  $\sim 60$  mas), obtained by combining eMERLIN and VLA visibilities. The filled area, shown at the bottom-left corner of the images, represents the restoring beam of the maps. Images reproduced from Baldi et al. (2021a), copyright by the author(s)

### 5.3 Radio SED

To reconstruct the typical broad-band radio SED of a FR 0, we collect the multi-frequency radio data from MHz to GHz for the FR0CAT objects, available from low and high frequency surveys and single dish observations. Figure 8 depicts the mean radio SED (black solid line) from 150 MHz to 22 GHz with  $1\sigma$  dispersion (considering only detections). The main result is the overall flat spectral index ( $-0.011 < \alpha < 0.025$ ), which confirms the general tendency of FR 0 population to be characterised by the lack of optically thin component throughout the frequencies. The mean FR0 radio SED is flatter than the typical one derived for classical RLAGN,  $\sim -0.6$  to  $0.7$  (Elvis et al. 1994), even selecting the low- $z$  sample of RLAGN (Shang et al. 2011). Non-thermal self-absorbed synchrotron emission from the basis of a core-dominated jet is most probably responsible to justify the observed spectral flatness.

At higher resolution, the (GHz-band) radio SED of the pc-scale cores is as flat as those derived from low-resolution radio observations (Fig. 6, Cheng and An 2018; Cheng et al. 2021). The jet components resolved with VLBI appear weak and have steeper spectra than those of cores,  $\sim -1$  to  $-2$ . This result confirms the small contribution of the extended optically thin jetted emission to the total radio emission in FR 0s (i.e. high core dominance) and, indeed, sub-kpc-scale jets can typically emerge from radio maps with hybrid angular resolution (e.g. combining short and long baselines) or with deep VLBI observations.

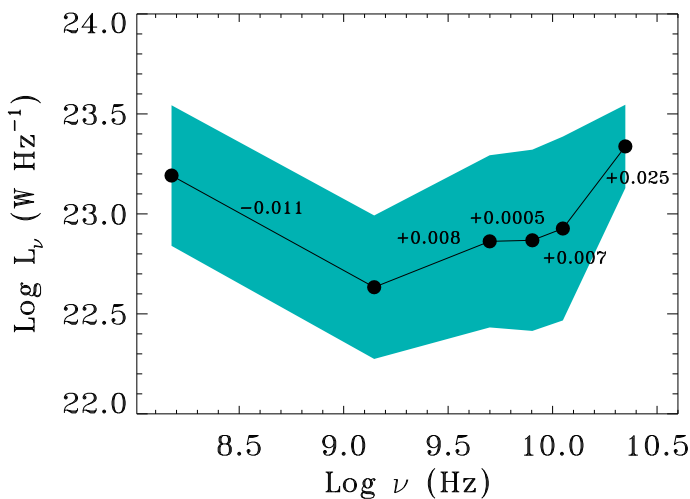


**Fig. 8** The mean radio spectra ( $L_\nu$  vs  $\nu$ ) of FR 0s from the FR0CAT (Baldi et al. 2018) from 150 MHz to 22.3 GHz. The data are taken: 150 MHz from Capetti et al. (2019, 2020a); 1.4 GHz from FIRST survey (Becker et al. 1995), 4.5–5 GHz from VLA data (Baldi et al. 2019a) and Green Bank 6 cm survey (GB6, Gregory et al. 1996); 7.5–8.2 GHz from VLA (Baldi et al. 2019a) and RATAN-600 telescope (Mikhailov and Sotnikova 2021b); 11.2 and 22.3 GHz from RATAN-600 telescope (Mikhailov and Sotnikova 2021b). The colour filled area represents the  $1\sigma$  distribution of the population. The numbers show the spectral indices in the 5 frequency segments ( $L_\nu \sim \nu^\alpha$ ) and are all consistent with a flat spectrum

## 6 Optical and infrared properties

In the optical band, the continuum and spectral information of genuine FR 0s is mostly limited to the SDSS data. For the FR0CAT host galaxies, the optical absolute magnitude distribution covers the range  $-21 \lesssim M_r \lesssim -23$ , corresponding to masses  $\sim 10^{10-11} M_\odot$ , consistent with massive ETGs, as also inferred from the infrared colours. Instead, from the nuclear point of view, a study of the optical and IR accretion-related emission of FR 0s, in analogy to what has been done with Hubble Space Telescope for nearby 3C/FR Is (Chiaberge et al. 1999; Baldi et al. 2010), is still missing. The lack of a proper optical nuclear power estimate leads to the assumption of the optical galaxy emission as upper limit on the optical AGN. Considering 5 mJy as radio flux cut from the FR0CAT sample, the radio-loudness parameter of the FR0CAT sources is at least  $> 11$ .

An optical-band quantity which is widely used to characterise the AGN emission is the [O III] $\lambda 5007$  emission line, that is produced by continuum radiation from the accretion disc or jet which photoionises and heats the ambient gas. Since it is easily observed and largely available from SDSS spectra, its luminosity is usually used as a proxy of the bolometric AGN power (Heckman et al. 2004) (see Sect. 8 for details and caveats). While the line luminosities of FR 0s do not correlate with the total radio luminosities in analogy to CoreG, but in opposition to classical RLAGN (upper panel, Fig. 9), they do with the radio core luminosities, once the sub-arcsec core emission is resolved. In fact, FR 0s lie on the radio-line correlation valid for FR Is and CoreG (Baldi et al. 2015, 2019a) (lower panel, Fig. 9). This common core-[O III] relation valid for LERG-type RGs (FR 0s, FR Is, FR IIs) is generally interpreted as measurement of non-thermal radiation from the jet base at different bands (see Sect. 8, e.g. Hardcastle and Worrall 2000; Baldi et al. 2019a). Since [O III] line is mostly isotropic, this shared correlation implies that the radio compactness of FR 0-like RGs is not due to geometric effects and also sets an universal accretion–ejection coupling at the nuclear level for all LERG-type RGs. Similarly, Miraghaei and Best (2017) found that compact RGs have  $L_{[\text{O III}]}$  distribution analogous to that of extended RGs,  $10^{39}–10^{40} \text{ erg s}^{-1}$ , when matched in radio core luminosities. Conversely, the total radio luminosity of the FR 0s and CoreG does not scale with AGN bolometric luminosity, as, instead, it is valid for LERG FR I and FR IIs (Buttiglione et al. 2010), but a strong deficit of total radio emission with respect to the 3C/FR Is (not due to orientation), by a factor 100–1000 lower at the same AGN power, is notable. This shortage of total jet power suggests a lower jet efficiency of FR 0s than that of the other RLAGN classes (see Sect. 8 for a deeper discussion).

The high detection rates of optical and IR nuclei and the lack of evidence for thermal emission at IR wavelengths have been interpreted as the absence of a dusty torus in 3C/FR Is and generally for LERGs (e.g. Chiaberge et al. 1999; Leipski et al. 2009; Baldi and Capetti 2010; van der Wolk et al. 2010; Antonucci 2012; Dicken et al. 2014; Tadhunter 2016a). This scenario has also been applied to LINER-like LLAGN in general (FR 0s included), which find similar optical and IR characteristics of FR Is (e.g. Ho 2008; Müller-Sánchez et al. 2013), consistent with a luminosity-

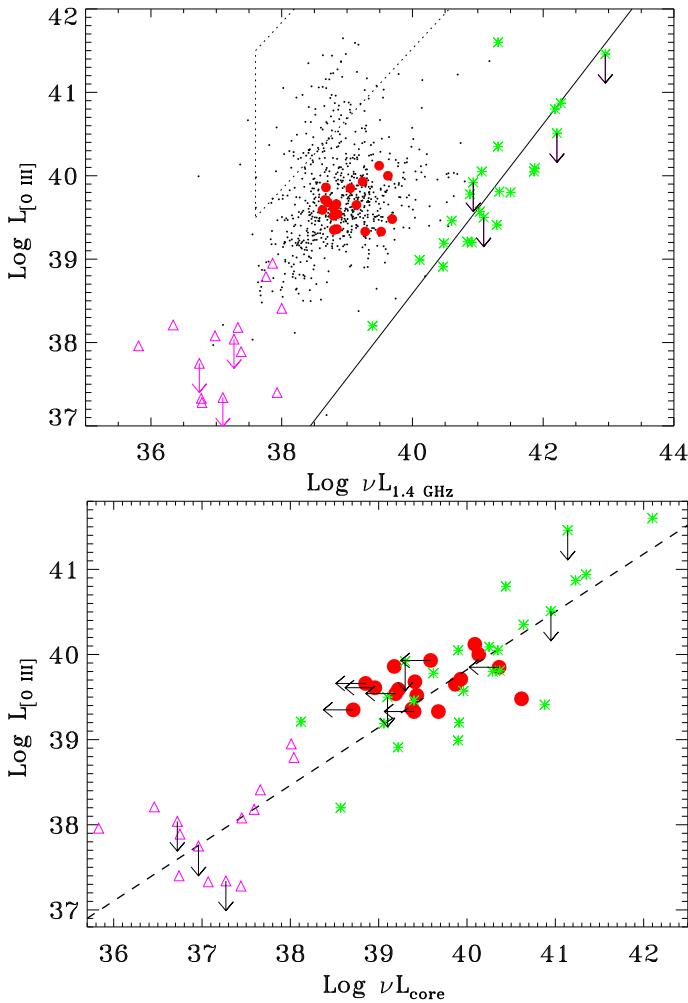


**Fig. 9** Upper panel: NVSS vs. [O III] line luminosity ( $\text{erg s}^{-1}$ ). The small points correspond to the SDSS/NVSS sample selected by Best and Heckman (2012). The solid line represents the correlation between line and radio luminosity derived for the 3C/FR I sample (green stars) (Baldi et al. 2019a). The dotted lines include the region where RQAGN (Seyferts) are found. The filled circles are FR 0s studied with the VLA by Baldi et al. (2019a) and the empty pink triangles are the CoreG. Lower panel: VLA radio core (5 GHz) vs [O III] line luminosity ( $\text{erg s}^{-1}$ ) for 3C/FR Is, FR 0s and CoreG and the dashed line represents their common radio-optical luminosity correlation

dependent model of a torus that disappears at very low accretion rates (Elitzur and Shlosman 2006; Balmaverde and Capetti 2015; González-Martín et al. 2015).

## 7 High-energy properties

The study of high-energy (HE,  $> 0.1$  keV) properties of jetted AGN can help to investigate the accretion and ejection mechanisms in action. The current and upcoming generations of HE detectors are revolutionising our picture of how the engines at the centre of the RLAGN are able to launch plasma at relativistic speeds and extend their spectra to very-high energies (up to TeV, Rani 2019; Rulten 2022). In addition, the detection of HE emission and neutrinos associated with low-luminosity, misaligned AGN and BL Lacs (e.g. Abdo et al. 2010; IceCube Collaboration et al. 2018, 2022; Torresi 2020) has opened a new window on the physics of particle accelerations and jets even in AGN with less extreme conditions than that expected in powerful blazars.

FR 0s,  $\sim 4.5$  times more numerous than FR 1s in the local Universe ( $z < 0.05$ ), represent potentially interesting targets at high and very-high energies (from X-ray to TeV) and could make a non-negligible contribution to the extragalactic HE background (Stecker et al. 2019). Here, we discuss the HE properties (from keV to TeV) of FR 0s, in analogy with the review by Baldi et al. (2019c).

### 7.1 X-ray

The X-ray emission represents an optimal proxy to study the accretion properties of active BHs, because the keV band can probe the HE photons produced by the corona and disc. Torresi et al. (2018) performed the first systematic study in the X-ray (2–10 keV) band of a sample of 19 nearby FR 0s selected from Best and Heckman (2012), for which X-ray data were available in the public archives of the *XMM-Newton*, *Chandra* and *Swift* satellites. Their FIRST 1.4 GHz flux densities ( $> 30$  mJy) are higher than those of the *FR0CAT* sources. Torresi et al. (2018) found that the X-ray spectra of these FR 0s are generally well represented by a power-law  $\Gamma \sim 1.9$  absorbed by Galactic column density and do not require an additional intrinsic absorber, confirming the optical-IR results on the absence of a dusty torus, similar to 3C/FR 1s (e.g. Donato et al. 2004; Balmaverde et al. 2006). In some cases, the addition of a thermal component is required by the data: this soft X-ray emission could be related to the extended inter-galactic medium or to the hot corona typical of nearby ETGs (Fabbiano et al. 1992). The X-ray luminosities of FR 0s,  $L_X$ , range between  $10^{40}$  and  $10^{43}$  erg s $^{-1}$ , similar to those of 3C/FR 1s (Balmaverde et al. 2006; Hardcastle and Worrall 2000).

When the X-ray luminosity is compared to that of the radio core, a statistically significant correlation is established (Fig. 10), valid for FR 1s and FR 0s. This result corroborates the common interpretation that the X-ray emission in low-power RGs, FR 0s, FR 1s and LERGs in general, has a non-thermal origin from the jet (e.g. Balmaverde and Capetti 2006; Hardcastle and Worrall 2000; Hardcastle et al. 2009). The X-ray luminosities of FR 0s also support the idea that the central engine of FR 0s is powered by a sub-Eddington RIAF-type disc,  $\dot{L}_E \sim 10^{-3} - 10^{-5}$ , analogous to 3C/FR 1s and different from powerful 3C/FR 1Is (HERGs) (Baum et al. 1995; Evans et al. 2006; Hardcastle et al. 2009). Since the study from Torresi et al. (2018) is

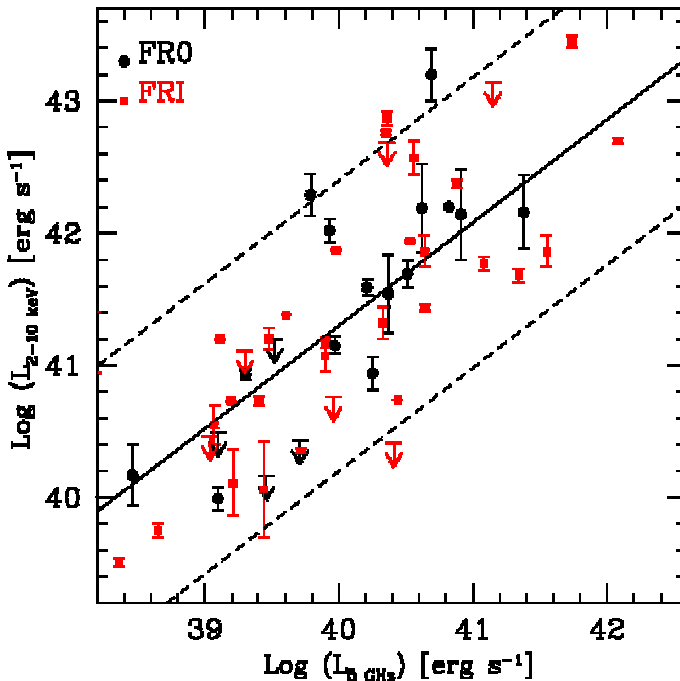


**Fig. 10** X-ray (2–10 keV) luminosity versus 5 GHz radio core luminosity for FR 0s (black circles) from SDSS/NVSS sample and 3C/FR Is (red squares). Arrows indicate upper limits. The black solid line is the linear regression for the overall sample of FR 0s and FR Is, excluding the upper limits. The black dashed lines represent the  $1\sigma$  uncertainties on the slope. Image reproduced with permission from Torresi et al. (2018), copyright by the author(s)

slightly biased towards high-luminous FR 0s, a dedicated study of the accretion properties with deep Chandra data would be required for a statistical confirmation.

## 7.2 Gamma-ray

Gamma rays ( $> 100$  keV) are generally produced under extreme relativistic conditions and offer a unique view of the physical mechanisms in jet launching and propagation (Blandford et al. 2019; Hada 2019). In such a band, blazars are known to be the most luminous class of  $\gamma$ -ray emitters and have been thoroughly studied (Abdollahi et al. 2022). Conversely, the HE properties of low-luminosity and misaligned AGN are generally less explored than their luminous counterparts, because of their lower flux densities (Abdo et al. 2010; Angioni et al. 2017; Rieger and Levinson 2018; de Menezes et al. 2020). In fact, there are only a few cases of  $\gamma$ -ray detection of FR 0s in literature.

Grandi et al. (2016) claimed the first Fermi  $\gamma$ -ray detection of a FR 0, Tol 1326-379, with a GeV luminosity of  $2 \times 10^{42}$  erg s $^{-1}$ , similar to FR Is. Its radio-GeV SED is double-peaked (Maraschi et al. 1992), similar to other jet-dominated RLAGN (Fig. 11, see the SEDs of M87, Abdo et al. 2009, and Cen A, H.E.S.S. Collaboration

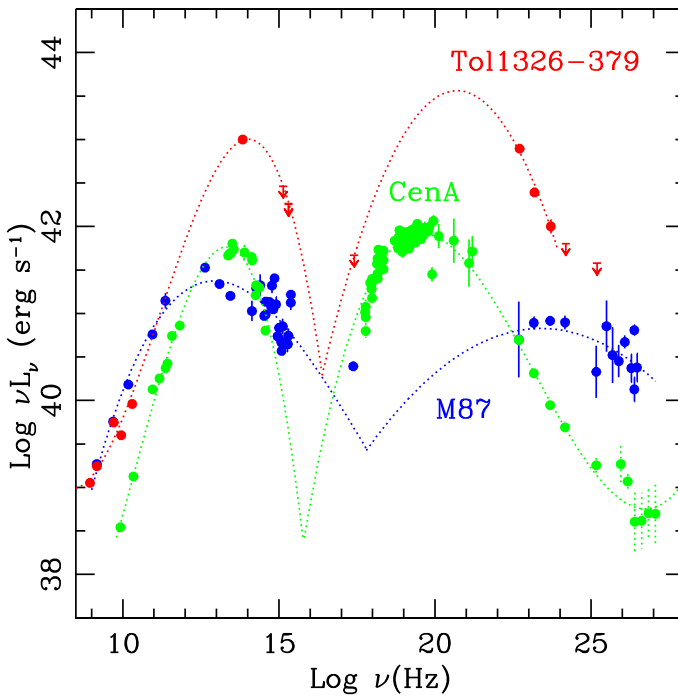


**Fig. 11** Multi-band SED (from radio to  $\gamma$ -ray) of the Fermi-detected FR 0, Tol 1326-379 (red symbols) compared to those of two nearby prototype FR Is, HE emitters: Cen A (green) and M 87 (blue). The dotted lines are polynomial functions connecting the data-points and do not represent model fits to data. Image reproduced with permission from Grandi et al. (2016), copyright by the author(s)

et al. 2020), where non-thermal synchrotron and inverse-Compton emission dominate in any band over the disc and host emission. While the GeV luminosity reconciles with the detection of local FR Is, the prominent Compton peak, brighter than the synchrotron one, makes this source similar to flat-spectrum radio quasars, while the steep  $\gamma$ -ray spectrum makes it conversely more similar to low-luminosity BL Lacs. Nevertheless, the best scenario which can reproduce the whole SED is a misaligned RG which emits synchrotron and synchrotron self-Compton radiation with a total energy flux of the order of a few  $10^{44} \text{ erg s}^{-1}$  (Grandi et al. 2016). Later, Paliya (2021) reports the  $\gamma$ -ray identification of the other three FR 0s from the FROCAT above 1 GeV using more than a decade of the Fermi Large Area Telescope (LAT) observations. By stacking present large datasets, other FR 0 candidates and compact core-dominated RGs have been recently claimed to be detected (Best and Bazo 2019; de Menezes et al. 2020). In addition, based on the sensitivities of upcoming MeV–TeV telescopes, a significant population of low-luminosity RGs emitting at HE will be unearthed in the near future (Baldi et al. 2019c; Balmaverde et al. 2020). In fact, it has been estimated that nearby core-dominated RGs (FR0s and CoreG) can account for  $\sim 4\text{--}18\%$  of the unresolved  $\gamma$ -ray background below 50 GeV observed by the LAT instrument on-board *Fermi* (Stecker et al. 2019; Harvey et al. 2020). Unfortunately, no evident FR 0s have been listed among the non-blazar

AGN list in the recently released Fourth LAT AGN Catalog (4LAC, Abdollahi et al. 2020; Ajello et al. 2022) and the  $\gamma$ -ray identification of Tol 1326-379 has also been questioned (Fu et al. 2022).

In addition, Tavecchio et al. (2018) proposed that FR 0s can accelerate HE protons in the jet and be powerful enough to sustain the neutrino production detectable by the IceCube experiment, above several tens of TeV (Jacobsen et al. 2015). Merten et al. (2021, 2022) argued that FR0 jets can generate ultra-high-energy cosmic rays through stochastic shear acceleration up to  $\sim 10^{18}$ – $10^{19}$  eV (Lundquist et al. 2022). In opposition, Mbarek and Caprioli (2021) argued that the lower bulk Lorentz factors of FR0 jets than those of FR I/IIIs could disfavour their HE emission in general.

In conclusions, although HE studies on FR 0s are still sparse, the main result is that FR 0s and FR Is share common X-ray and  $\gamma$ -ray properties, suggesting similar generic accretion and ejection phenomena in the vicinity of the BH (e.g. accretion disc properties and relativistic acceleration of particles at GeV energies in the jet).

## 8 Accretion and ejection

Current magneto-hydrodynamic simulations have produced a wide range of accretion discs coupled with jets (e.g. Meier et al. 2001; Ohsuga et al. 2009; Yuan and Narayan 2014). In the low-accretion regime (where  $\dot{L}_E$  is typically less than 2% of the Eddington limit, Heckman and Best 2014), ADAF discs are akin to launch jets (Narayan and Yi 1995). An ADAF system can evolve under standard and normal evolution (SANE, e.g. Narayan et al. 2012) and magnetically arrested disc (MAD, e.g. Bisnovatyi-Kogan and Ruzmaikin 1974; Narayan et al. 2003; Tchekhovskoy et al. 2011) configurations: in the former the disc is not significantly threaded with poloidal magnetic flux, while in the latter the magnetic flux threading the BH horizon becomes so large that the magnetic pressure of the jet can temporarily stop the flow of matter into the BH. Current interest in MAD accretion is driven by the discovery that it leads to low and powerful relativistic jets. In fact, for M87, only strongly magnetised (MAD) disc models remain the most favourable solutions to reproduce the EHT results (e.g. Event Horizon Telescope Collaboration et al. 2021). This result strengthens the common interpretation that low-power RGs (generally FR Is, such as M 87) are probably powered by ADAF (MAD-type?) discs with low  $\dot{m}$  and low radiative efficiencies, which channel a small fraction of the disc plasma into the relativistic jet (e.g. Nagar et al. 2000; Falcke et al. 2000; Ho 2002; Hardcastle and Worrall 2000; Balmaverde and Capetti 2006; Zanni et al. 2007; Ho 2008; Balmaverde et al. 2008; Hardcastle et al. 2009). To study the accretion and ejection characteristics of low-power RGs, broad-band empirical relations have been used to gauge the disc and jet energetics.

For the accretion-related argument, we must rely on various proxies for the bolometric AGN luminosity based on the radiation that is not fully obscured by the torus and escapes or is reprocessed. For its large availability, the radiative bolometric luminosity or accretion power can be estimated from the optical [O III] emission line,  $L_{\text{Bol}} = 3500 L_{[\text{O III}]}$  (for LLAGN, Heckman et al. 2004), as the AGN emission excites the gas clouds in the narrow line region, which re-emit [O III] line almost

isotropically. This quantity is a good, but not optimal, proxy since internal obscuration and stellar contamination can affect the measurement.  $L_{[\text{O III}]}$  represents an upper limit on the accretion power for jet-dominated AGN, LERGs (generally not affected by nuclear dust obscuration), where jet shocks can cause [O III] emission, instead of the underluminous RIAF disc (Capetti et al. 2005).

The AGN jets are observable through their synchrotron emission. The mechanical (kinetic) power of the jets,  $L_{\text{Mech}}$  has been estimated using different assumptions. Monochromatic radio luminosity represents only a small fraction of the energy carried by the jets, about 2 orders of magnitude smaller than total  $L_{\text{mech}}$  (Scheuer 1974). However, recalibrating this relationship with physical constraints (e.g. synchrotron spectral ageing, radiative loss, content of particles and magnetic fields) has yielded to

$$L_{\text{mech}} = 7 \times 10^{36} f (L_{1.4\text{GHz}} / 10^{25} \text{ W Hz}^{-1})^{0.68} \text{ W} \quad (3)$$

estimated by Heckman and Best (2014). This relation was obtained by studying the jet mechanical energy as  $pV$  work done by the jet to inflate cavities found in hot X-ray emitting halos (Rafferty et al. 2006; Bîrzan et al. 2008; Cavagnolo et al. 2010). The jet energy can also be estimated from synchrotron emission using the minimum energy condition in the radio lobes in an equipartition regime (i.e. the internal energy is almost equally divided between magnetic field and relativistic particles) (Willott et al. 1999; O'Dea et al. 2009; Daly et al. 2012). The  $f$  factor includes all the uncertainties on the physical state of the lobes, such as for example the particle composition, SED, volume filling factor, possible deviation from the equipartition and adiabatic condition, turbulence, additional heating from shocks. Heckman and Best (2014) adopted  $f = 4$  based on the best linear relation of the data. We note that these empirical assumptions, set on samples of FR Is and FR IIs, may not be entirely applicable to FR 0s (Grandi et al. 2021). However we choose to use this value to be consistent with previous works on low-power RGs (e.g. Heckman and Best 2014).

Left panel of Fig. 12 depicts the Eddington ratio ( $L_{\text{Bol}}/L_{\text{Edd}}$ ) distributions for FROCAT, FRICAT and CoreG galaxies. FR 0s and FR Is have similar rates,  $10^{-5}$ – $10^{-2}$ . A Kolmogorov–Smirnov (KS) statistic test confirms that two distributions are not drawn from different populations with a probability  $P = 0.0059$ . Conversely, CoreG have significantly lower accretion rates  $< 10^{-4}$ .

Since a large amount of the falling gas is launched into the jet without feeding the BH (Zanni et al. 2007), another method to estimate the total accretion is by adding the jet kinetic power to the radiative power as follows  $\dot{L}_{\text{E,tot}} = (L_{\text{Bol}} + L_{\text{Mech}})/L_{\text{Edd}}$ . The right panel of Fig. 12 shows the distribution of this total accretion rate estimator for the different groups of sources. The CoreG generally have lower total accretion rates than the FR 0s and FR Is. However, there is a considerable overlap between the populations of FR 0s and FR Is,  $\dot{L}_{\text{E,tot}} \sim 10^{-4}$ – $10^{-2}$ . A KS test confirms that the cumulative distribution function of FR0s is not significantly different from that of FR Is ( $P = 5.0 \times 10^{-17}$ ). These results confirm the X-ray study from Torresi et al. (2018) that FR 0 BHs are fed at low rates, consistent with a jet-mode AGN and RIAF-type accretion states (Heckman and Best 2014). CoreG, being low-power FR 0s, also have lower accretion rates than FROCAT objects.

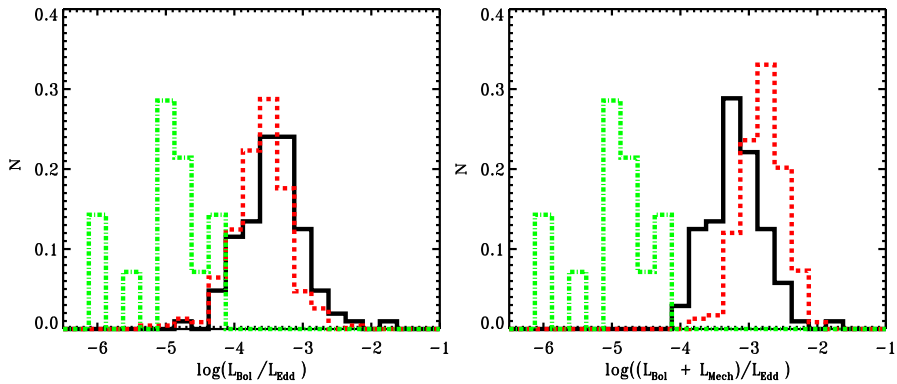


**Fig. 12** Histograms of BH-accretion rates estimated as Eddington ratio,  $L_{\text{Bol}}/L_{\text{Edd}}$  (left panel), and as total accretion rate,  $(L_{\text{Bol}} + L_{\text{Mech}})/L_{\text{Edd}}$  (right panel) for FR0CAT objects (black solid line), FRICAT objects (red dashed line) and CoreG (green dot-dashed line)

Broad-band proxies for accretion and kinetic jet powers are expected to broadly correlate in RLAGN, corresponding to two parallel empirical relations valid for the two accretion states (e.g. Rawlings and Saunders 1991; Willott et al. 1999; Buttiglione et al. 2010; Capetti et al. 2023). For AGN-dominated RLAGN (HERGs), the correlation between radio and optical (continuum) or X-ray emission probably results from a combination of thermal and non-thermal emission from disc and jet (e.g. Chiaberge et al. 2002; Hardcastle and Worrall 2000; Baldi et al. 2019b). For jet-dominated RLAGN (LERGs), the correlation between two luminosity proxies is best explained as the result of a single emission process in the two bands,<sup>10</sup> i.e. non-thermal synchrotron emission from the relativistic jet (e.g. Chiaberge et al. 1999; Balmaverde et al. 2006; Mingo et al. 2014), launched by a RIAF disc as supported by multiple theoretical and analytical studies (e.g. Meier 2001; Begelman 2012; McKinney et al. 2012). This result has also been found valid for low-luminosity AGN, where compact jet dominates the broad-band continuum emission (e.g. Nagar et al. 2002b; Ho 2008; Fernández-Ontiveros et al. 2023). Balmaverde et al. (2008) found that for 3C/FR Is and CoreG the accretion power correlates linearly with the jet power, with an efficiency of conversion from rest mass into jet power of  $\sim 0.012$ . An [O III]-radio correlation found for FR Is, FR 0s, CoreG, and RL low-power LINERs (e.g. Verdoes Kleijn et al. 2002; Nagar et al. 2005; Balmaverde and Capetti 2006; Baldi et al. 2015, 2019a, 2021b, see also Fig. 9) suggests a similar ionising central source, where a scaled-down accretion rate for the core-dominated sources explains a likewise scaled-down jet power with respect to the more powerful 3C/FR Is (Balmaverde et al. 2008). By focussing on the parsec-scale radio emission, the higher resolution of VLBI observation probes a section of the jet base ‘closer’ to the launching site, which is thus more sensitive to the BH-accretion properties, than that detected with the VLA at arcsec resolution. In fact, an analogous  $L_{[\text{O III}]}-L_{\text{VLBI core}}$  correlation has been reported by Baldi et al. (2021a) over  $\sim 4$  orders of magnitudes

<sup>10</sup> The caveat is that the optical and X-ray emission represent only an upper limit on the actual accretion power for LERGs.

(Fig. 13) for RGs with comparable properties, e.g. hosted in massive ETGs and characterised by a LINER spectrum (FR I, FR 0s, CoreG, RL LLAGN). By also including the new VLBI data for FR 0s from Giovannini et al. (2023), we fit the data points present in this sequence with a power-law relation. We find a robust correlation in the form  $L_{[\text{O III}]} \propto L_{\text{VLBI core}}^{0.58 \pm 0.06}$  with a Pearson correlation coefficient of 0.767 which indicates that the two quantities do not correlate with a probability smaller than  $8 \times 10^{-14}$ . This statistically robust relationship corroborates the idea that the model of RIAF disc with core-brightened jets of FR Is is also applicable to FR 0s and LINER-like RLAGN in general. The large scatter of the correlation,  $\sim 0.28$  dex, could be caused by Doppler boosting, nuclear variability and non-flat spectral index (1.4–8 GHz). However, there is no clear evidence for strong Doppler-boosted effect in FR 0s (higher radio luminosities than implied by the linear correlation) for the one-sided jets or highly variable sources, suggesting that the jet spine is not highly relativistic and/or prominent (see Sect. 12 for more discussion on jet structure).

The accretion–ejection coupling can also be explored by comparing the core dominance, a proxy of the jet brightness structure (i.e. how much the core shines over the extended jet emission), with the total accretion rate,  $\dot{L}_{\text{E, tot}}$ . Figure 14 presents the distribution of these two quantities for FR0CAT, FRICAT and CoreG galaxies (excluding the few sources with core dominance  $> 1$  possibly due to variability or systematic errors). Although the core dominance naturally saturates at 1 as the source becomes weaker (and radio spectrum flatter, Dabhade and Gopal-Krishna 2023), there is a general tendency for RGs to increase their core dominance with decreasing accretion rate. These results suggest that the capability of a RG to develop kpc-scale structures is related to accretion properties: more core-brightened structures are associated with lower- $\dot{m}$  sources.

The jet efficiency, i.e. the fraction of the kinetic jet power produced with respect to the AGN accretion power, offers a good diagnostic to investigate the nature of the nuclei of RGs. The  $L_{\text{Mech}}/L_{\text{Bol}} \sim \eta/\epsilon$  ratio ( $\eta$  and  $\epsilon$  are the fraction of gravitational energy converted into jet power and thermal radiation, respectively) directly measures the ability of the system to channel gravitational energy into the jet rather than to dissipate it in thermal radiation. Figure 15 depicts  $\eta/\epsilon$  for FR0CAT, FRICAT and FRIICAT objects (Grandi et al. 2021). Neglecting the  $f$  and  $M_{\text{BH}}$  effect on the jet efficiency, whereas HERGs favour a thermal dissipation of the gravitational power, different LERG types, powered by similar inefficient accretion flows, launch jets with different luminosities and different jet efficiencies: FR 0s appear less efficient in extracting energy from the BHs into the jets than FR Is.

At parsec scale, a comparison between FR 0 and classical 3C/FR I jets can help us understand the reason why FR 0s do not develop large structures. 3C/FR Is generally exhibit core-brightened radio morphologies with VLBI observations (Fanti et al. 1987; Venturi et al. 1995; Giovannini et al. 2005) and FR 0s show occasionally similar morphologies when resolved. However, the degree of jet asymmetry and the ratio between one-sided and two-sided jets appears different between the two classes. In FR Is, the effect of Doppler boosting on the jet sidedness, i.e. the jet-to-counter-jet flux ratio, decreases from VLBI to VLA observations and is typically larger than 3 at

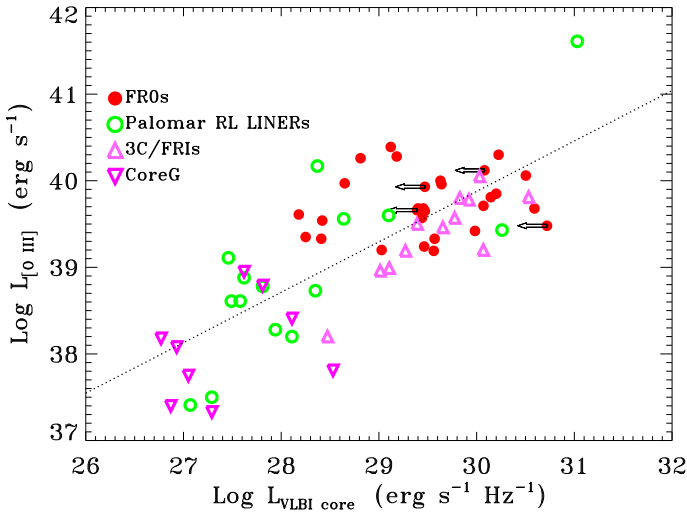


**Fig. 13** Parsec-scale core radio power ( $\text{erg s}^{-1} \text{Hz}^{-1}$ ) vs.  $[\text{O III}]$  line luminosity ( $\text{erg s}^{-1}$ ) for different samples of LINER-type RLAGN hosted in ETGs with core-brightened morphologies (see the legend): FR 0s (red filled dots) from Cheng and An (2018), Cheng et al. (2021), Baldi et al. (2021a) and Giovannini et al. (2023), RL LINERs from the Palomar sample from Ho et al. (1995) (green empty dots), 3C/FR Is (upwards orange triangles), Core Galaxies (downward pink triangles). The dotted line indicates the best linear correlation

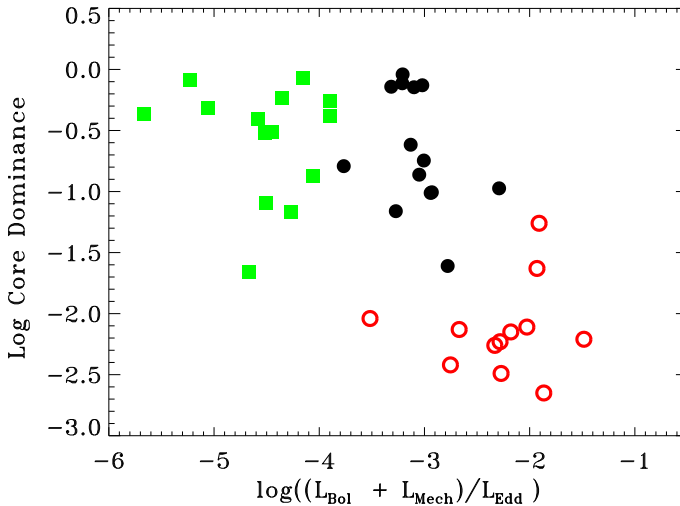


**Fig. 14** The core dominance measured as ratio between VLA 5 GHz core and NVSS 1.4 GHz flux densities for FR0CAT sources (black filled dots), FRICAT sources (red circles) and CoreG (green squares) as function of total accretion rate  $(L_{\text{Bol}} + L_{\text{Mech}})/L_{\text{Edd}}$ . We exclude sources with core dominance  $> 1$  because probably affected by variability or systematic errors

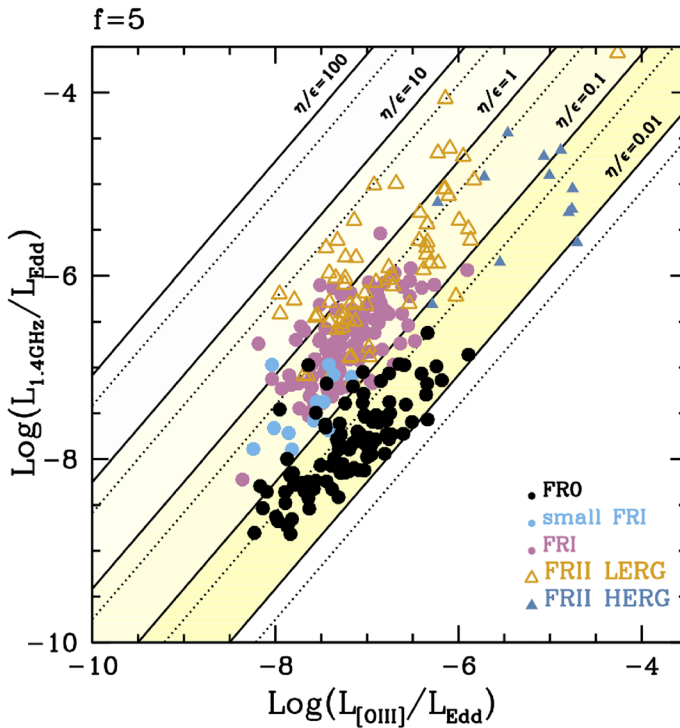


**Fig. 15**  $L_{1.4\text{GHz}}/L_{\text{Edd}}$  versus  $L_{[\text{OIII}]} / L_{\text{Edd}}$  of FRCAT sources (FR 0, FR Is and FR IIs) compared to the predicted values of kinetic jet power estimated by Eq. 3 assuming  $f = 5$ . Each line in the plots corresponds to a different value of  $\eta/\epsilon$ . Since a change of the BH mass can have a minor impact on the predicted  $\eta/\epsilon$  curves, we plot (solid and dotted) lines corresponds to  $M_{\text{BH}} = 10^{7.5}$  and  $M_{\text{BH}} = 10^{9.5} M_{\odot}$ . Image reproduced with permission from Grandi et al. (2021), copyright by the author(s)

parsec scale (Bridle 1984; Parma et al. 1987; Giovannini et al. 1990; Venturi et al. 1995; Xu et al. 2000; Giovannini et al. 2001). On the basis of the presence of a link between jet speed and asymmetry, this result is interpreted as a change of the FR I jet bulk speed from relativistic,  $\Gamma > 3$ , to sub-relativistic speeds on kpc scales by decelerating, possibly due to entrainment of external material (Bicknell 1984, 1995; Bowman et al. 1996; Laing and Bridle 2014; Perucho et al. 2014). For FR 0s the jet sidedness is less prominent: only one third of FR 0s has jet sidedness larger than 2 at parsec scale (Fig. 16). This is a clear observational evidence that the jet bulk speed of FR 0s is significantly smaller than that of FR Is. Following the procedure discussed by Bassi et al. (2018), we can roughly estimate the bulk Lorentz  $\Gamma$  factor of the jet, but with a strong assumption on the unknown orientation: the  $\Gamma_{\text{bulk}}$  for the angle of the jet to the line of sight  $\theta_m$  that maximises  $\beta = v/c$ . With these assumptions, considering the range of jet sidedness observed  $< 10$ ,  $\Gamma_{\text{bulk}}$  for FR 0s is typically  $< 2.5$ . This result concurs with the low jet proper motions studied by Cheng and An (2018) and Cheng et al. (2021). In conclusion, although FR 0 and FR Is share comparable accretion properties, the jets of the former appear less efficient and slower, mildly relativistic at parsec scales with a bulk velocity which does not exceed

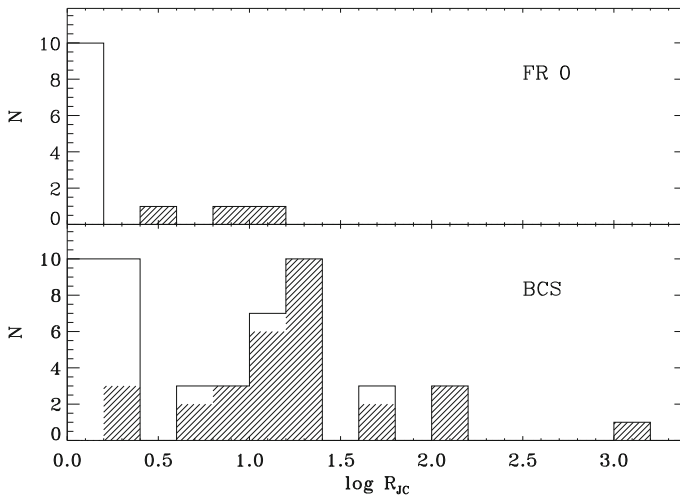


**Fig. 16** Distributions of the logarithm of the  $R_{JC}$ , the jet-to-counter-jet flux ratio for the FR 0 (top panel) from Giovannini et al. (2023) and FR I/FR II RGs from the Bologna Complete Sample (BCS, bottom panel, from Liuzzo et al. 2009). The dashed histograms correspond to lower limit on the jet sidedness. Image reproduced with permission from Giovannini et al. (2023), copyright by the authors

0.5c. However, a proper systematic analysis on larger samples of FR 0s is needed to draw a final conclusion on their accretion–ejection state.

## 9 Environment

The kpc- and Mpc-scale environmental properties (e.g. clustering, ICM, location within the cluster/group, relative galaxy velocity) can regulate the accretion and ejection states of an active BH: e.g. bright cluster galaxies at the centre of dense environments typically host a RG and have different merger histories and fueling properties than galaxies at the cluster outskirts moving away from the centre (e.g. Lin et al. 2010; Vattakunnel et al. 2010; Shlosman 2013; Kormendy and Ho 2013; Conselice 2014). The understanding of the relationship between RLAGN activity and their environment is essential for a comprehension of BH–host evolution, AGN triggering and life cycles, and for calibrating feedback processes in cosmological models (e.g. Huško et al. 2023). However, the role of the environment in shaping RLAGN is still not clear (e.g. Best 2004; Ineson et al. 2013, 2015; Ching et al. 2017; Macconi et al. 2020). The FR I/II dichotomy is believed to depend on jet interaction with the environment (e.g. Laing et al. 1994; Kaiser et al. 1997), or due to host properties (Ledlow and Owen 1996), apart from mechanisms associated with jet production itself (e.g. Meier 2001).

At small scales, the similarity between the host types of FR 0s and FR Is suggests that the galactic gas conditions between the two classes are rather comparable. Precisely, the smaller optical host masses of the FR 0s than those of FR Is argue against the idea of a dense galaxy-scale environment which could cause the jet deceleration and disruption through the interaction with ISM (Kaiser and Best 2007).

No evidence of a denser hot-gas halo with respect to that of FR Is hosts, which typically permeates the atmosphere of elliptical galaxies, can be inferred from the sparse X-ray studies of FR 0s.

The large-scale environment is typically invoked to explain the deceleration and confinement of FR I jets with respect to FR IIs, since FR Is typically reside in denser environment (denser coronae and richer groups/cluster, e.g. Prestage and Peacock 1988; Hill and Lilly 1991; Zirbel 1997; Gendre et al. 2013; Laing and Bridle 2014; Massaro et al. 2019, 2020b). Several studies on the Mpc-scale environment of RL CRSs have confirmed that they inhabit dense environment, but the presence of environmental differences with respect to FR Is have been questioned. Torresi et al. (2018) found that at least 50% of the FR0s live in a dense X-ray environment, which reflects massive dark matter halos in which these objects are embedded. Vardoulaki et al. (2021), studying the VLA-COSMOS Large Project, found that FR I/IIs and compact AGN are found in all types and density environments (group or cluster, filaments, field), regardless of their radio structures. Miraghaei and Best (2017) only found a marginal trend of RL CRSs in denser environments. In this direction, Capetti et al. (2020b) found that FR0CAT sources do indeed live in rich environment but with lower density by a factor of 2 on average, than FR Is, and that about two thirds of FR 0s are located in groups containing  $< 15$  members. A similar result was found by Prestage and Peacock (1988) who argued that RL CRSs lie in regions of lower galactic density than extended sources. In addition, Massaro et al. (2020a) concluded that nearby BL Lacs share similar clustering properties with FR 0s, suggesting a common parental population. In conclusion, there is growing evidence of an environmental difference (at least at large scales) between FR 0s and FR Is (and extended RGs in general), which would imply a different cosmological evolution between the two classes.

## 10 Feedback

AGN feedback comes in two flavours: quasar and radio (or maintenance) mode (e.g. see Croton et al. 2006; Best 2007; Fabian 2012; Bower et al. 2012; Heckman and Best 2014; Harrison 2017). While the former mode is associated with powerful radiatively dominated AGN, i.e. quasars (and HERGs), associated with high Eddington ratios ( $\dot{L}_E > 0.01$ ), the radio mode is attributed to BHs with low-accretion rates ( $\dot{L}_E < 0.01$ , mainly LERGs). The latter releases most of their energy in the form of jets, preventing strong cooling flows in galaxy clusters (e.g. Fabian et al. 2003), and regulating the level of SF in their host galaxies (e.g. Best et al. 2006). It is only with the advent of deep multi-band radio surveys, with their combination of high sensitivity to both compact and extended emission (Shimwell et al. 2017) that we are now able to systematically study the effects of galactic-scale feedback from RL CRSs (e.g. Bicknell et al. 2018). In opposition, powerful quasars have jets that rapidly “drill” through the ISM, depositing most of the energy in the inter-galactic medium. Observational evidence continues to mount that lower-power ( $L_{1.4\text{GHz}} \lesssim 10^{24} \text{ W Hz}^{-1}$ ) jetted AGN may have a significant impact on their hosts through jet-ISM interactions on small ( $\sim 1\text{--}10$  kpc) scales, where the jets heat,

expel, or shock the ambient ISM, thereby altering the SF efficiency (e.g. Nyland et al. 2013; Jarvis et al. 2019, 2021; Webster et al. 2021a, b; Grandi et al. 2021; Venturi et al. 2021). State-of-the-art jet simulations (e.g. Sutherland and Bicknell 2007; Wagner and Bicknell 2011; Mukherjee et al. 2016, 2018; Bicknell et al. 2018; Rossi et al. 2020; Talbot et al. 2022; Tanner and Weaver 2022) provide further support to this scenario, demonstrating that lower-power jets are susceptible to disruption and entrainment, which increases the volume and timescale of the feedback, as well as the amount of energy transferred to the ISM ( $> 5\text{--}10\%$  of bolometric power).

FR 0s, showing galaxy-scale jetted emission, could play a critical role in the radio-mode feedback. In fact, they are the best candidates to offer continuous energy injection into the ISM, although at low regimes ( $\dot{L}_E < 0.02$ ), but fully inserted in the host and with most of the energy deposited in the ISM, on smaller physical (galactic medium) scales than those (inter-galactic medium) affected by the full-fledged jets of FR I/II. Nevertheless, the role of FR0s and the jetted population of LLAGN in general in the context of feedback has just started to be explored (e.g. Kharb and Silpa 2023; Krause 2023; Goold et al. 2023).

Vardoulaki et al. (2021) showed a comparable radio-mode quenching of SF in the hosts of RL CRSs and of FR I/II. In fact, while compact RGs can also be found in less massive hosts ( $10^{9.5}\text{--}10^{11.5} M_\odot$ ) than FR I/II, the former also have low specific SF rates and large time from the last burst of SF derived from SED fitting (Delvecchio et al. 2017) similar to those of the latter. RL CRS hosts lie in cooler X-ray groups than extended RGs with average inter-galactic medium temperatures of  $\sim 1$  keV. Additionally, the older the episode of SF, the cooler the X-ray group in which RL CRSs lie, suggesting a SF shutdown by kinetic feedback.

A dense cold- or hot-phase in the ISM can increase the chances of detecting signatures of an active radio-mode feedback. Best et al. (2000) showed that compact radio sources smaller than 90 kpc have emission line nebulae with lower ionisation, higher luminosity, and broader line widths than in larger radio sources, consistent with shocks driven by the jets or outflows, typically observed in dust-shrouded young RGs. Low-luminosity jet can also carry enough power to shock and remove the cold/hot gas (e.g. Morganti et al. 2018, 2021b; Murthy et al. 2022), as demonstrated by some cases with observed disturbed gas kinematics, absorption features and LINER-like line emission in compact sources (e.g. Holt et al. 2008; Glowacki et al. 2017; Baldi et al. 2019b; Tadhunter et al. 2021). The detection of X-ray cavities in low-power RLAGN ( $< 10^{23} \text{ W Hz}^{-1}$ ) demonstrates the ability of their jets to inflate bubbles in the hot-gas atmosphere (Birzan et al. 2004; Allen et al. 2006). Nevertheless, ordinary FR 0s are not expected to drive strong outflows in dense ISM.

The first dedicated study which has observationally addressed the radio-mode feedback for FR 0s is by Ubertosi et al. (2021a), who found two putative X-ray cavities and two prominent cold fronts possibly associated with the jet activity of a FR 0 (with a bolometric luminosity of the order of  $10^{40} \text{ erg s}^{-1}$ ), associated with a brightest cluster galaxy (cluster Abell 795) (Fig. 17). The estimated cavity power and the cooling luminosity of the ICM follow the well-known scaling relations (e.g. McNamara and Nulsen 2007, 2012), providing a strong evidence for the self-

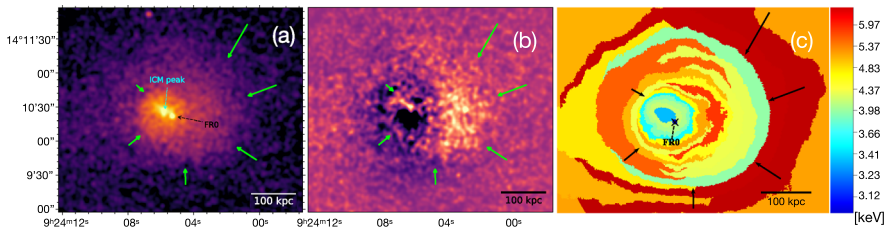


**Fig. 17** **a** Chandra image (0.5–2 keV) of the cluster A795; the ICM peak and the position of the FR 0 are indicated. **b** ICM brightness profile model subtracted to the Chandra image over the same region of **a**. **c** Temperature map of A795. In each panel, the arrows highlight the ICM spiral geometry. Image reproduced with permission from Ubertosi et al. (2021b), copyright by the author(s)

regulated feedback in this source. Being fuelled by the inflow of a cold spiral-shape ICM, the central AGN inflate radio cocoons that excavate X-ray depressions and drive shocks in the ICM which slosh and heat gas, establishing a feedback loop. However, a systematic study of the feedback for a large sample of FR 0s is still missing, mainly because of the great difficulty to detect low-brightness X-ray cavities related to small jets.

To roughly estimate the impact of FR 0 jets on galaxies, assuming that the X-ray atmosphere is regulated by the jet activity, we compare the internal energy within the jets with the energy of the hot X-ray emitting gas in the host, similar to the analysis performed by Webster et al. (2021b) for galaxy-scale jets. First, to calculate the jet energetics, we assume that the radio emission comes from a cylindrical region of  $5''$  long with a radius of  $0.3''$  (radio observation based, Baldi et al. 2019a). Using a Python code (pysynch,<sup>11</sup> Hardcastle et al. 1998) we derive the minimum energy density and the minimum total energy, which is of the order of  $\sim 5 \times 10^{48} - 10^{50}$  J, by considering radio flux densities between 5 and 500 mJy, consistent with FR0CAT sources. Second, to estimate energy within the hot ISM, several assumptions are needed. Since the small jets of FR 0s should have a larger impact on the bulge, we estimate the bulge mass from the BH mass distribution of FR0CAT,  $10^{7.5} - 10^9 M_{\odot}$ , using the McConnell and Ma (2013) scaling relation for ETGs. Then we fix the hot-gas mass fraction to 5% (e.g. Dai et al. 2010; Trinchieri et al. 2012). Then assuming an average particle mass of  $0.62 m_{\text{proton}}$  and a typical gas temperature of 0.5 keV (Goulding et al. 2016), we are able to estimate the internal energy of the hot phase in the bulge, which is of the order of  $\sim 10^{50} - 3 \times 10^{51}$  J. Finally, the total jet energy of FR 0s turns out to be  $\sim 3 - 5\%$  of the total binding energy of the bulge. However, bear in mind that minimum jet energy estimates represent only a lower limit, since the jets must also displace the ISM and produce shocks and its enthalpy for a relativistic gas undergoing adiabatic expansion could be  $> 4$  pV (Bîrzan et al. 2004; Croston et al. 2007; Hardcastle and Krause 2013). In addition, the internal estimated jet energy could be lower than the kinetic jet energy, which can be calculated using the method by Willott et al. (1999) using the 151 MHz luminosity. In fact, by considering the LOFAR 150 MHz luminosity of the FR0CAT,  $10^{38} - 10^{40} \text{ erg s}^{-1}$ , the jet output is of

<sup>11</sup> <https://github.com/mhardcastle/pysynch>.

the order  $1 \times 10^{43} - 4 \times 10^{44} \text{ erg s}^{-1}$ . This evaluation also considers the uncertainties on the factor  $f$  ( $< 20$ , Hardcastle et al. 2007 for FR Is), which includes the effect from the jet structure and its environment (Willott et al. 1999). Assuming a lifetime of the jet activity of  $10^7$  year, the kinetic jet energy would range  $\sim 3 \times 10^{50} - 6 \times 10^{51} \text{ J}$ . These can be considered as upper limits of the jet energetics. In this case, the ISM energy would balance jet energetics. We conclude that the FR0 jets are potentially capable of affecting the ISM properties, at least in the bulge.

Current hydrodynamical simulations (Horizon-AGN, Dubois et al. 2014a; Illustris, Vogelsberger et al. 2014; EAGLE, Schaye et al. 2015; MUFASA, Davé et al. 2016; SIMBA, Davé et al. 2019; SWIFT, Schaller et al. 2023) implement quasar- and radio-mode feedback with a typical efficiency of 5–10%, assuming that the energy deposited back into the ISM, scales directly with accretion rate. The ratio  $(L_{\text{Mech}})/(L_{\text{Bol}} + L_{\text{Mech}})$  provides a measure of the fraction of the total accreted energy released back into the ISM in mechanical form in jets. We measured this ratio for FR 0 and FR Is from FRCAT and found that all deposit more than 10% (on average 30% for FR 0s) of their accreted energy back into the galaxy. This calculation confirms the result from Whittam et al. (2018, 2022) that LERGs in general have higher feedback efficiencies and thus thought to be more responsible for the maintenance mode of mechanical feedback than HERGs, which, as more powerful FR IIs on average than LERGs, generally deposit their energy at larger distances in the ICM.

## 11 Comparison with FR II LERGs

Deep optical-radio surveys have unearthed a large population of low-luminosity FR II LERGs (Capetti et al. 2017b; Jimenez-Gallardo et al. 2019; Webster et al. 2021b), which show kpc-scale edge-brightened radio morphologies, smaller ( $> 30 \text{ kpc}$ ) and less luminous ( $\sim 10^{41} \text{ erg s}^{-1}$ ) than the Mpc-scale powerful 3C/FR II LERGs. Their nuclear properties (luminosity, accretion rates) can still be reproduced by a RIAF disc, consistent with the general jet-mode LERG population (Heckman and Best 2014). Macconi et al. (2020) suggested that FR II LERGs are characterised by intermediate properties between FR Is and FR II HERGs, since they populate an intermediate region of a correlation between accretion rates and environmental richness. Conversely, Capetti et al. (2023) found FR II LERGs are among the most luminous radio sources in the Universe (up to radio power  $10^{35} \text{ erg s}^{-1} \text{ Hz}^{-1}$ ). Tadhunter (2016a) argued that FR II LERGs represent a phase of the RG evolution, when the accretion has recently switched off or levelled down from an FR II HERG high state, after exhausting the cold gas. However, preliminary studies on the properties of the warm ionised and cold molecular gas in RGs (Balmaverde et al. 2019; Torresi et al. 2022) possibly rule out the presence of a statistical difference between FR II LERGs and HERGs, weakening the evolution scenario and, instead, suggesting that jet properties in powerful FR IIs do not depend on the accretion mode or the disc structure (Capetti et al. 2023).

The connection between FR 0 and FR II LERGs is established by their common affinity with FR Is, since they all share a LERG optical spectrum and are generally

interpreted to be jet-dominated RGs powered by a RIAF disc. In fact, Baldi et al. (2018) envisaged that FR 0s, FR Is and FR II LERGs belong to a single continuous population, with similar BH mass, galaxy and accretion properties, regardless of their different jet morphologies. Differences related to intrinsic intimate BH properties (spin and magnetic field at its horizon, and marginally different BH mass) shape the whole LERG population (Miraghaei and Best 2017; Grandi et al. 2021): when these parameters are maximised, highly relativistic jets are launched and form full-fledged FR I/FR II LERGs, while FR 0s would originate from less extreme values of these parameters (see Baldi et al. 2018 and Sect. 12 for discussion).

## 12 Models for FR 0s

Here we will discuss two possible scenarios to account for the multi-band results on FR 0s where the jet and nuclear properties of FR 0s (1) are intrinsically different from those of the other FR classes and do not evolve; (2) evolve within a context of RLAGN population where FR 0 represents a particular phase of this evolution.

### 12.1 Static scenarios

In a non-evolutionary scenario, where the intrinsic properties of the FR 0 class remain unchanged across their lifetime, we will review the main features which can determine the accretion and ejection in FR 0s in relation to FR Is.

Magneto-hydrodynamic simulations of jet launching (e.g. McKinney and Gammie 2004; Hawley and Krolik 2006; McKinney 2006; Tchekhovskoy et al. 2011) predict the formation of a light, relativistic outflow powered by the rotational energy of the BH, as described in the work of Blandford and Znajek (1977) (BZ), as well as of a heavier and mildly relativistic outflow powered by the accretion disc, as originally proposed by Blandford and Payne (1982) (BP). LERGs, which are jet-dominated sources, are generally interpreted as BZ powered, while HERGs, which have quasar-type discs, are generally interpreted as powered by BZ and BP for the presence of both relativistic jets and strong outflows (Heckman and Best 2014). FR 0s as well as FR Is are expected to launch BZ jets (with a possible contribution from a BP process for the outer jet layer in case of a stratified jet, see below).

For RLAGN jets generated by BZ-type process in RIAF discs (Tchekhovskoy et al. 2011; Liska et al. 2022), the ratio of jet and accretion powers (jet efficiency) is maximum when the BH is both rapidly spinning and has accumulated a substantial amount of large-scale poloidal magnetic flux by accretion (see e.g. Komissarov 2001; Tchekhovskoy et al. 2010). The BZ-jet power does not directly depend on the accretion rate, but the outflowing plasma is surely a fraction of the accreting flow. As discussed in Sect. 8, although they can share similar accretion rates, core-dominated RGs and FR 0s show a less jet efficiency than more powerful FR Is. The small fraction of plasma within the disc that is actually channelled into the jet could justify the paucity of matter to accelerate to relativistic speeds in the FR 0 jets.

The BZ-jet power depends on  $M_{\text{BH}}$ , the magnetic field strength  $B$  threading the BH and the magnitude of its spin  $\bar{a}$  (Chen et al. 2021). In Newtonian physics, in a

ballistic model, the jet height is proportional to the ratio of initial speed to gravity. Since the gravity is proportional to the BH mass and the initial jet speed is set by BZ process as the  $\sim E_{\text{kin}}^{1/2} \bar{a}^2 M_{\text{BH}}^2 B^2$ , the maximum jet length is  $\sim \bar{a} B$ . This mathematical approximation suggests that the limited length of FR 0 jets could, in fact, depend on spin and magnetic field.

$M_{\text{BH}}$ , the mass of the central compact object is often used as an indicator of BH activity as AGN are preferentially associated with massive systems (e.g. Chiaberge and Marconi 2011). The jet power roughly establishes the likelihood of the source being radio-jet dominated (Cattaneo and Best 2009). Kinetic jet power and BH masses are connected in radio active nuclei, as AGN tend to become more radio powerful (i.e. more radio loud) at larger BH masses (e.g. Best et al. 2005a). Furthermore, the  $L_{\text{mech}}-M_{\text{BH}}$  relation mirrors the mass dependence on the accretion rate estimated with the Bondi accretion flow expected from the hot hydrostatic gas halos surrounding the galaxies (e.g. Allen et al. 2006; Balmaverde et al. 2008). The slightly smaller BH masses of FR 0s can constitute a limit on the jet power, but cannot simply justify the substantial lack of extended jet emission.

Magnetic field  $B$  plays a primary role in the processes of jet formation, acceleration, and collimation (e.g. Blandford and Znajek 1977; Blandford and Payne 1982; Nakamura et al. 2001; Lovelace et al. 2002). Its azimuthal and poloidal components, originated by rotation of the accretion disc and BH, are required to form and then hold the jet, which extracts angular momentum from the disc surface by torque. The magnetic field integrated on BH horizon sets the jet power. The magnetic flux paradigm by Sikora and Begelman (2013) suggests that the radio loudness is determined by the deposition of magnetic flux close to the BH, which occurs more efficiently during the hot RIAF-type (ADAF) phase and facilitates the jet launching. In fact, as counter-example to stress the important role of  $B$  in jet production, the low magnetic field strength measured with VLBI in the radio-intermediate quasar III Zw 2 has possibly determined its failure to develop a powerful jet (Chamani et al. 2021). The amount of magnetic flux accumulation and the geometry of the external field can differentiate between powerful and weak RGs, including FR 0s (O'Sullivan et al. 2015; Grandi et al. 2021). Moderate jet activity as in FR 0s can also be triggered by the dissipation of turbulent fields in accretion disc coronae (Balbus and Hawley 1991; Brandenburg et al. 1995). In conclusion, a low intensity of the magnetic field structure of FR 0s represents a plausible scenario to describe their limited jet capabilities, although there is not still clear evidence.

BH spin  $\bar{a}$  is the primary ingredient in separating the formation of different jets: the spin paradigm for AGN (Sikora et al. 2007; Garofalo et al. 2010) is a phenomenological scale-invariant framework based on BH-disc parameters for understanding BH feeding, feedback and jet launching mechanisms across the BH mass scale. This model, also named gap paradigm, involves the physics of energy extraction from BH via the BZ effect, the extraction of accretion disc rotational energy via BP jets and disc winds (Pringle 1981; Kuncic and Bicknell 2004, 2007). The total outflow power (BZ jet, BP jet, disc wind) is based on the size of the gap region between the BH event horizon and the disc. The BH spin still mediates launching the jet and determines the upper bound on the radio loudness (Sikora et al.

2007). Retrograde and prograde BH spin configuration with the accreting material rotating opposite or parallel to the direction of the BH can determine the gap region and so jet power: high retrograde BH spin for greater jet power and low-spinning prograde BHs for weak jets (Garofalo 2009). The latter scenario would fit with the FR 0 class.

Recently, in the framework of BZ-jet model, it has been found that the measured poloidal jet magnetic field  $\phi_{\text{jet}}$  threading a BH (Narayan et al. 2003; Tchekhovskoy et al. 2011; McKinney et al. 2012; Yuan and Narayan 2014) correlates over seven orders of magnitudes with the disc luminosity for a sample of aligned and misaligned RLAGN, in the form  $\phi_{\text{jet}} \sim L_{\text{Bol}}^{1/2} M_{\text{BH}}$  (Zamaninasab et al. 2014), as predicted by a MAD model. This relation suggests that the magnetic field twisted by the rotation of the BHs which powers the BZ jets, dominates the plasma dynamics of the MAD disc, prevents the gas infall, and slows down the rotation by removing angular momentum into collimated relativistic outflow. Although we cannot directly measure field strength at the BH horizon  $\phi_{\text{BH}}$ , this quantity is the same as  $\phi_{\text{jet}}$  by the flux freezing approximation for BZ jets. Assuming that  $\phi_{\text{jet}}$  is set by the BZ mechanism,  $\phi_{\text{jet}} \sim L_{\text{jet}}^{1/2} \bar{a}^{-1} M_{\text{BH}}^{-1}$ , and the empirical relation from Zamaninasab et al. (2014), we can derive a rough estimate of the BH spin as  $\bar{a} \sim L_{\text{Mech}}^{1/2} M_{\text{BH}}^{-2} L_{\text{Bol}}^{-1/2}$  by deriving accretion and jet power, respectively, from [O III] and radio luminosities (Eq. 3). This approximate calculation performed for the FR0CAT and FRICAT leads to the conclusion that FR 0s have on average a smaller BH spin than those of FR 1s by a factor  $0.7 \pm 0.3$ . A similar result is obtained if the BH spin is estimated using the empirical correlation with jet power (Narayan and McClintock 2012).

The smaller BH spin of FR 0s would reflect to a lower bulk Lorentz factor  $\Gamma$  than those of FR 1s, as suggested by Baldi et al. (2015, 2019a). The maximisation of the BH parameters ( $M_{\text{BH}}, B, \bar{a}$ ) would lead to high- $\Gamma$  jets with a FR I/II morphology. This is in line with theoretical works which suggest a link between BH spin and jet speeds (e.g. Thorne et al. 1986; Meier 1999; Maraschi et al. 2012; Chai et al. 2012). While an initial disc-jet magnetisation is needed, high spins are possibly required to launch the most relativistic jets, but observational evidence for the connection between BH spin and the jet is controversial and RQAGN with high spins have been observed (Reynolds 2014), breaking the one-to-one correspondence between high BH spins and presence of jets. However, the lower BH spin of FR 0s would certainly contribute to the lower jet bulk speeds, observed in the form of lower jet sidedness than that of FR 1s.

To reconcile the common pc-scale  $L_{\text{core}}-L_{\text{Bol}}$  luminosity correlations valid for FR 0s and FR 1s, the lower jet sidedness of FR 0s, their lack of kpc-scale emission, their putative  $\gamma$ -ray emission, the invoked (static, but valid also for a dynamic scenario) jet model for FR 0s comes from the well-known (stratified jet) “two-flow model” (Sol et al. 1989): an outer jet layer with a mildly relativistic velocity ( $v \sim 0.5c$ ) surrounds an inner electron-positron jet spine, which moves at much higher relativistic speeds (bulk Lorentz factor  $\sim 10$ ). The existence of two flows at different velocities provided a good agreement with both theoretical and observational constraints of RGs in general (Ghisellini et al. 2005). This model can provide a

simple way to solve the discrepancy between the required high Lorentz factors to produce the observed  $\gamma$ -ray emission and the slower observed motion in jets at pc scales (Cheng and An 2018; Chen et al. 2021). Based on this model, the inner beam of FR 0 jets is slower than that of FR I'. Similarly to what happens in FR I jets (Bicknell 1984, 1995; Bowman et al. 1996; Laing and Bridle 2014; Perucho et al. 2014), the jet spine of FR 0s could decelerate on kpc scale to sub-relativistic speeds for entrainment of external material. As suggested by the similar Mpc-scale environment, the unification of the FR 0s and weak BL Lacs in a single class of RGs characterised by a fainter slower spine than that of FR Is, finds supports from recent results which identify a large number of BL Lacs showing 'non classical' blazar-like properties and analogies with FR 0s (e.g. Liuzzo et al. 2013; Massaro et al. 2017; D'Ammando et al. 2018).

Another parameter which can play a role in two-model flow jets for FR 0s is the prominence of one of the two components over the other. In fact, the picture of FR I jets as decelerating flows with transverse velocity gradients and with an intrinsic emissivity (prominence) differences between the spine and the sheath (a slow-moving boundary layer being more prominent than faster material near the centre, Komissarov 1990) finds observational support in resolved jet structures of individual sources (e.g. 3C 84, Giovannini et al. 2018; Cen A, Janssen et al. 2021). Similarly, in FR 0s, the large loss of radio emission from pc-scale structure with respect to the arcsec-scale cores indicates that the jet emissivity does not remain constant and the sheath emission dominates over the spine emission, which is hardly seen, even if boosted, with VLBI observations. In addition, an intrinsically weak spine and a brighter slower shear, supported by BZ and BP processes respectively, could account for the possible loss of jet stability for galaxy medium entertainment. On kpc scale, the spine dies out, dragging the layer to disruption. Another advantage of a sheath-dominated jet is the formation of relativistic shocks between the jet layer of the two flows moving at different speeds, which can accelerate particles along the shock front and produce  $\gamma$ -ray emission by Inverse Compton (Wang et al. 2023). This would justify the  $\gamma$ -ray detection of FR 0 candidates (Baldi et al. 2019c).

Another parameter which takes part in shaping the jet structure is the composition, which is one of the major uncertainties in AGN physics. In powerful RGs, protons (or huge Poynting flux with a very low particle content) are needed in the spine to support the jet kinetic energy (De Young 2006). Conversely, pure leptonic pair (electrons/positrons) jets are excluded, because the jet would be slowed down by Compton interactions. Croston et al. (2018) suggested that FR Is are likely dominated by hadrons (mostly protons) and FR IIs are dominated by leptons, FR 0 jets could be lighter than FR I/II jets, with a smaller hadronic component. This scenario would reduce the necessity for very high bulk  $\Gamma$  factors for FR 0 jets and consequently would probably favour their jet instability by crossing the host galaxy.

## 12.2 Dynamic scenarios

The inclusion of a temporal variation of the accretion–ejection parameters across the RG lifetime span can better reproduce the different observed classes of RLAGN. The tracks in Fig. 18 based on parametric modelling present the expected evolutionary

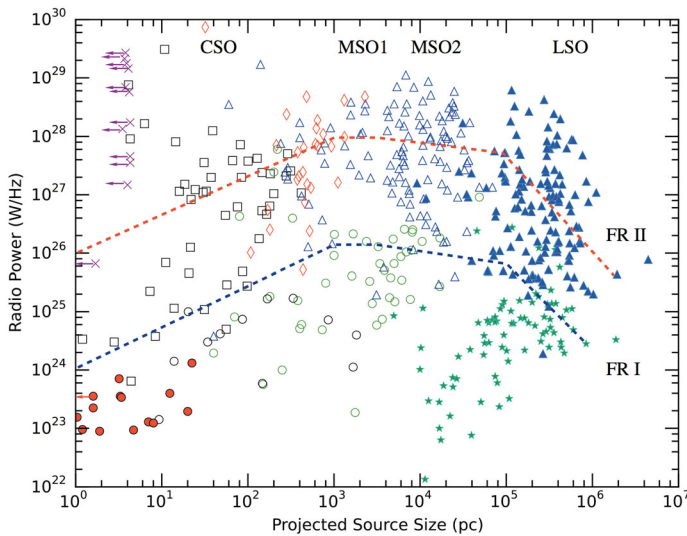


**Fig. 18** Radio power vs. source size ( $P$ – $D$  diagram) of RGs adopted from Cheng and An (2018) with data take from An and Baan (2012). Black squares are CSO, black circles are low-power GPSs, red diamonds are high-power GPSs, purple crosses are HFPs, green circles are low-power CSSs, blue open triangles are high-power CSSs, blue filled triangles are FR IIs, and green filled stars are FR Is. A further morphological sub-classification is also considered that distinguishes among CSO ( $< 1$  kpc), MSO (1–15 kpc), and large symmetric objects (LSO;  $> 15$  kpc, FR I/IIs) (Readhead 1995). Red and blue dashed lines are illustrative of the evolutionary tracks based on parametric modelling for the high-power and low-power sources, respectively. The pc-scale FR 0s (red filled circles) studied by Cheng and An (2018) are situated in the bottom-left corner, occupied by low-power CSOs and some compact low-power MSOs

routes of a radio source that begins as a CSO and successfully evolves to FR I or FR IIs under conditions of long-duration AGN activity. If this standard evolutionary scenario is also applicable to the FR 0s and we consider FR 0s as progenitors of FR Is, FR 0s would correspond to the population of the low-power ( $P_{1.4\text{ GHz}} < 10^{24} \text{ W Hz}^{-1}$ ) CSOs in their earliest evolutionary phase. Instead, the VLBI-resolved FR 0s with pc-scale jets may shift horizontally their position in the  $P$ – $D$  diagram into the region of MSOs. According to the evolutionary model of FR 0s into low-power FR Is proposed by An and Baan (2012), it is necessary for the jet structure to remain preserved before breaking out of the host galaxy and for the AGN activity to last longer than  $10^4$  year. However, due to their low radio power and susceptibility to jet fragmentation, only a small fraction of FR 0s would be capable of evolving beyond a few tens of kpc and becoming low-power FR Is. Furthermore, the much larger space density of FR 0s with respect to FR Is clearly clashes against the picture of all FR 0s as young FR Is and necessarily, not all RL CRSs may be destined to evolve into double RGs (Fanti et al. 1990, 1995). In fact, a uniform distribution of total lifetimes of RLGN in the range 0–1000 Myr, estimated from low radio frequencies data, reproduces well the distributions of projected linear sizes of the powerful sources,  $10^{25} \lesssim L_{150\text{ MHz}} \lesssim 10^{27} \text{ W Hz}^{-1}$ , but diverges from the expectations for the large number of compact/small sources at lower luminosities, even when surface-brightness selection effects are taken into account (Hardcastle et al. 2019). To

break this tension, the presence of RLAGN populations with distinct lifetime distributions or accretion–ejection mechanisms (e.g. FR 0 vs FR I/II) needs to be considered.

A possible scenario to resolve the problem of the large abundance of compact RGs concerns an intermittent AGN activity. Baldi et al. (2018) stated that a radio activity recurrence, with the duration of the active phase covering a wide range of values and with short active periods of a few thousand years strongly favoured with respect to longer ones, might account for the large density number of FR 0s. This would explain why their jets do not develop at large scales (Sadler et al. 2014). An occasional fueling of the central BH can significantly reduce the accretion rate and cause a discontinuous plasma injection in the jet and its possible rapid deceleration and instability within the galaxy. Particular conditions of magnetic field loop, which trap gas and grow magnetic instabilities, could lead to a strangulated BH (Czerny et al. 2009; Yuan and Narayan 2014; Inayoshi et al. 2020). An ‘aborted’ jet scenario was invoked by Ghisellini et al. (2004) to account for the jetted RQAGN where the BH fails to eject an extended relativistic particle jet, if the central engine works intermittently. According to this model, a small difference in BH masses, as seen between FR Is and FR 0s, could play a role in aborting the nascent extended jets. Gopal-Krishna et al. (2008) suggested that a dependence of the jet phenomenon on the BH mass probably could drive a large amount of gas tidally stripped from stars by the central BH, which could truncate the jets in the BH vicinity due to mass loading from the stellar debris. In addition, there is recent evidence that some compact sources, possibly a fraction of the FR 0 population, are turning-off/fading (e.g. Kunert-Bajraszewska et al. 2005, 2006; Giroletti et al. 2005; Orienti et al. 2010) and short-lived due to accretion-related criticality (e.g. Czerny et al. 2009; Kunert-Bajraszewska et al. 2010; An and Baan 2012; Kiehlmann et al. 2023). However, there is not still observational proof of different nuclear gas distribution between FR 0s and FR Is, which might lead to an intermittent BH feeding or a jet frustration of the former with respect to the long-lasting secular accretion and ejection of the latter (Balmaverde et al. 2006).

A temporal evolution of the BH spin within the gap paradigm predicts a FR 0 as a specific phase of a continuous activity in the family of RLAGN (Garofalo et al. 2010). As the gap region reduces in size with BH spin, the BZ/BP jet decreases in power. Instead, continuous mass accretion spins the BH up towards the angular momentum value of the accretion flow. An evolution of the BH spin configuration with the disc angular momentum can reduce or increase the gap region and change the BH spin magnitude. This dynamic process can accommodate the formation of a FR 0 population within two different scenarios: an accretion-driven or a merger-driven one.

In a scenario where the BH spin depends on the accretion history of the system, the gap paradigm has been applied to FR 0s as low, prograde, spinning BHs whose progenitors are powerful FR II quasars (Garofalo and Singh 2019) (Fig. 19). In gas rich mergers, powerful (FR II) HERGs emerge from a BH accreting in a cold mode, surrounded by a thin REAF disc with a retrograde accretion. Due to the powerful jet feedback, the disc moves into a RIAF disc on a timescale of about a few million years. The continuous accretion across the duty cycles will spin down the BHs,

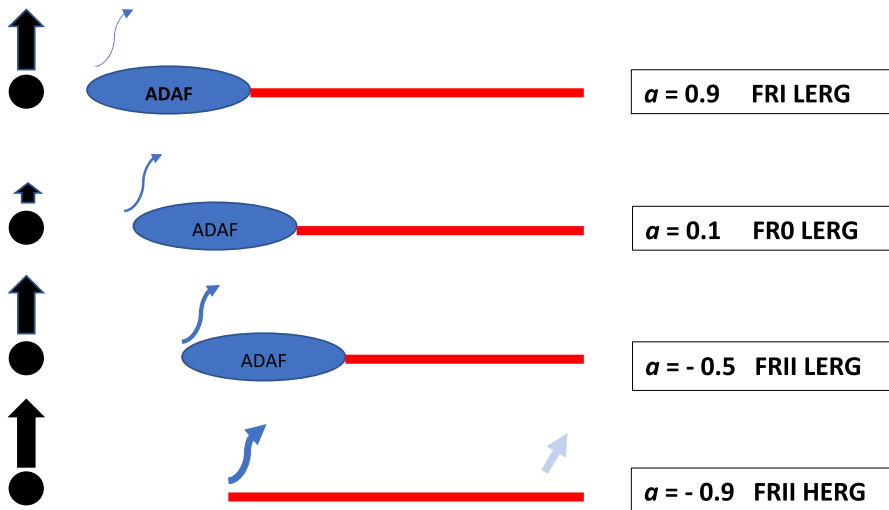


**Fig. 19** Focus on the temporal evolution of RGs according to the gap paradigm from high-powered FR II HERGs to FR I LERGs in an accretion-driven scenario. FR 0s represent a stage of this evolution, as prograde low-spinning BHs.  $\alpha$  is the BH spin, the black thick and the blue curved arrows represent the BZ and BP jets, the blue oval and the red line represent the ADAF and the REAF discs, while the grey arrow in the REAF disc represents the disc wind, which is absent in ADAF states. Image reproduced with permission from Garofalo and Singh (2019), copyright by AAS

moving the system to lower luminosities with a FR II jet, as the retrograde BH approaches to zero (LERGs). As the BH spin moves to a prograde regime, the BZ-jet power increases as the spin increases. In this low BH spinning regime, jet is weaker than in the FR II stage and tends to level off in a stable state. In this region of BH-jet parameter space, FR 0s find their location, where weak, compact jets are found. As the system keeps on feeding the low-spinning prograde BH, the FR 0 moves to a full-fledged FR I, when the spin is sufficiently higher than 0.2 and the BH must accumulate 30% of its original mass.

The large abundance of FR 0s with respect to the other FR classes can also be interpreted as a result of the limited gas availability in nearby ETGs. The paucity of gas in the FR 0 (small- and large-scale) environments slows down the transition from FR 0s to FR Is because of the low-accretion rates. Therefore, FR 0s are not young sources, but they are the result of a prolonged slow accretion of prograde low-spinning massive BHs over timescales of hundreds of millions–billions of years. One-sixth of this population succeeds to funnel sufficient fuel to the BH and ultimately turns into a FR I. The poorer Mpc-scale environment of FR 0s and the slightly smaller BH masses (galaxy masses) than those of FR Is are the two main evidences of a different cosmological evolution of FR 0s with respect to that of FR Is. Therefore, FR 0s are predicted to grow both in small groups (primarily) and in rich clusters.

In a merger-driven scenario, major mergers are known to be the main mechanism for spinning-up BHs (Martínez-Sansigre and Rawlings 2011; Bustamante and Springel 2019). Since such objects are the result of BH–BH coalescence event,

galaxies with higher masses are more likely to have undergone more mergers and, therefore, own high-spinning BHs. The simulations performed by Dubois et al. (2014b) indicate that indeed the most massive BHs ( $M_{\text{BH}} \gtrsim 10^8 M_{\odot}$ ), in particular those associated with gas-poor galaxies, acquire most of their mass through BH coalescence. In a poor environment, major mergers of galaxies with similar masses are rare, causing a limit on the formation of highly spinning BHs. Although large-scale environment seems to generate a sort of difference in the BH spin distribution, the nature of the connection between environment and BH spin is still under debate, because opposite results have also been found (e.g. Smethurst et al. 2019; Beckmann et al. 2023). However, in the standard picture, this merger-driven scenario would agree with the observational result that FR 0s and FR Is live in different environment. Consequently, in this scenario, a positive link between local galaxy density, BH parameters (mass and spin), and accretion rate is set. The poorer neighbourhood of FR 0s, on a statistical basis, determines a longer phase of their lower BH spin than those of their companions FR Is, which live in richer environment. FR 0s in clusters of galaxies are likely formed recently and have not yet accreted a sufficient amount of mass onto their central BH to turn into a FR I. Conversely, rare FR Is in poor groups have likely undergone particular conditions (magnetic field, gas availability, reciprocal galaxy velocity, position in the cluster/group), which have led to an acceleration on their evolution from a FR 0 stage or a different duty cycle. However, the physical process which controls the connection between large-scale environment (Mpc scale) and the BH accretion (Bondi radius, tens and hundred pc) still remains to be understood and there is currently limited observational evidence to support the two proposed scenarios.

In the nearby Universe,  $\sim 70\text{--}80\%$  of the RLAGN phase is spent in a compact-jet configuration. Given that  $\sim 30\%$  of the most massive galaxies are active and the activity must be constantly re-triggered so that the galaxy spends over a quarter of its time in an active state (Best et al. 2005a), the FR 0 phase is an important stage of the evolution of an ETG where their galactic-scale jets are continuously operating in maintenance mode. The large excess of RL CRSs over what would be expected from models in which all sources live to the same age (i.e. constant age models), particularly evident at lower radio luminosities (Shabala et al. 2008; Hardcastle et al. 2019; Shabala et al. 2020), suggests that the actual process of FR 0 evolution is longer than the phase spent as FR I and FR II. Assuming a monotonic jet expansion, the limited size of FR 0s would point to irregular duty cycles, where shorter active phases occur more often than the longer ones (Baldi et al. 2018, 2019a). However, this would conflict with the LOFAR result that the most massive galaxies are always switched on at some level at  $L_{150\text{ MHz}} \gtrsim 10^{21} \text{ W Hz}^{-1}$  (Sabater et al. 2019). Therefore, the large uncertainties on the origin and nature of FR 0 jets, the role of environmental and internal conditions on the duration of the compact phase, complicate the estimate of the duty cycle of FR 0s.

### 13 Conclusions and future perspective

The BH accretion–ejection mechanism provides a major power source in the Universe and is believed to regulate the evolution of galaxies, by injecting energy and momentum. However, the details of how and when this occurs remain uncertain, particularly at low luminosities, where the majority of active BHs are expected. There is compelling evidence, supported by numerical simulations, that low-luminosity RGs channel the bulk of their accretion power into compact and galactic-scale jets ( $\sim 1\text{--}10$  kpc) which may have a significant impact on their hosts, regulating the SF, because they plough energy in the ISM more efficiently than powerful jets. Yet, a poor characterisation of the jet physics and the AGN–host connection at low luminosities hampers our comprehension of the accretion–ejection paradigm, feedback and hence the galaxy evolution. The cross-correlation of high-sensitivity radio and optical surveys showed that the vast majority of local RGs ( $\sim 80\%$ ) appear unresolved on arcsecond scales and shed light on a ‘new’ class of low-luminosity RGs, *FR 0s*, which lack of kpc-scale extended radio emission. This review about recent results on the multi-band properties of FR 0s collected enough evidence to conclude that FR 0s constitute a unique class of CRSs, which *can* launch pc-scale jets with mildly relativistic bulk speeds, probably due to small (prograde) BH spins or lower magnetic fields in the BH vicinity.

To solve the long-lasting question about the large abundance of RL CRSs with respect to what expected by standard RG evolution models, the puzzling nature of FR 0s and their impact on BH–galaxy evolution, an accurate census of the accretion–jet properties is needed with the following characteristics: (i) a statistically complete sample to include all galaxy and AGN diversity to explore the role of each physical parameter that controls the accretion–ejection and feedback processes; (ii) in the radio band, because long-baseline radio arrays can isolate the low-brightness nuclear emission far better than any other instruments at higher energies; (iii) at luminosities as low as possible to probe the very end of luminosity functions, ideally down to Sgr A\* luminosity ( $\sim 10^{15.5}$  W Hz); (iv) in the local Universe to enable pc-scale spatial resolution to disentangle the relative AGN–SF contribution and probe small jet structures.

The current and upcoming generation of radio arrays and surveys done with these facilities, LOFAR (Best and The LOFAR-UK Consortium 2008; Shimwell et al. 2019; Hardcastle and Croston 2020) and the International LOFAR Telescope (Morabito et al. 2022a, b), ASKAP (Norris et al. 2011; Riggì et al. 2021), MeerKAT (Jarvis et al. 2016; Heywood et al. 2022), SKA (Falcke et al. 2004; Kapinska et al. 2015), ngVLA (Nyland et al. 2018a, b), uGMRT (Gupta et al. 2017; Lal et al. 2021), DSA-2000 (Hallinan et al. 2021) and other radio antennae (e.g. ALMA, WSRT), will provide the cornerstone of our understanding of BH activity in the local Universe at low luminosities, across a wide range of galaxy types and environments. Because of their sub-arcsecond resolution and  $\mu\text{Jy}$ -level sensitivity, they will uncover the bulk population of CRSs, opening a new window onto the physical properties of FR 0s. For example, within the wide sky coverage of the LOFAR observations, the census of nearby active BHs at 150 GHz will count  $\sim 3000$  LLAGN with luminosities

$< 10^{40} \text{ erg s}^{-1}$  at  $z < 0.03$  (Sabater et al. 2019). The next step will be with the advent of SKA and ngVLA, which will survey vast numbers of nearby galaxies with unprecedented sensitivities at sub-arcsecond resolutions on a large range of radio frequencies (reaching  $\sim 1 \mu\text{Jy}$  at  $< 1 \text{ GHz}$  over  $30 \text{ deg}^2$  will detect  $\sim 300\,000$  LLAGN, Prandoni and Seymour 2015; Padovani 2016). A multi-band cross-match with other surveys at higher frequencies (optical, X-ray) will trace a demography of local low-power jetted BHs and their interplay with galaxies, providing firmer constraints on models of accretion–ejection coupling in ordinary AGN (not quasar type) (Prandoni and Seymour 2014, 2015).

Low-frequency ( $< 1 \text{ GHz}$ ) radio surveys with SKA precursors (e.g. ASKAP, MWA), LOFAR and GMRT are already extremely valuable for studying the putative extended emissions of FR 0s, because it remains crudely true that the observed duty cycle of AGN increases with decreasing frequency: this is because of the longer synchrotron lifetimes of the lower energy relativistic particles at lower frequencies. Deep sub-arcsecond international LOFAR telescope observations could reveal the true extent of the penetration of FR 0 jet into the galaxy, by discovering synchrotron-aged plasma from past injection events. This would lead to a better characterisation of the physical properties, duty cycles and kinetic power of FR 0 jets.

Combining hundreds-MHz information with GHz-observations can help to characterise the spectral shape of FR 0s to infer the fraction of optically thin, hence extended, emission present in FR 0 jets and eventually isolate the fraction of genuine young radio sources erroneously included in this class. High-resolution radio observations with long baseline arrays (e.g. eMERLIN, EVN, VLBA) are crucial to establish the fraction of jetted FR 0s on pc scale and derive the jet asymmetry and velocity distribution.

With those ideas in mind, the future research on FR 0s will address the following key topics:

- **Pc-scale accretion–ejection.** The origin of the inability of such a large population to grow kpc-scale jets is still a mystery. The separation of the genuine population of FR 0s with respect to other compact impostors (star-forming galaxies, RQAGN, young RGs, blazars) is fundamental to identify the crucial aspects which can diagnose their jet limitations. Accretion and ejection studied with non-radio high-resolution data (e.g. Chandra, eROSITA, JWST, VLT, ELT) can help to disentangle the different contribution in RL CRS population and constraining models of disc and jets.
- **High energy.** Several FR 0 as  $\gamma$ -ray emitters have been detected at the present time and are expected to be multi-messenger sources. It is important to continue the search for  $\gamma$ -ray emission from RL CRSs and LLAGN in general to study particle acceleration mechanisms at low powers.
- **AGN feedback.** Several studies point to the result that RL CRSs can have a more efficient feedback on galaxy than powerful extended RGs. A single studied case of FR 0 driving turbulence and creating cavities in the X-ray atmosphere of a cluster is not sufficient to derive robust results on the effect of low-power jets of FR 0s in the surrounding medium. Systematic studies with deep multi-band data,

combined with VLBI observations will provide a unique data set for advancing our comprehension of the interaction of the FR 0s with their environments.

- **High redshifts.** There is evidence that the local FR 0 population has an important counterpart also at higher redshifts ( $z > 1$ ). A systematic study of the genuine FR 0s at the cosmic noon from deep fields would help to understand the formation and cosmic evolution of low-power RLAGN with respect to the other classes of RGs.
- **Numerical simulations.** High resolution, 3D numerical simulations of low-power jets (total jet power  $< 10^{44} \text{ erg s}^{-1}$ ) can help to clarify the formation, propagation and impact of FR 0 jets in the galactic medium.

**Acknowledgements** I am very grateful to friends and colleagues who provided thoughtful comments on the manuscript, especially A. Capetti, who helped me through fruitful discussions and inspired this review, and M. Brienza, G. Giovannini, P. Grandi, G. Migliori, and E. Torresi, who triggered a productive discussion on FR 0s. I thank the anonymous referees for constructive comments and suggestions that greatly helped improve the manuscript. I thank L. Ferretti for offering me this wonderful opportunity to write this review. R.D.B. acknowledges financial support from INAF mini-grant “FR0 radio galaxies” (Bando Ricerca Fondamentale INAF 2022). This research has made use of NASA’s Astrophysics Data System Bibliographic Services. This research has made use of the NASA/IPAC Extragalactic Database (NED), which is funded by the National Aeronautics and Space Administration and operated by the California Institute of Technology.

**Funding** Open access funding provided by Istituto Nazionale di Astrofisica within the CRUI-CARE Agreement.

## Declarations

**Conflict of interest** The author has no conflicts of interest to declare.

**Open Access** This article is licensed under a Creative Commons Attribution 4.0 International License, which permits use, sharing, adaptation, distribution and reproduction in any medium or format, as long as you give appropriate credit to the original author(s) and the source, provide a link to the Creative Commons licence, and indicate if changes were made. The images or other third party material in this article are included in the article's Creative Commons licence, unless indicated otherwise in a credit line to the material. If material is not included in the article's Creative Commons licence and your intended use is not permitted by statutory regulation or exceeds the permitted use, you will need to obtain permission directly from the copyright holder. To view a copy of this licence, visit <http://creativecommons.org/licenses/by/4.0/>.

## References

- Abdo AA, Ackermann M, Ajello M et al (2009) Fermi Large Area Telescope gamma-ray detection of the radio galaxy M87. *ApJ* 707(1):55–60. <https://doi.org/10.1088/0004-637X/707/1/55>. arXiv:0910.3565 [astro-ph.HE]
- Abdo AA, Ackermann M, Ajello M et al (2010) Fermi Large Area Telescope observations of misaligned active galactic nuclei. *ApJ* 720(1):912–922. <https://doi.org/10.1088/0004-637X/720/1/912>. arXiv:1007.1624 [astro-ph.HE]
- Abdollahi S, Acero F, Ackermann M et al (2020) Fermi Large Area Telescope fourth source catalog. *ApJS* 247(1):33. <https://doi.org/10.3847/1538-4365/ab6bcb>. arXiv:1902.10045 [astro-ph.HE]
- Abdollahi S, Acero F, Baldini L et al (2022) Incremental Fermi Large Area Telescope fourth source catalog. *ApJS* 260(2):53. <https://doi.org/10.3847/1538-4365/ac6751>. arXiv:2201.11184 [astro-ph.HE]

- Ajello M, Baldini L, Ballet J et al (2022) The fourth catalog of active galactic nuclei detected by the Fermi Large Area Telescope: data release 3. *ApJS* 263(2):24. <https://doi.org/10.3847/1538-4365/ac9523>. [arXiv:2209.12070](https://arxiv.org/abs/2209.12070) [astro-ph.HE]
- Alexander P, Leahy JP (1987) Ageing and speeds in a representative sample of 21 classical double radio sources. *MNRAS* 225:1–26
- Allen SW, Dunn RJH, Fabian AC, Taylor GB, Reynolds CS (2006) The relation between accretion rate and jet power in X-ray luminous elliptical galaxies. *MNRAS* 372:21–30. <https://doi.org/10.1111/j.1365-2966.2006.10778.x>. [arXiv:astro-ph/0602549](https://arxiv.org/abs/astro-ph/0602549)
- An T, Baan WA (2012) The dynamic evolution of young extragalactic radio sources. *ApJ* 760(1):77. <https://doi.org/10.1088/0004-637X/760/1/77>. [arXiv:1211.1760](https://arxiv.org/abs/1211.1760) [astro-ph.CO]
- An T, Hong XY, Hardcastle MJ et al (2010) Kinematics of the parsec-scale radio jet in 3C 48. *MNRAS* 402(1):87–104. <https://doi.org/10.1111/j.1365-2966.2009.15899.x>. [arXiv:0910.3782](https://arxiv.org/abs/0910.3782) [astro-ph.CO]
- An T, Wu F, Yang J et al (2012) VLBI observations of 10 compact symmetric object candidates: expansion velocities of hot spots. *ApJS* 198(1):5. <https://doi.org/10.1088/0067-0049/198/1/5>. [arXiv:1111.3710](https://arxiv.org/abs/1111.3710) [astro-ph.CO]
- Angioni R, Grandi P, Torresi E, Vignali C, Knödseder J (2017) Radio galaxies with the Cherenkov Telescope Array. *Astropart Phys* 92:42–48. <https://doi.org/10.1016/j.astropartphys.2017.02.010>. [arXiv:1702.05926](https://arxiv.org/abs/1702.05926) [astro-ph.HE]
- Antonucci R (1993) Unified models for active galactic nuclei and quasars. *ARA&A* 31:473–521. <https://doi.org/10.1146/annurev.aa.31.090193.002353>
- Antonucci R (2012) A panchromatic review of thermal and nonthermal active galactic nuclei. *Astron Astrophys Trans* 27(4):557–602 [arXiv:1210.2716](https://arxiv.org/abs/1210.2716) [astro-ph.CO]
- Balbus SA, Hawley JF (1991) A powerful local shear instability in weakly magnetized disks. I. Linear analysis. *ApJ* 376:214. <https://doi.org/10.1086/170270>
- Baldi RD, Capetti A (2008) Recent star formation in nearby 3CR radio-galaxies from UV HST observations. *A&A* 489:989–1002. <https://doi.org/10.1051/0004-6361/20078745>. [arXiv:0808.1555](https://arxiv.org/abs/0808.1555)
- Baldi RD, Capetti A (2009) Radio and spectroscopic properties of miniature radio galaxies: revealing the bulk of the radio-loud AGN population. *A&A* 508:603–614. <https://doi.org/10.1051/0004-6361/200913021>. [arXiv:0910.4261](https://arxiv.org/abs/0910.4261)
- Baldi RD, Capetti A (2010) Spectro-photometric properties of the bulk of the radio-loud AGN population. *A&A* 519:A48. <https://doi.org/10.1051/0004-6361/201014446>. [arXiv:1005.3223](https://arxiv.org/abs/1005.3223) [astro-ph.CO]
- Baldi RD, Chiaberge M, Capetti A et al (2010) The 1.6  $\mu\text{m}$  near-infrared nuclei of 3C radio galaxies: jets, thermal emission, or scattered light? *ApJ* 725:2426–2443. <https://doi.org/10.1088/0004-637X/725/2/2426>. [arXiv:1010.5277](https://arxiv.org/abs/1010.5277) [astro-ph.CO]
- Baldi RD, Capetti A, Giovannini G (2015) Pilot study of the radio-emitting AGN population: the emerging new class of FR 0 radio-galaxies. *A&A* 576:A38. <https://doi.org/10.1051/0004-6361/201425426>. [arXiv:1502.00427](https://arxiv.org/abs/1502.00427)
- Baldi RD, Capetti A, Giovannini G (2016) The new class of FR 0 radio galaxies. *Astron Nachr* 337(1–2):114. <https://doi.org/10.1002/asna.201512275>. [arXiv:1510.04272](https://arxiv.org/abs/1510.04272) [astro-ph.GA]
- Baldi RD, Capetti A, Massaro F (2018) FR0CAT: a FIRST catalog of FR 0 radio galaxies. *A&A* 609:A1. <https://doi.org/10.1051/0004-6361/201731333>. [arXiv:1709.00015](https://arxiv.org/abs/1709.00015)
- Baldi RD, Capetti A, Giovannini G (2019a) High-resolution VLA observations of FR0 radio galaxies: the properties and nature of compact radio sources. *MNRAS* 482(2):2294–2304. <https://doi.org/10.1093/mnras/sty2703>. [arXiv:1810.01894](https://arxiv.org/abs/1810.01894) [astro-ph.GA]
- Baldi RD, Rodríguez Zaurín J, Chiaberge M et al (2019b) Hubble Space Telescope emission-line images of nearby 3CR radio galaxies: two photoionization, accretion, and feedback modes. *ApJ* 870(1):53. <https://doi.org/10.3847/1538-4357/aaf002>. [arXiv:1811.04946](https://arxiv.org/abs/1811.04946) [astro-ph.GA]
- Baldi RD, Torresi E, Migliori G, Balmaverde B (2019c) The high energy view of FR0 radio galaxies. *Galaxies* 7(3):76. <https://doi.org/10.3390/galaxies7030076>. [arXiv:1909.04113](https://arxiv.org/abs/1909.04113) [astro-ph.HE]
- Baldi RD, Giovannini G, Capetti A (2021a) The eMERLIN and EVN view of FR 0 radio galaxies. *Galaxies* 9(4):106. <https://doi.org/10.3390/galaxies9040106>. [arXiv:2111.09899](https://arxiv.org/abs/2111.09899) [astro-ph.GA]
- Baldi RD, Williams DRA, Beswick RJ et al (2021b) LeMMINGs III. The e-MERLIN legacy survey of the Palomar sample: exploring the origin of nuclear radio emission in active and inactive galaxies through the [O III]-radio connection. *MNRAS* 508(2):2019–2038. <https://doi.org/10.1093/mnras/stab2613>. [arXiv:2109.06205](https://arxiv.org/abs/2109.06205) [astro-ph.GA]
- Baldwin JE (1982) Evolutionary tracks of extended radio sources. In: Heeschen DS, Wade CM (eds) *Extragalactic radio sources*. IAU Symposium, vol 97. Springer, Dordrecht, pp 21–24. [https://doi.org/10.1007/978-94-009-7781-5\\_3](https://doi.org/10.1007/978-94-009-7781-5_3)

- Balmaverde B, Capetti A (2006) The host galaxy/AGN connection in nearby early-type galaxies. Is there a miniature radio-galaxy in every “core” galaxy? *A&A* 447:97–112. <https://doi.org/10.1051/0004-6361:20054031>
- Balmaverde B, Capetti A (2015) The naked nuclei of low ionization nuclear emission line regions. *A&A* 581:A76. <https://doi.org/10.1051/0004-6361/201526496>
- Balmaverde B, Capetti A, Grandi P (2006) The Chandra view of the 3C/FR I sample of low luminosity radio-galaxies. *A&A* 451:35–44. <https://doi.org/10.1051/0004-6361:20053799>. [arXiv:astro-ph/0601175](https://arxiv.org/abs/astro-ph/0601175)
- Balmaverde B, Baldi RD, Capetti A (2008) The accretion mechanism in low-power radio galaxies. *A&A* 486:119–130. <https://doi.org/10.1051/0004-6361:200809810>. [arXiv:0805.3920](https://arxiv.org/abs/0805.3920)
- Balmaverde B, Capetti A, Marconi A et al (2019) The MURALES survey. II. Presentation of MUSE observations of 20 3C low- $z$  radio galaxies and first results. *A&A* 632:A124. <https://doi.org/10.1051/0004-6361/201935544>. [arXiv:1903.10768](https://arxiv.org/abs/1903.10768) [astro-ph.GA]
- Balmaverde B, Caccianiga A, Della Ceca R et al (2020) Te-REX: a sample of extragalactic TeV-emitting candidates. *MNRAS* 492(3):3728–3741. <https://doi.org/10.1093/mnras/stz3532>. [arXiv:1912.07613](https://arxiv.org/abs/1912.07613) [astro-ph.HE]
- Balogh ML, Morris SL, Yee HKC, Carlberg RG, Ellingson E (1999) Differential galaxy evolution in cluster and field galaxies at  $z \sim 0.3$ . *ApJ* 527:54–79. <https://doi.org/10.1086/308056>. [arXiv:astro-ph/9906470](https://arxiv.org/abs/astro-ph/9906470)
- Barausse E, Shankar F, Bernardi M, Dubois Y, Sheth RK (2017) Selection bias in dynamically measured supermassive black hole samples: scaling relations and correlations between residuals in semi-analytic galaxy formation models. *MNRAS* 468:4782–4791. <https://doi.org/10.1093/mnras/stx799>. [arXiv:1702.01762](https://arxiv.org/abs/1702.01762)
- Barthel PD (1989) Is every quasar beamed? *ApJ* 336:606–611
- Bassi T, Migliori G, Grandi P et al (2018) Faint  $\gamma$ -ray sources at low redshift: the radio galaxy IC 1531. *MNRAS* 481(4):5236–5246. <https://doi.org/10.1093/mnras/sty2622>. [arXiv:1810.02668](https://arxiv.org/abs/1810.02668) [astro-ph.HE]
- Baum SA, Zirbel EL, O’Dea CP (1995) Toward understanding the Fanaroff–Riley dichotomy in radio source morphology and power. *ApJ* 451:88. <https://doi.org/10.1086/176202>
- Becker RH, White RL, Helfand DJ (1995) The FIRST survey: faint images of the radio sky at twenty centimeters. *ApJ* 450:559. <https://doi.org/10.1086/176166>
- Beckmann RS, Smethurst RJ, Simmons BD et al (2023) Supermassive black holes in merger-free galaxies have higher spins which are preferentially aligned with their host galaxy. *MNRAS*. <https://doi.org/10.1093/mnras/stad1795>. [arXiv:2211.13614](https://arxiv.org/abs/2211.13614) [astro-ph.GA]
- Begelman MC (2012) Radiatively inefficient accretion: breezes, winds and hyperaccretion. *MNRAS* 420:2912–2923. <https://doi.org/10.1111/j.1365-2966.2011.20071.x>. [arXiv:1110.5356](https://arxiv.org/abs/1110.5356) [astro-ph.HE]
- Bennett AS (1962) The revised 3C catalogue of radio sources. *MmRAS* 68:163
- Best PN (2004) The environmental dependence of radio-loud AGN activity and star formation in the 2dFGRS. *MNRAS* 351(1):70–82. <https://doi.org/10.1111/j.1365-2966.2004.07752.x>. [arXiv:astro-ph/0402523](https://arxiv.org/abs/astro-ph/0402523)
- Best PN (2007) Feedback from radio-loud AGN. *New Astron Rev* 51(1–2):168–173. <https://doi.org/10.1016/j.newar.2006.11.014>
- Best S, Bazo J (2019) Gamma-ray counterparts of radio astrophysical sources. *J Cosmol Astropart Phys* 12:004. <https://doi.org/10.1088/1475-7516/2019/12/004>. [arXiv:1906.01664](https://arxiv.org/abs/1906.01664) [astro-ph.GA]
- Best PN, Heckman TM (2012) On the fundamental dichotomy in the local radio-AGN population: accretion, evolution and host galaxy properties. *MNRAS* 421:1569–1582. <https://doi.org/10.1111/j.1365-2966.2012.20414.x>. [arXiv:1201.2397](https://arxiv.org/abs/1201.2397) [astro-ph.CO]
- Best PN et al (2008) LOFAR-UK WhitePaper: a science case for UK involvement in LOFAR. [arXiv:0802.1186](https://arxiv.org/abs/0802.1186) [astro-ph]
- Best PN, Röttgering HJA, Longair MS (2000) Ionization, shocks and evolution of the emission-line gas of distant 3CR radio galaxies. *MNRAS* 311(1):23–36. <https://doi.org/10.1046/j.1365-8711.2000.03028.x>. [arXiv:astro-ph/9908211](https://arxiv.org/abs/astro-ph/9908211)
- Best PN, Kauffmann G, Heckman TM et al (2005a) The host galaxies of radio-loud active galactic nuclei: mass dependences, gas cooling and active galactic nuclei feedback. *MNRAS* 362:25–40. <https://doi.org/10.1111/j.1365-2966.2005.09192.x>. [arXiv:astro-ph/0506269](https://arxiv.org/abs/astro-ph/0506269)
- Best PN, Kauffmann G, Heckman TM, Ivezić Ž (2005b) A sample of radio-loud active galactic nuclei in the Sloan Digital Sky Survey. *MNRAS* 362:9–24. <https://doi.org/10.1111/j.1365-2966.2005.09283.x>. [arXiv:astro-ph/0506268](https://arxiv.org/abs/astro-ph/0506268)

- Best PN, Kaiser CR, Heckman TM, Kauffmann G (2006) AGN-controlled cooling in elliptical galaxies. *MNRAS* 368(1):L67–L71. <https://doi.org/10.1111/j.1745-3933.2006.00159.x>. [arXiv:astro-ph/0602171](#)
- Best PN, Kondapally R, Williams WL et al (2023) The LOFAR Two-metre Sky Survey: deep fields data release 1. V. Survey description, source classifications and host galaxy properties. *MNRAS*. <https://doi.org/10.1093/mnras/stad1308>
- Bicknell GV (1984) A model for the surface brightness of a turbulent low Mach number jet. I. Theoretical development and application to 3C 31. *ApJ* 286:68–87. <https://doi.org/10.1086/162577>
- Bicknell GV (1995) Relativistic jets and the Fanaroff–Riley classification of radio galaxies. *ApJS* 101:29. <https://doi.org/10.1086/192232>. [arXiv:astro-ph/9406064](#)
- Bicknell GV, Mukherjee D, Wagner AY, Sutherland RS, Nesvadba NPH (2018) Relativistic jet feedback—II. Relationship to gigahertz peak spectrum and compact steep spectrum radio galaxies. *MNRAS* 475(3):3493–3501. <https://doi.org/10.1093/mnras/sty070>. [arXiv:1801.06518](#) [astro-ph.GA]
- Birzan L, Rafferty DA, McNamara BR, Wise MW, Nulsen PEJ (2004) A systematic study of radio-induced X-ray cavities in clusters, groups, and galaxies. *ApJ* 607:800–809. <https://doi.org/10.1086/383519>. [arXiv:astro-ph/0402348](#)
- Birzan L, McNamara BR, Nulsen PEJ, Carilli CL, Wise MW (2008) Radiative efficiency and content of extragalactic radio sources: toward a universal scaling relation between jet power and radio power. *ApJ* 686(2):859–880. <https://doi.org/10.1086/591416>. [arXiv:0806.1929](#) [astro-ph]
- Bisnovatyi-Kogan GS, Ruzmaikin AA (1974) The accretion of matter by a collapsing star in the presence of a magnetic field. *Ap & SS* 28(1):45–59. <https://doi.org/10.1007/BF00642237>
- Blandford RD, Payne DG (1982) Hydromagnetic flows from accretion disks and the production of radio jets. *MNRAS* 199:883–903. <https://doi.org/10.1093/mnras/199.4.883>
- Blandford RD, Znajek RL (1977) Electromagnetic extraction of energy from Kerr black holes. *MNRAS* 179:433–456
- Blandford R, Meier D, Readhead A (2019) Relativistic jets from active galactic nuclei. *ARA&A* 57:467–509. <https://doi.org/10.1146/annurev-astro-081817-051948>. [arXiv:1812.06025](#) [astro-ph.HE]
- Bonato M, Liuzzo E, Giannetti A et al (2018) ALMACAL IV: a catalogue of ALMA calibrator continuum observations. *MNRAS* 478(2):1512–1519. <https://doi.org/10.1093/mnras/sty1173>. [arXiv:1805.00024](#) [astro-ph.GA]
- Bonato M, Liuzzo E, Herranz D et al (2019) ALMA photometry of extragalactic radio sources. *MNRAS* 485(1):1188–1195. <https://doi.org/10.1093/mnras/stz465>. [arXiv:1901.08976](#) [astro-ph.GA]
- Bondi M, Zamorani G, Ciliegi P et al (2018) Linear radio size evolution of  $\mu$ Jy populations. *A&A* 618:L8. <https://doi.org/10.1051/0004-6361/201834243>. [arXiv:1810.04095](#) [astro-ph.GA]
- Bonzini M, Padovani P, Mainieri V et al (2013) The sub-mJy radio sky in the Extended Chandra Deep Field-South: source population. *MNRAS* 436:3759–3771. <https://doi.org/10.1093/mnras/stt1879>. [arXiv:1310.1248](#)
- Bower RG, Benson AJ, Crain RA (2012) What shapes the galaxy mass function? Exploring the roles of supernova-driven winds and active galactic nuclei. *MNRAS* 422(4):2816–2840. <https://doi.org/10.1111/j.1365-2966.2012.20516.x>. [arXiv:1112.2712](#) [astro-ph.CO]
- Bowman M, Leahy JP, Komissarov SS (1996) The deceleration of relativistic jets by entrainment. *MNRAS* 279:899. <https://doi.org/10.1093/mnras/279.3.899>
- Brandenburg A, Nordlund A, Stein RF, Torkelsson U (1995) Dynamo-generated turbulence and large-scale magnetic fields in a Keplerian shear flow. *ApJ* 446:741. <https://doi.org/10.1086/175831>
- Bridle AH (1984) Sidedness, field configuration, and collimation of extragalactic radio jets. *AJ* 89:979–986. <https://doi.org/10.1086/113593>
- Burns JO, Feigelson ED, Schreier EJ (1983) The inner radio structure of Centaurus A: clues to the origin of the jet X-ray emission. *ApJ* 273:128–153
- Bustamante S, Springel V (2019) Spin evolution and feedback of supermassive black holes in cosmological simulations. *MNRAS* 490(3):4133–4153. <https://doi.org/10.1093/mnras/stz2836>. [arXiv:1902.04651](#) [astro-ph.GA]
- Buttiglione S, Capetti A, Celotti A et al (2010) An optical spectroscopic survey of the 3CR sample of radio galaxies with  $z < 0.3$ . II. Spectroscopic classes and accretion modes in radio-loud AGN. *A&A* 509:A6. <https://doi.org/10.1051/0004-6361/200913290>. [arXiv:0911.0536](#)
- Callingham JR, Ekers RD, Gaensler BM et al (2017) Extragalactic peaked-spectrum radio sources at low frequencies. *ApJ* 836(2):174. <https://doi.org/10.3847/1538-4357/836/2/174>. [arXiv:1701.02771](#) [astro-ph.GA]

- Capetti A, Brienza M (2023) The LOFAR view of massive early-type galaxies: transition from radio AGN to host emission. *A&A* 676:A102. <https://ui.adsabs.harvard.edu/abs/2023A%26A...676A.102C/abstract>. <https://doi.org/10.1051/0004-6361/202346529>
- Capetti A, Raiteri CM (2015) Looking for the least luminous BL Lacertae objects. *A&A* 580:A73. <https://doi.org/10.1051/0004-6361/201525890>. arXiv:1506.08043
- Capetti A, Verdoes Kleijn GA, Chiaberge M (2005) The HST view of the nuclear emission line region in low luminosity radio-galaxies. *A&A* 439:935–946. <https://doi.org/10.1051/0004-6361:20041609>
- Capetti A, Kharb P, Axon DJ, Merritt D, Baldi RD (2009) A very large array radio survey of early-type galaxies in the Virgo cluster. *AJ* 138:1990–1997. <https://doi.org/10.1088/0004-6256/138/6/1990>. arXiv:0910.4102
- Capetti A, Massaro F, Baldi RD (2017a) FRICAT: a FIRST catalog of FR I radio galaxies. *A&A* 598:A49. <https://doi.org/10.1051/0004-6361/201629287>. arXiv:1610.09376 [astro-ph.HE]
- Capetti A, Massaro F, Baldi RD (2017b) FRIICAT: a FIRST catalog of FR II radio galaxies. *A&A* 601:A81. <https://doi.org/10.1051/0004-6361/201630247>. arXiv:1703.03427 [astro-ph.HE]
- Capetti A, Baldi RD, Brienza M, Morganti R, Giovannini G (2019) The low-frequency properties of FR 0 radio galaxies. *A&A* 631:A176. <https://doi.org/10.1051/0004-6361/201936254>. arXiv:1910.06618 [astro-ph.GA]
- Capetti A, Brienza M, Baldi RD et al (2020a) The LOFAR view of FR 0 radio galaxies. *A&A* 642:A107. <https://doi.org/10.1051/0004-6361/202038671>. arXiv:2008.08099 [astro-ph.GA]
- Capetti A, Massaro F, Baldi RD (2020b) Large-scale environment of FR 0 radio galaxies. *A&A* 633:A161. <https://doi.org/10.1051/0004-6361/201935962>. arXiv:2009.03330 [astro-ph.GA]
- Capetti A, Brienza M, Balmaverde B et al (2022) The LOFAR view of giant, early-type galaxies: radio emission from active nuclei and star formation. *A&A* 660:A93. <https://doi.org/10.1051/0004-6361/202142911>. arXiv:2202.08593 [astro-ph.GA]
- Capetti A, Balmaverde B, Baldi RD et al (2023) The MURALES survey. VII. Optical spectral properties of the nuclei of 3C radio sources at  $0.3 < z < 0.82$ . *A&A* 671:A32. <https://doi.org/10.1051/0004-6361/202244606>. arXiv:2210.05407 [astro-ph.GA]
- Carvalho JC (1994) The age of GHz-peaked-spectrum radio sources. *A&A* 292:392–394
- Carvalho JC (1998) The evolution of GHz-peaked-spectrum radio sources. *A&A* 329:845–852
- Cattaneo A, Best PN (2009) On the jet contribution to the active galactic nuclei cosmic energy budget. *MNRAS* 395:518–523. <https://doi.org/10.1111/j.1365-2966.2009.14557.x>. arXiv:0812.1562
- Cavagnolo KW, McNamara BR, Nulsen PEJ et al (2010) A relationship between AGN jet power and radio power. *ApJ* 720(2):1066–1072. <https://doi.org/10.1088/0004-637X/720/2/1066>. arXiv:1006.5699 [astro-ph.CO]
- Chai B, Cao X, Gu M (2012) What governs the bulk velocity of the jet components in active galactic nuclei? *ApJ* 759:114. <https://doi.org/10.1088/0004-637X/759/2/114>. arXiv:1209.4702 [astro-ph.CO]
- Chamani W, Savolainen T, Hada K, Xu MH (2021) Testing the magnetic flux paradigm for AGN radio loudness with a radio-intermediate quasar. *A&A* 652:A14. <https://doi.org/10.1051/0004-6361/202140676>. arXiv:2106.01089 [astro-ph.HE]
- Chen Y, Gu Q, Fan J et al (2021) The powers of relativistic jets depend on the spin of accreting supermassive black holes. *ApJ* 913(2):93. <https://doi.org/10.3847/1538-4357/abf4ff>. arXiv:2104.04242 [astro-ph.HE]
- Chen BY, Bower GC, Dexter J et al (2023) Testing the linear relationship between black hole mass and variability timescale in low-luminosity AGNs at submillimeter wavelengths. *ApJ* 951(2):93. <https://doi.org/10.3847/1538-4357/acd250>. arXiv:2305.06529 [astro-ph.HE]
- Cheng XP, An T (2018) Parsec-scale radio structure of 14 Fanaroff–Riley type 0 radio galaxies. *ApJ* 863(2):155. <https://doi.org/10.3847/1538-4357/aad22c>. arXiv:1807.02505 [astro-ph.HE]
- Cheng X, An T, Sohn BW, Hong X, Wang A (2021) Parsec-scale properties of eight Fanaroff–Riley type 0 radio galaxies. *MNRAS* 506(2):1609–1622. <https://doi.org/10.1093/mnras/stab1388>. arXiv:2105.05396 [astro-ph.HE]
- Chhetri R, Ekers RD, Mahony EK et al (2012) Spectral properties and the effect on redshift cut-off of compact active galactic nuclei from the AT20G survey. *MNRAS* 422(3):2274–2281. <https://doi.org/10.1111/j.1365-2966.2012.20775.x>. arXiv:1202.5406 [astro-ph.CO]
- Chhetri R, Ekers RD, Jones PA, Ricci R (2013) The AT20G high-angular-resolution catalogue. *MNRAS* 434(2):956–965. <https://doi.org/10.1093/mnras/stt975>. arXiv:1306.0990 [astro-ph.CO]
- Chhetri R, Kimball A, Ekers RD et al (2020) WISE mid-infrared properties of compact active galactic nuclei selected from the high radio frequency AT20G survey. *MNRAS* 494(1):923–940. <https://doi.org/10.1093/mnras/staa513>. arXiv:2002.07429 [astro-ph.GA]

- Chiaberge M, Marconi A (2011) On the origin of radio loudness in active galactic nuclei and its relationship with the properties of the central supermassive black hole. *MNRAS* 416:917–926. <https://doi.org/10.1111/j.1365-2966.2011.19079.x>. arXiv:1105.4889 [astro-ph.CO]
- Chiaberge M, Capetti A, Celotti A (1999) The HST view of FR I radio galaxies: evidence for non-thermal nuclear sources. *A&A* 349:77–87
- Chiaberge M, Capetti A, Celotti A (2002) Understanding the nature of FR II optical nuclei: a new diagnostic plane for radio galaxies. *A&A* 394:791–800
- Chiaberge M, Capetti A, Macchetto FD (2005) The Hubble Space Telescope view of LINER nuclei: evidence for a dual population? *ApJ* 625:716–726. <https://doi.org/10.1086/429612>
- Ching JHY, Croom SM, Sadler EM et al (2017) Galaxy And Mass Assembly (GAMA): the environments of high- and low-excitation radio galaxies. *MNRAS* 469(4):4584–4599. <https://doi.org/10.1093/mnras/stx1173>. arXiv:1705.04502 [astro-ph.GA]
- Cohen MH, Moffet AT, Shaffer D et al (1969) Compact radio source in the nucleus of M87. *ApJ* 158:L83. <https://doi.org/10.1086/180437>
- Condon JJ (1989) The 1.4 GHz luminosity function and its evolution. *ApJ* 338:13. <https://doi.org/10.1086/167176>
- Condon JJ (1992) Radio emission from normal galaxies. *ARA&A* 30:575–611. <https://doi.org/10.1146/annurev.aa.30.090192.003043>
- Condon JJ, Dressel LL (1978) Compact radio sources in and near bright galaxies. *ApJ* 221:456–467. <https://doi.org/10.1086/156047>
- Condon JJ, Ransom SM (2016) Essential radio astronomy. Princeton University Press, Princeton
- Condon JJ, Cotton WD, Greisen EW et al (1998) The NRAO VLA Sky Survey. *AJ* 115:1693–1716. <https://doi.org/10.1086/300337>
- Conselice CJ (2014) The evolution of galaxy structure over cosmic time. *ARA&A* 52:291–337. <https://doi.org/10.1146/annurev-astro-081913-040037>. arXiv:1403.2783 [astro-ph.GA]
- Conway JE (2002) Compact symmetric objects—newborn radio galaxies? *New Astron Rev* 46(2–7):263–271. [https://doi.org/10.1016/S1387-6473\(01\)00191-9](https://doi.org/10.1016/S1387-6473(01)00191-9)
- Croston JH, Kraft RP, Hardcastle MJ (2007) Shock heating in the nearby radio galaxy NGC 3801. *ApJ* 660(1):191–199. <https://doi.org/10.1086/513500>. arXiv:astro-ph/0702094
- Croston JH, Ineson J, Hardcastle MJ (2018) Particle content, radio-galaxy morphology, and jet power: all radio-loud AGN are not equal. *MNRAS* 476(2):1614–1623. <https://doi.org/10.1093/mnras/sty274>. arXiv:1801.10172 [astro-ph.GA]
- Croton DJ, Springel V, White SDM et al (2006) The many lives of active galactic nuclei: cooling flows, black holes and the luminosities and colours of galaxies. *MNRAS* 365:11–28. <https://doi.org/10.1111/j.1365-2966.2005.09675.x>. arXiv:astro-ph/0508046
- Czerny B, Siemiginowska A, Janiuk A, Nikiel-Wroczyński B, Stawarz Ł (2009) Accretion disk model of short-timescale intermittent activity in young radio sources. *ApJ* 698(1):840–851. <https://doi.org/10.1088/0004-637X/698/1/840>. arXiv:0903.3940 [astro-ph.CO]
- Dabhade P, Gopal-Krishna (2023) The spectral index-flux density relation for extragalactic radio sources selected at metre and decametre wavelengths. *A&A* 675:L3. <https://doi.org/10.1051/0004-6361/202346593>. arXiv:2306.11205 [astro-ph.GA]
- Dai X, Bregman JN, Kochanek CS, Rasia E (2010) On the baryon fractions in clusters and groups of galaxies. *ApJ* 719(1):119–125. <https://doi.org/10.1088/0004-637X/719/1/119>. arXiv:0911.2230 [astro-ph.CO]
- Dallacasa D, Stanghellini C, Centonza M, Fanti R (2000) High frequency peakers. I. The bright sample. *A&A* 363:887–900. arXiv:astro-ph/0012428
- Daly RA, Sprinkle TB, O’Dea CP, Kharb P, Baum SA (2012) The relationship between beam power and radio power for classical double radio sources. *MNRAS* 423(3):2498–2502. <https://doi.org/10.1111/j.1365-2966.2012.21060.x>. arXiv:1204.1307 [astro-ph.CO]
- D’Ammando F, Giroletti M, Rainó S (2018) Exploring the bulk of the BL Lacertae object population. II. Gamma-ray properties. *A&A* 618:A175. <https://doi.org/10.1051/0004-6361/201833540>. arXiv:1809.01173 [astro-ph.HE]
- Davé R, Thompson R, Hopkins PF (2016) MUFASA: galaxy formation simulations with meshless hydrodynamics. *MNRAS* 462(3):3265–3284. <https://doi.org/10.1093/mnras/stw1862>. arXiv:1604.01418 [astro-ph.GA]
- Davé R, Anglés-Alcázar D, Narayanan D et al (2019) SIMBA: cosmological simulations with black hole growth and feedback. *MNRAS* 486(2):2827–2849. <https://doi.org/10.1093/mnras/stz937>. arXiv:1901.10203 [astro-ph.GA]

- Davis F, Kaviraj S, Hardcastle MJ et al (2022) Radio AGN in nearby dwarf galaxies: the important role of AGN in dwarf galaxy evolution. *MNRAS* 511(3):4109–4122. <https://doi.org/10.1093/mnras/stac068>. [arXiv:2201.09903](https://arxiv.org/abs/2201.09903) [astro-ph.GA]
- de Menezes R, Nemmen R, Finke JD, Almeida I, Rani B (2020) Gamma-ray observations of low-luminosity active galactic nuclei. *MNRAS* 492(3):4120–4130. <https://doi.org/10.1093/mnras/staa083>. [arXiv:2001.03184](https://arxiv.org/abs/2001.03184) [astro-ph.HE]
- De Young DS (2006) The particle content of extragalactic jets. *ApJ* 648(1):200–208. <https://doi.org/10.1086/505861>. [arXiv:astro-ph/0605734](https://arxiv.org/abs/astro-ph/0605734)
- Delvecchio I, Smolčić V, Zamorani G et al (2017) The VLA-COSMOS 3 GHz large project: AGN and host-galaxy properties out to  $z \lesssim 6$ . *A&A* 602:A3. <https://doi.org/10.1051/0004-6361/201629367>. [arXiv:1703.09720](https://arxiv.org/abs/1703.09720) [astro-ph.GA]
- Dicken D, Tadhunter C, Morganti R et al (2014) Spitzer mid-IR spectroscopy of powerful 2Jy and 3CRR radio galaxies. II. AGN power indicators and unification. *ApJ* 788:98. <https://doi.org/10.1088/0004-637X/788/2/98>. [arXiv:1405.0670](https://arxiv.org/abs/1405.0670)
- Doi A, Nakanishi K, Nagai H, Kohno K, Kamen S (2011) Millimeter radio continuum emissions as the activity of supermassive black holes in nearby early-type galaxies and low-luminosity active galactic nuclei. *AJ* 142(5):167. <https://doi.org/10.1088/0004-6256/142/5/167>. [arXiv:1106.5627](https://arxiv.org/abs/1106.5627) [astro-ph.CO]
- Donato D, Sambruna RM, Gliozzi M (2004) Obscuration and origin of nuclear X-ray emission in FR I radio galaxies. *ApJ* 617(2):915–929. <https://doi.org/10.1086/425575>. [arXiv:astro-ph/0408451](https://arxiv.org/abs/astro-ph/0408451)
- Dubois Y, Pichon C, Welker C et al (2014a) Dancing in the dark: galactic properties trace spin swings along the cosmic web. *MNRAS* 444(2):1453–1468. <https://doi.org/10.1093/mnras/stu1227>. [arXiv:1402.1165](https://arxiv.org/abs/1402.1165) [astro-ph.CO]
- Dubois Y, Volonteri M, Silk J (2014b) Black hole evolution—III. Statistical properties of mass growth and spin evolution using large-scale hydrodynamical cosmological simulations. *MNRAS* 440(2):1590–1606. <https://doi.org/10.1093/mnras/stu373>. [arXiv:1304.4583](https://arxiv.org/abs/1304.4583) [astro-ph.CO]
- Dullo BT, Knapen JH, Williams DRA et al (2018) The nuclear activity and central structure of the elliptical galaxy NGC 5322. *MNRAS*. <https://doi.org/10.1093/mnras/sty069>. [arXiv:1801.03660](https://arxiv.org/abs/1801.03660)
- Ekers RD, Ekers JA (1973) A survey of elliptical galaxies at 6 CM. *A&A* 24:247
- Elitzur M, Shlosman I (2006) The AGN-obscuring torus: the end of the “Doughnut” paradigm? *ApJ* 648(2):L101–L104. <https://doi.org/10.1086/508158>. [arXiv:astro-ph/0605686](https://arxiv.org/abs/astro-ph/0605686)
- Elvis M, Wilkes BJ, McDowell JC et al (1994) Atlas of quasar energy distributions. *ApJS* 95:1–68
- Evans DA, Worrall DM, Hardcastle MJ, Kraft RP, Birkinshaw M (2006) Chandra and XMM-Newton observations of a sample of low-redshift FR I and FR II radio galaxy nuclei. *ApJ* 642:96–112. <https://doi.org/10.1086/500658>. [arXiv:astro-ph/0512600](https://arxiv.org/abs/astro-ph/0512600)
- Event Horizon Telescope Collaboration, Akiyama K, Algaba JC et al (2021) First M87 Event Horizon Telescope results. VIII. Magnetic field structure near the event horizon. *ApJ* 910(1):L13. <https://doi.org/10.3847/2041-8213/abe4de>. [arXiv:2105.01173](https://arxiv.org/abs/2105.01173) [astro-ph.HE]
- Fabbiano G, Kim DW, Trinchieri G (1992) An X-ray catalog and atlas of galaxies. *ApJS* 80:531–644. <https://doi.org/10.1086/191675>
- Faber SM, Tremaine S, Ajhar EA et al (1997) The centers of early-type galaxies with HST. IV. Central parameter relations. *AJ* 114:1771
- Fabian AC (2012) Observational evidence of active galactic nuclei feedback. *ARA&A* 50:455–489. <https://doi.org/10.1146/annurev-astro-081811-125521>. [arXiv:1204.4114](https://arxiv.org/abs/1204.4114) [astro-ph.CO]
- Fabian AC, Sanders JS, Allen SW et al (2003) A deep Chandra observation of the Perseus cluster: shocks and ripples. *MNRAS* 344:L43–L47. <https://doi.org/10.1046/j.1365-8711.2003.06902.x>. [arXiv:astro-ph/0306036](https://arxiv.org/abs/astro-ph/0306036)
- Falcke H, Nagar NM, Wilson AS, Ulvestad JS (2000) Radio sources in low-luminosity active galactic nuclei. II. Very long baseline interferometry detections of compact radio cores and jets in a sample of LINERs. *ApJ* 542:197–200
- Falcke H, Körding E, Nagar NM (2004) Compact radio cores: from the first black holes to the last. *New Astron Rev* 48(11–12):1157–1171. <https://doi.org/10.1016/j.newar.2004.09.029>. [arXiv:astro-ph/0409125](https://arxiv.org/abs/astro-ph/0409125)
- Fanaroff BL, Riley JM (1974) The morphology of extragalactic radio sources of high and low luminosity. *MNRAS* 167:31P–36P. <https://doi.org/10.1093/mnras/167.1.31P>
- Fanidakis N, Baugh CM, Benson AJ et al (2011) Grand unification of AGN activity in the  $\Lambda$ CDM cosmology. *MNRAS* 410(1):53–74. <https://doi.org/10.1111/j.1365-2966.2010.17427.x>. [arXiv:0911.1128](https://arxiv.org/abs/0911.1128) [astro-ph.CO]
- Fanti R, Gioia I, Lari C, Ulrich MH (1978) A new complete sample of radio galaxies. *A&AS* 34:341–362

- Fanti C, Fanti R, Parma P, Schilizzi RT, van Breugel WJM (1985) Compact steep spectrum 3 CR radio sources. VLBI observations at 18 cm. *A&A* 143:292–306
- Fanti C, Fanti R, de Ruiter HR, Parma P (1986) VLA observations of low luminosity radio galaxies. III. The A-array observations. *A&AS* 65:145–188
- Fanti C, Fanti R, de Ruiter HR, Parma P (1987) VLA observations of low luminosity radio galaxies. IV. The B2 sample revisited. *A&AS* 69:57–76
- Fanti R, Fanti C, Schilizzi RT et al (1990) On the nature of compact steep spectrum radio sources. *A&A* 231:333–346
- Fanti C, Fanti R, Dallacasa D et al (1995) Are compact steep-spectrum sources young? *A&A* 302:317
- Fanti C, Pozzi F, Dallacasa D et al (2001) Multi-frequency VLA observations of a new sample of CSS/GPS radio sources. *A&A* 369:380–420. <https://doi.org/10.1051/0004-6361:20010051>
- Fernández-Ontiveros JA, López-López X, Prieto A (2023) Compact jets dominate the continuum emission in low-luminosity active galactic nuclei. *A&A* 670:A22. <https://doi.org/10.1051/0004-6361/202243547>. [arXiv:2211.09828](https://arxiv.org/abs/2211.09828) [astro-ph.HE]
- Filho ME, Barthel PD, Ho LC (2000) The nature of composite LINER/H II galaxies as revealed from high-resolution VLA observations. *ApJS* 129:93–110. <https://doi.org/10.1086/313412>. [arXiv:astro-ph/0002404](https://arxiv.org/abs/astro-ph/0002404)
- Filho ME, Barthel PD, Ho LC (2002a) Light-year scale radio cores in four LINER galaxies. *A&A* 385:425–430. <https://doi.org/10.1051/0004-6361:20020138>. [arXiv:astro-ph/0201505](https://arxiv.org/abs/astro-ph/0201505)
- Filho ME, Barthel PD, Ho LC (2002b) The radio properties of composite LINER/H II galaxies. *ApJS* 142(2):223–238. <https://doi.org/10.1086/341786>. [arXiv:astro-ph/0205196](https://arxiv.org/abs/astro-ph/0205196)
- Filho ME, Fraternali F, Markoff S et al (2004) Further clues to the nature of composite LINER/H II galaxies. *A&A* 418:429–443
- Floyd DJE, Axon D, Baum S et al (2010) Hubble Space Telescope near-infrared snapshot survey of 3CR radio source counterparts. III. Radio galaxies and quasars in context. *ApJ* 713(1):66–81. <https://doi.org/10.1088/0004-637X/713/1/66>. [arXiv:1003.2467](https://arxiv.org/abs/1003.2467) [astro-ph.CO]
- Fu WJ, Zhang HM, Zhang J et al (2022) Is TOL 1326–379 a prototype of  $\gamma$ -ray emitting FR0 radio galaxy? *RAA* 22(3):035005. <https://doi.org/10.1088/1674-4527/ac4410>
- Gallimore JF, Axon DJ, O’Dea CP, Baum SA, Pedlar A (2006) A survey of kiloparsec-scale radio outflows in radio-quiet active galactic nuclei. *AJ* 132:546–569. <https://doi.org/10.1086/504593>. [arXiv:astro-ph/0604219](https://arxiv.org/abs/astro-ph/0604219)
- Gallo E, Sesana A (2019) Exploring the local black hole mass function below  $10^6$  solar masses. *ApJ* 883(1):L18. <https://doi.org/10.3847/2041-8213/ab40c6>. [arXiv:1909.02585](https://arxiv.org/abs/1909.02585) [astro-ph.HE]
- Garofalo D (2009) The spin dependence of the Blandford–Znajek effect. *ApJ* 699(1):400–408. <https://doi.org/10.1088/0004-637X/699/1/400>. [arXiv:0904.3486](https://arxiv.org/abs/0904.3486) [astro-ph.HE]
- Garofalo D, Singh CB (2019) FR0 radio galaxies and their place in the radio morphology classification. *ApJ* 871(2):259. <https://doi.org/10.3847/1538-4357/aaf056>. [arXiv:1811.05383](https://arxiv.org/abs/1811.05383) [astro-ph.HE]
- Garofalo D, Evans DA, Sambruna RM (2010) The evolution of radio-loud active galactic nuclei as a function of black hole spin. *MNRAS* 406:975–986. <https://doi.org/10.1111/j.1365-2966.2010.16797.x>. [arXiv:1004.1166](https://arxiv.org/abs/1004.1166)
- Gendre MA, Best PN, Wall JV, Ker LM (2013) The relation between morphology, accretion modes and environmental factors in local radio AGN. *MNRAS* 430:3086–3101. <https://doi.org/10.1093/mnras/stt116>. [arXiv:1301.1526](https://arxiv.org/abs/1301.1526)
- Ghisellini G (2011) Extragalactic relativistic jets. In: Aharonian FA, Hofmann W, Rieger FM (eds) American Institute of Physics conference series, vol 1381. pp 180–198. <https://doi.org/10.1063/1.3635832>. [arXiv:1104.0006](https://arxiv.org/abs/1104.0006)
- Ghisellini G, Haardt F, Matt G (2004) Aborted jets and the X-ray emission of radio-quiet AGNs. *A&A* 413:535–545. <https://doi.org/10.1051/0004-6361:20031562>. [arXiv:astro-ph/0310106](https://arxiv.org/abs/astro-ph/0310106)
- Ghisellini G, Tavecchio F, Chiaferge M (2005) Structured jets in TeV BL Lac objects and radiogalaxies. Implications for the observed properties. *A&A* 432(2):401–410. <https://doi.org/10.1051/0004-6361:20041404>. [arXiv:astro-ph/0406093](https://arxiv.org/abs/astro-ph/0406093)
- Giovannini G, Feretti L, Comoretto G (1990) VLBI observations of a complete sample of radio galaxies. I. Snapshot data. *ApJ* 358:159. <https://doi.org/10.1086/168970>
- Giovannini G, Cotton WD, Feretti L, Lara L, Venturi T (2001) VLBI observations of a complete sample of radio galaxies: 10 years later. *ApJ* 552:508–526. <https://doi.org/10.1086/320581>. [arXiv:astro-ph/0101096](https://arxiv.org/abs/astro-ph/0101096)

- Giovannini G, Taylor GB, Feretti L et al (2005) The Bologna complete sample of nearby radio sources. *ApJ* 618:635–648. <https://doi.org/10.1086/426106>. [arXiv:astro-ph/0409624](#)
- Giovannini G, Savolainen T, Orienti M et al (2018) A wide and collimated radio jet in 3C84 on the scale of a few hundred gravitational radii. *Nat Astron* 2:472–477. <https://doi.org/10.1038/s41550-018-0431-2>. [arXiv:1804.02198](#) [astro-ph.GA]
- Giovannini G, Baldi RD, Capetti A, Giroletti M, Lico R (2023) Jets in FR0 radio galaxies. *A&A* 672: A104. <https://doi.org/10.1051/0004-6361/202245395>. [arXiv:2302.12657](#) [astro-ph.GA]
- Giroletti M, Giovannini G, Taylor GB (2005) Low power compact radio galaxies at high angular resolution. *A&A* 441(1):89–101. <https://doi.org/10.1051/0004-6361:20053347>. [arXiv:astro-ph/0506497](#)
- Glowacki M, Allison JR, Sadler EM et al (2017) H I absorption in nearby compact radio galaxies. *MNRAS* 467(3):2766–2786. <https://doi.org/10.1093/mnras/stx214>. [arXiv:1701.07036](#) [astro-ph.GA]
- González-Martín O, Masegosa J, Márquez I et al (2015) Nuclear obscuration in LINERs. Clues from Spitzer/IRS spectra on the Compton thickness and the existence of the dusty torus. *A&A* 578:A74. <https://doi.org/10.1051/0004-6361/201425254>
- Goold K, Seth A, Molina M et al (2023) ReveaLLAGN 0: first look at JWST MIRI data of Sombrero and NGC 1052. Submitted to *ApJ*. [arXiv e-prints. arXiv:2307.01252](#) [astro-ph.GA]
- Gopal-Krishna Mangalam A, Wiita PJ (2008) Stellar disruption by supermassive black holes and the quasar radio loudness dichotomy. *ApJ* 680(1):L13. <https://doi.org/10.1086/589739>. [arXiv:0806.1464](#) [astro-ph]
- Goulding AD, Greene JE, Ma CP et al (2016) The MASSIVE survey. IV. The X-ray halos of the most massive early-type galaxies in the nearby universe. *ApJ* 826(2):167. <https://doi.org/10.3847/0004-637X/826/2/167>. [arXiv:1604.01764](#) [astro-ph.GA]
- Grandi P, Capetti A, Baldi RD (2016) Discovery of a Fanaroff–Riley type 0 radio galaxy emitting at  $\gamma$ -ray energies. *MNRAS* 457(1):2–8. <https://doi.org/10.1093/mnras/stv2846>. [arXiv:1512.01242](#) [astro-ph.GA]
- Grandi P, Torresi E, Macconi D, Boccardi B, Capetti A (2021) Jet-accretion system in the nearby mJy radio galaxies. *ApJ* 911(1):17. <https://doi.org/10.3847/1538-4357/abe776>. [arXiv:2102.08922](#) [astro-ph.HE]
- Greene JE (2012) Low-mass black holes as the remnants of primordial black hole formation. *Nat Commun* 3:1304. <https://doi.org/10.1038/ncomms2314>. [arXiv:1211.7082](#) [astro-ph.CO]
- Gregory PC, Scott WK, Douglas K, Condon JJ (1996) The GB6 catalog of radio sources. *ApJS* 103:427. <https://doi.org/10.1086/192282>
- Grossová R, Werner N, Massaro F et al (2022) Very Large Array radio study of a sample of nearby X-ray and optically bright early-type galaxies. *ApJS* 258(2):30. <https://doi.org/10.3847/1538-4365/ac366c>. [arXiv:2111.02430](#) [astro-ph.HE]
- Gugliucci NE, Taylor GB, Peck AB, Giroletti M (2005) Dating COINS: kinematic ages for compact symmetric objects. *ApJ* 622(1):136–148. <https://doi.org/10.1086/427934>. [arXiv:astro-ph/0412199](#)
- Gupta Y, Ajithkumar B, Kale HS et al (2017) The upgraded GMRT: opening new windows on the radio Universe. *Curr Sci* 113(4):707–714. <https://doi.org/10.18520/cs/v113/i04/707-714>
- Gürkan G, Hardcastle MJ, Smith DJB et al (2018) LOFAR/H-ATLAS: the low-frequency radio luminosity–star formation rate relation. *MNRAS* 475(3):3010–3028. <https://doi.org/10.1093/mnras/sty016>. [arXiv:1801.02629](#) [astro-ph.GA]
- Hada K (2019) Relativistic jets from AGN viewed at highest angular resolution. *Galaxies* 8(1):1. <https://doi.org/10.3390/galaxies8010001>
- Hallinan G, Ravi V, Deep Synoptic Array Team (2021) The DSA-2000: a radio survey camera. In: American Astronomical Society Meeting abstracts, vol 53. p 316.05. <https://ui.adsabs.harvard.edu/abs/2021AAS...23731605H/abstract>
- Hancock PJ, Sadler EM, Mahony EK, Ricci R (2010) Observations and properties of candidate high-frequency GPS radio sources in the AT20G survey. *MNRAS* 408(2):1187–1206. <https://doi.org/10.1111/j.1365-2966.2010.17199.x>. [arXiv:1008.1401](#) [astro-ph.GA]
- Hardcastle MJ, Croston JH (2020) Radio galaxies and feedback from AGN jets. *New Astron Rev* 88:101539. <https://doi.org/10.1016/j.newar.2020.101539>. [arXiv:2003.06137](#) [astro-ph.HE]
- Hardcastle MJ, Krause MGH (2013) Numerical modelling of the lobes of radio galaxies in cluster environments. *MNRAS* 430(1):174–196. <https://doi.org/10.1093/mnras/sts564>. [arXiv:1301.2531](#) [astro-ph.CO]
- Hardcastle MJ, Worrall DM (2000) Radio, optical and X-ray nuclei in nearby 3CRR radio galaxies. *MNRAS* 314:359–363

- Hardcastle MJ, Birkinshaw M, Worrall DM (1998) Magnetic field strengths in the hotspots of 3C 33 and 111. *MNRAS* 294:615–621. <https://doi.org/10.1111/j.1365-8711.1998.01159.x>. [arXiv:astro-ph/9709228](#)
- Hardcastle MJ, Evans DA, Croston JH (2007) Hot and cold gas accretion and feedback in radio-loud active galaxies. *MNRAS* 376:1849–1856. <https://doi.org/10.1111/j.1365-2966.2007.11572.x>. [arXiv:astro-ph/0701857](#)
- Hardcastle MJ, Evans DA, Croston JH (2009) The active nuclei of  $z < 1.0$  3CRR radio sources. *MNRAS* 396:1929–1952. <https://doi.org/10.1111/j.1365-2966.2009.14887.x>. [arXiv:0904.1323](#)
- Hardcastle MJ, Williams WL, Best PN et al (2019) Radio-loud AGN in the first LoTSS data release. The lifetimes and environmental impact of jet-driven sources. *A&A* 622:A12. <https://doi.org/10.1051/0004-6361/201833893>. [arXiv:1811.07943](#) [astro-ph.GA]
- Harrison CM (2017) Impact of supermassive black hole growth on star formation. *Nat Astron* 1:0165. <https://doi.org/10.1038/s41550-017-0165>. [arXiv:1703.06889](#) [astro-ph.GA]
- Harvey M, Rulten CB, Chadwick PM (2020) A search for  $\gamma$ -ray emission from a sample of local Universe low-frequency selected radio galaxies. *MNRAS* 496(1):903–912. <https://doi.org/10.1093/mnras/staa1593>. [arXiv:2006.02831](#) [astro-ph.HE]
- Hawley JF, Krolik JH (2006) Magnetically driven jets in the Kerr metric. *ApJ* 641(1):103–116. <https://doi.org/10.1086/500385>. [arXiv:astro-ph/0512227](#)
- Heckman TM (1980) An optical and radio survey of the nuclei of bright galaxies. Activity in normal galactic nuclei. *A&A* 500:187–199
- Heckman TM, Best PN (2014) The coevolution of galaxies and supermassive black holes: insights from surveys of the contemporary universe. *ARA&A* 52:589–660. <https://doi.org/10.1146/annurev-astro-081913-035722>. [arXiv:1403.4620](#)
- Heckman TM, Kauffmann G, Brinchmann J et al (2004) Present-day growth of black holes and bulges: the Sloan Digital Sky Survey perspective. *ApJ* 613:109–118
- Heeschen DS (1970) Radio observations of E and SO galaxies. *AJ* 75:523–529. <https://doi.org/10.1086/110987>
- Hernán-Caballero A, Alonso-Herrero A, Pérez-González PG et al (2013) SHARDS: stellar populations and star formation histories of a mass-selected sample of  $0.65 < z < 1.1$  galaxies. *MNRAS* 434(3):2136–2152. <https://doi.org/10.1093/mnras/stt1165>. [arXiv:1306.5581](#) [astro-ph.CO]
- HESS Collaboration, Abdalla H, Adam R et al (2020) Resolving acceleration to very high energies along the jet of Centaurus A. *Nature* 582(7812):356–359. <https://doi.org/10.1038/s41586-020-2354-1>. [arXiv:2007.04823](#) [astro-ph.HE]
- Heywood I, Jarvis MJ, Hale CL et al (2022) MIGHTEE: total intensity radio continuum imaging and the COSMOS/XMM-LSS Early Science fields. *MNRAS* 509(2):2150–2168. <https://doi.org/10.1093/mnras/stab3021>. [arXiv:2110.00347](#) [astro-ph.GA]
- Hill GJ, Lilly SJ (1991) A change in the cluster environments of radio galaxies with cosmic epoch. *ApJ* 367:1. <https://doi.org/10.1086/169597>
- Hine RG, Longair MS (1979) Optical spectra of 3CR radio galaxies. *MNRAS* 188:111–130
- Ho LC (2002) On the relationship between radio emission and black hole mass in galactic nuclei. *ApJ* 564:120–132
- Ho LC (2008) Nuclear activity in nearby galaxies. *ARA&A* 46:475–539. <https://doi.org/10.1146/annurev.astro.45.051806.110546>. [arXiv:0803.2268](#)
- Ho LC, Filippenko AV, Sargent WL (1995) A search for “dwarf” Seyfert nuclei. 2: an optical spectral atlas of the nuclei of nearby galaxies. *ApJS* 98:477–593. <https://doi.org/10.1086/192170>
- Holt J, Tadhunter CN, Morganti R (2008) Fast outflows in compact radio sources: evidence for AGN-induced feedback in the early stages of radio source evolution. *MNRAS* 387(2):639–659. <https://doi.org/10.1111/j.1365-2966.2008.13089.x>. [arXiv:0802.1444](#) [astro-ph]
- Hota A, Sirothia SK, Ohya Y et al (2011) Discovery of a spiral-host episodic radio galaxy. *MNRAS* 417(1):L36–L40. <https://doi.org/10.1111/j.1745-3933.2011.01115.x>. [arXiv:1107.4742](#) [astro-ph.CO]
- Huško F, Lacey CG, Schaye J, Nobels FSJ, Schaller M (2023) Winds versus jets: a comparison between black hole feedback modes in simulations of idealized galaxy groups and clusters. Submitted to *MNRAS*. [arXiv e-prints. arXiv:2307.01409](#) [astro-ph.GA]
- IceCube Collaboration, Aartsen MG, Ackermann M et al (2018) Multimessenger observations of a flaring blazar coincident with high-energy neutrino IceCube-170922A. *Science* 361(6398):eaat1378. <https://doi.org/10.1126/science.aat1378>. [arXiv:1807.08816](#) [astro-ph.HE]

- IceCube Collaboration, Abbasi R, Ackermann M et al (2022) Evidence for neutrino emission from the nearby active galaxy NGC 1068. *Science* 378(6619):538–543. <https://doi.org/10.1126/science.abg3395>. [arXiv:2211.09972](https://arxiv.org/abs/2211.09972) [astro-ph.HE]
- Inayoshi K, Ichikawa K, Ho LC (2020) Universal transition diagram from dormant to actively accreting supermassive black holes. *ApJ* 894(2):141. <https://doi.org/10.3847/1538-4357/ab8569>. [arXiv:2001.11032](https://arxiv.org/abs/2001.11032) [astro-ph.GA]
- Ineson J, Croston JH, Hardcastle MJ et al (2013) Radio-loud active galactic nucleus: is there a link between luminosity and cluster environment? *ApJ* 770(2):136. <https://doi.org/10.1088/0004-637X/770/2/136>. [arXiv:1305.1050](https://arxiv.org/abs/1305.1050) [astro-ph.CO]
- Ineson J, Croston JH, Hardcastle MJ et al (2015) The link between accretion mode and environment in radio-loud active galaxies. *MNRAS* 453(3):2682–2706. <https://doi.org/10.1093/mnras/stv1807>. [arXiv:1508.01033](https://arxiv.org/abs/1508.01033) [astro-ph.GA]
- Ishwara-Chandra CH, Taylor AR, Green DA et al (2020) A wide-area GMRT 610-MHz survey of ELAIS N1 field. *MNRAS* 497(4):5383–5394. <https://doi.org/10.1093/mnras/staa2341>. [arXiv:2008.02530](https://arxiv.org/abs/2008.02530)
- Jackson N, Rawlings S (1997) [O III] 500.7 spectroscopy of 3C galaxies and quasars at redshift  $z > 1$ . *MNRAS* 286:241–256
- Jacobsen IB, Wu K, On AYL, Saxton CJ (2015) High-energy neutrino fluxes from AGN populations inferred from X-ray surveys. *MNRAS* 451(4):3649–3663. <https://doi.org/10.1093/mnras/stv1196>. [arXiv:1506.05916](https://arxiv.org/abs/1506.05916) [astro-ph.HE]
- Janssen M, Falcke H, Kadler M et al (2021) Event Horizon Telescope observations of the jet launching and collimation in Centaurus A. *Nat Astron* 5:1017–1028. <https://doi.org/10.1038/s41550-021-01417-w>. [arXiv:2111.03356](https://arxiv.org/abs/2111.03356) [astro-ph.GA]
- Jarvis M, Taylor R, Agudo I et al (2016) The MeerKAT International GHz Tiered Extragalactic Exploration (MIGHTEE) Survey. In: MeerKAT science: on the pathway to the SKA. p 6. <https://doi.org/10.22323/1.277.0006>. [arXiv:1709.01901](https://arxiv.org/abs/1709.01901) [astro-ph.GA]
- Jarvis ME, Harrison CM, Thomson AP et al (2019) Prevalence of radio jets associated with galactic outflows and feedback from quasars. *MNRAS* 485(2):2710–2730. <https://doi.org/10.1093/mnras/stz556>. [arXiv:1902.07727](https://arxiv.org/abs/1902.07727) [astro-ph.GA]
- Jarvis ME, Harrison CM, Mainieri V et al (2021) The quasar feedback survey: discovering hidden Radio-AGN and their connection to the host galaxy ionized gas. *MNRAS* 503(2):1780–1797. <https://doi.org/10.1093/mnras/stab549>. [arXiv:2103.00014](https://arxiv.org/abs/2103.00014) [astro-ph.GA]
- Jimenez-Gallardo A, Massaro F, Capetti A et al (2019) COMP2CAT: hunting compact double radio sources in the local Universe. *A&A* 627:A108. <https://doi.org/10.1051/0004-6361/201935104>. [arXiv:1905.02212](https://arxiv.org/abs/1905.02212) [astro-ph.HE]
- Jones DH, Read MA, Saunders W et al (2009) The 6dF Galaxy Survey: final redshift release (DR3) and southern large-scale structures. *MNRAS* 399(2):683–698. <https://doi.org/10.1111/j.1365-2966.2009.15338.x>. [arXiv:0903.5451](https://arxiv.org/abs/0903.5451) [astro-ph.CO]
- Kaiser CR, Best PN (2007) Luminosity function, sizes and FR dichotomy of radio-loud AGN. *MNRAS* 381(4):1548–1560. <https://doi.org/10.1111/j.1365-2966.2007.12350.x>. [arXiv:0708.3733](https://arxiv.org/abs/0708.3733) [astro-ph]
- Kaiser CR, Dennett-Thorpe J, Alexander P (1997) Evolutionary tracks of FR II sources through the P-D diagram. *MNRAS* 292(3):723–732. <https://doi.org/10.1093/mnras/292.3.723>. [arXiv:astro-ph/9710104](https://arxiv.org/abs/astro-ph/9710104)
- Kapinska AD, Hardcastle M, Jackson C et al (2015) Unravelling lifecycles and physics of radio-loud AGN in the SKA Era. In: Advancing astrophysics with the Square Kilometre Array (AASKA14). p 173. <https://doi.org/10.22323/1.215.0173>. [arXiv:1412.5884](https://arxiv.org/abs/1412.5884) [astro-ph.GA]
- Kaviraj S, Shabala SS, Deller AT, Middelberg E (2015) Radio AGN in spiral galaxies. *MNRAS* 454(2):1595–1604. <https://doi.org/10.1093/mnras/stv1957>. [arXiv:1412.5602](https://arxiv.org/abs/1412.5602) [astro-ph.GA]
- Kawamuro T, Ricci C, Imanishi M et al (2022) BASS XXXII: studying the nuclear millimeter-wave continuum emission of AGNs with ALMA at scales  $\lesssim 100$ –200 pc. *ApJ* 938(1):87. <https://doi.org/10.3847/1538-4357/ac8794>. [arXiv:2208.03880](https://arxiv.org/abs/2208.03880) [astro-ph.GA]
- Kellermann KI (1980) Radio galaxies and quasars. In: Ninth Texas symposium on relativistic astrophysics, vol 336, pp 1–11. <https://doi.org/10.1111/j.1749-6632.1980.tb15914.x>
- Kellermann KI, Pauliny-Toth IIK (1981) Compact radio sources. *ARA&A* 19:373–410. <https://doi.org/10.1146/annurev.aa.19.090181.002105>
- Kellermann KI, Sramek R, Schmidt M, Shaffer DB, Green R (1989) VLA observations of objects in the Palomar Bright Quasar Survey. *AJ* 98:1195. <https://doi.org/10.1086/115207>

- Kewley LJ, Groves B, Kauffmann G, Heckman T (2006) The host galaxies and classification of active galactic nuclei. *MNRAS* 372:961–976. <https://doi.org/10.1111/j.1365-2966.2006.10859.x>. arXiv:astro-ph/0605681
- Kharb P, Silpa S (2023) Looking for signatures of AGN feedback in radio-quiet AGN. *Galaxies*. <https://doi.org/10.3390/galaxies11010027>
- Kharb P, Capetti A, Axon DJ et al (2012) Examining the radio-loud/radio-quiet dichotomy with new Chandra and VLA observations of 13 UGC galaxies. *AJ* 143:78. <https://doi.org/10.1088/0004-6256/143/4/78>. arXiv:1201.4175
- Kiehlmann S, Readhead ACS, O'Neill S et al (2023) Compact symmetric objects: a distinct population of jetted active galaxies. arXiv e-prints. <https://doi.org/10.48550/arXiv.2303.11359>. arXiv:2303.11359 [astro-ph.HE]
- Kim M, Ho LC, Peng CY, Barth AJ, Im M (2017) Stellar photometric structures of the host galaxies of nearby type 1 active galactic nuclei. *ApJS* 232(2):21. <https://doi.org/10.3847/1538-4365/aa8a75>. arXiv:1710.02194 [astro-ph.GA]
- Komissarov SS (1990) Emission by relativistic jets with boundary layers. *Sov Astron Lett* 16:284
- Komissarov SS (2001) Direct numerical simulations of the Blandford–Znajek effect. *MNRAS* 326(3):L41–L44. <https://doi.org/10.1046/j.1365-8711.2001.04863.x>
- Kormendy J, Ho LC (2013) Coevolution (or not) of supermassive black holes and host galaxies. *ARA&A* 51:511–653. <https://doi.org/10.1146/annurev-astro-082708-101811>. arXiv:1304.7762
- Kotilainen JK, León-Tavares J, Olguín-Iglesias A et al (2016) Discovery of a pseudobulge galaxy launching powerful relativistic jets. *ApJ* 832(2):157. <https://doi.org/10.3847/0004-637X/832/2/157>. arXiv:1609.02417 [astro-ph.GA]
- Kozieł-Wierzbowska D, Stasińska G, Vale Asari N et al (2017a) Pair-matching of radio-loud and radio-quiet AGNs. *Front Astron Space Sci* 4:39. <https://doi.org/10.3389/fspas.2017.00039>. arXiv:1711.00085 [astro-ph.GA]
- Kozieł-Wierzbowska D, Vale Asari N, Stasińska G et al (2017b) What distinguishes the host galaxies of radio-loud and radio-quiet AGNs? *ApJ* 846(1):42. <https://doi.org/10.3847/1538-4357/aa8326>. arXiv:1709.09912 [astro-ph.GA]
- Kozieł-Wierzbowska D, Goyal A, Zywucka N (2020) Radio sources associated with optical galaxies and having unresolved or extended morphologies (ROGUE). I. A catalog of SDSS galaxies with FIRST core identifications. *ApJS* 247(2):53. <https://doi.org/10.3847/1538-4365/ab63d3>. arXiv:1912.09959 [astro-ph.GA]
- Kratzer RM, Richards GT (2015) Mean and extreme radio properties of quasars and the origin of radio emission. *AJ* 149(2):61. <https://doi.org/10.1088/0004-6256/149/2/61>. arXiv:1405.2344 [astro-ph.GA]
- Krause MGH (2023) Jet feedback in star-forming galaxies. *Galaxies*. <https://doi.org/10.3390/galaxies11010029>
- Kuncic Z, Bicknell GV (2004) Dynamics and energetics of turbulent, magnetized disk accretion around black holes: a first-principles approach to disk-corona-outflow coupling. *ApJ* 616(2):669–687. <https://doi.org/10.1086/425032>. arXiv:astro-ph/0402421
- Kuncic Z, Bicknell GV (2007) Towards a new standard model for black hole accretion. *Ap & SS* 311(1–3):127–135. <https://doi.org/10.1007/s10509-007-9522-8>. arXiv:0705.0791 [astro-ph]
- Kunert M, Marecki A, Spencer RE, Kus AJ, Niezgoda J (2002) FIRST-based survey of Compact Steep Spectrum sources. I. MERLIN images of arc-second scale objects. *A&A* 391:47–54. <https://doi.org/10.1051/0004-6361:20020532>. arXiv:astro-ph/0112511
- Kunert-Bajraszewska M (2016) Dichotomy in the population of young AGN: optical, radio, and X-ray properties. *Astron Nachr* 337(1–2):27. <https://doi.org/10.1002/asna.201512259>. arXiv:1510.09061 [astro-ph.GA]
- Kunert-Bajraszewska M, Marecki A, Thomasson P, Spencer RE (2005) FIRST-based survey of Compact Steep Spectrum sources. II. MERLIN and VLA observations of medium-sized symmetric objects. *A&A* 440:93–105. <https://doi.org/10.1051/0004-6361:20042496>. arXiv:astro-ph/0505435
- Kunert-Bajraszewska M, Marecki A, Thomasson P (2006) FIRST-based survey of compact steep spectrum sources. IV. Multifrequency VLBA observations of very compact objects. *A&A* 450:945–958. <https://doi.org/10.1051/0004-6361:20054428>. arXiv:astro-ph/0601288
- Kunert-Bajraszewska M, Gawroński MP, Labiano A, Siemiginowska A (2010) A survey of low-luminosity compact sources and its implication for the evolution of radio-loud active galactic nuclei-I. Radio data. *MNRAS* 408:2261–2278. <https://doi.org/10.1111/j.1365-2966.2010.17271.x>. arXiv:1009.5235 [astro-ph.CO]

- Kunert-Bajraszewska M, Labiano A, Gawronski MP (2011) Emission line-radio correlation for Low Luminosity Compact sources. Evolution schemes. In: Proceedings of 10th European VLBI network symposium and EVN users meeting: VLBI and the new generation of radio arrays—PoS(10th EVN symposium). PoS, vol 125, p 079. <https://doi.org/10.22323/1.125.0079>. arXiv:1106.5918 [astro-ph.CO]
- Lacy M, Baum SA, Chandler CJ et al (2020) The Karl G. Jansky Very Large Array Sky Survey (VLASS). Science case and survey design. PASP 132(1009):035001. <https://doi.org/10.1088/1538-3873/ab63eb>. arXiv:1907.01981 [astro-ph.IM]
- Laing RA, Bridle AH (2014) Systematic properties of decelerating relativistic jets in low-luminosity radio galaxies. MNRAS 437:3405–3441. <https://doi.org/10.1093/mnras/stt2138>. arXiv:1311.1015
- Laing RA, Jenkins CR, Wall JV, Unger SW (1994) Spectrophotometry of a complete sample of 3CR radio sources: implications for unified models. The First Stromlo Symposium. In: Bicknell GV, Dopita MA, Quinn PJ (eds) The physics of active galaxies. Astronomical Society of the Pacific conference series, vol 54, p 201
- Lal DV, Legodi P, Fanaroff B et al (2021) Viewing classical radio galaxies with the upgraded GMRT and MeerKAT—a progress report. Galaxies 9(4):87. <https://doi.org/10.3390/galaxies9040087>
- Laor A (2000) On black hole masses and radio loudness in active galactic nuclei. ApJ 543:L111–L114. <https://doi.org/10.1086/317280>. arXiv:astro-ph/0009192
- Ledlow MJ, Owen FN (1996) 20 CM VLA survey of Abell clusters of galaxies. VI. Radio/optical luminosity functions. AJ 112:9
- Leipke C, Antonucci R, Ogle P, Whyson D (2009) The Spitzer view of FR I radio galaxies: on the origin of the nuclear mid-infrared continuum. ApJ 701(2):891–914. <https://doi.org/10.1088/0004-637X/701/2/891>. arXiv:0906.2152 [astro-ph.CO]
- Lin YT, Shen Y, Strauss MA, Richards GT, Lunnan R (2010) On the populations of radio galaxies with extended morphology at  $z < 0.3$ . ApJ 723:1119–1138. <https://doi.org/10.1088/0004-637X/723/2/1119>. arXiv:1006.5452
- Liska MTP, Musoke G, Tchekhovskoy A, Porth O, Beloborodov AM (2022) Formation of magnetically truncated accretion disks in 3D radiation-transport two-temperature GRMHD simulations. ApJ 935 (1):L1. <https://doi.org/10.3847/2041-8213/ac84db>. arXiv:2201.03526 [astro-ph.HE]
- Liuzzo E, Giovannini G, Giroletti M, Taylor GB (2009) The Bologna complete sample of nearby radio sources. II. Phase referenced observations of faint nuclear sources. A&A 505(2):509–520. <https://doi.org/10.1051/0004-6361/200912586>. arXiv:0908.4391 [astro-ph.CO]
- Liuzzo E, Giroletti M, Giovannini G et al (2013) Exploring the bulk of the BL Lacertae object population. I. Parsec-scale radio structures. A&A 560:A23. <https://doi.org/10.1051/0004-6361/201322144>. arXiv:1309.2774 [astro-ph.HE]
- Lobanov A (2006) Compact radio jets and nuclear regions in active galaxies. In: Baan W, Bachiller R, Booth R et al (eds) Proceedings of the 8th European VLBI network symposium. September 26–29, 2006, Torun, p 3
- Lovelace RVE, Li H, Koldoba AV, Ustyugova GV, Romanova MM (2002) Poynting jets from accretion disks. ApJ 572(1):445–455. <https://doi.org/10.1086/340292>. arXiv:astro-ph/0210571
- Lundquist JP, Merten L, Vorobiov S et al (2022) Extrapolating FR-0 radio galaxy source properties from the propagation of multi-messenger ultra-high-energy cosmic rays. In: 37th International cosmic ray conference, p 989. <https://doi.org/10.22323/1.395.0989>
- Macconi D, Torresi E, Grandi P, Boccardi B, Vignali C (2020) Radio morphology-accretion mode link in Fanaroff–Riley type II low-excitation radio galaxies. MNRAS 493(3):4355–4366. <https://doi.org/10.1093/mnras/staa560>. arXiv:2002.09360 [astro-ph.HE]
- Macfarlane C, Best PN, Sabater J et al (2021) The radio loudness of SDSS quasars from the LOFAR Two-metre Sky Survey: ubiquitous jet activity and constraints on star formation. MNRAS 506(4):5888–5907. <https://doi.org/10.1093/mnras/stab1998>. arXiv:2107.09141 [astro-ph.GA]
- Magliocchetti M (2022) Hosts and environments: a (large-scale) radio history of AGN and star-forming galaxies. A&A Rev 30(1):6. <https://doi.org/10.1007/s00159-022-00142-1>. arXiv:2206.15286 [astro-ph.CO]
- Mahony EK, Morganti R, Prandoni I et al (2016) The Lockman Hole project: LOFAR observations and spectral index properties of low-frequency radio sources. MNRAS 463(3):2997–3020. <https://doi.org/10.1093/mnras/stw2225>. arXiv:1609.00537 [astro-ph.GA]
- Mao MY, Blanchard JM, Owen F et al (2018) The first VLBI detection of a spiral DRAGN core. MNRAS 478(1):L99–L104. <https://doi.org/10.1093/mnras/sty081>. arXiv:1805.03039 [astro-ph.GA]

- Maoz D (2007) Low-luminosity active galactic nuclei: are they UV faint and radio loud? *MNRAS* 377 (4):1696–1710. <https://doi.org/10.1111/j.1365-2966.2007.11735.x>. arXiv:astro-ph/0702292
- Maraschi L, Ghisellini G, Celotti A (1992) A jet model for the gamma-ray-emitting blazar 3C 279. *ApJ* 397:L5. <https://doi.org/10.1086/186531>
- Maraschi L, Colpi M, Ghisellini G, Perego A, Tavecchio F (2012) On the role of black hole spin and accretion in powering relativistic jets in AGN. *J Phys Conf Ser* 355(1):012016. <https://doi.org/10.1088/1742-6596/355/1/012016>
- Martí-Vidal I, Muller S (2017) High-sensitivity AGN polarimetry at sub-millimeter wavelengths. *Galaxies*. <https://doi.org/10.3390/galaxies5040065>
- Martínez-Sansigre A, Rawlings S (2011) Evidence for cosmic evolution in the spin of the most massive black holes. *MNRAS* 418(1):L84–L88. <https://doi.org/10.1111/j.1745-3933.2011.01148.x>. arXiv:1109.0997 [astro-ph.HE]
- Massardi M, Ekers RD, Murphy T et al (2011) The Australia Telescope 20 GHz (AT20G) Survey: analysis of the extragalactic source sample. *MNRAS* 412(1):318–330. <https://doi.org/10.1111/j.1365-2966.2010.17917.x>. arXiv:1010.5942 [astro-ph.CO]
- Massaro F, Marchesini EJ, D’Abrusco R et al (2017) Radio-weak BL Lac objects in the Fermi era. *ApJ* 834 (2):113. <https://doi.org/10.3847/1538-4357/834/2/113>. arXiv:1701.06067 [astro-ph.HE]
- Massaro F, Álvarez-Crespo N, Capetti A et al (2019) Deciphering the large-scale environment of radio galaxies in the local universe: where are they born? Where do they grow? Where do they die? *ApJS* 240(2):20. <https://doi.org/10.3847/1538-4365/aaf1c7>. arXiv:1811.11179 [astro-ph.HE]
- Massaro F, Capetti A, Paggi A et al (2020a) Dragon’s lair: on the large-scale environment of BL Lac objects. *ApJ* 900(2):L34. <https://doi.org/10.3847/2041-8213/abac56>. arXiv:2009.03318 [astro-ph.GA]
- Massaro F, Capetti A, Paggi A et al (2020b) Deciphering the Large-scale environment of radio galaxies in the local universe. II. A statistical analysis of environmental properties. *ApJS* 247(2):71. <https://doi.org/10.3847/1538-4365/ab799e>. arXiv:2004.02969 [astro-ph.HE]
- Mauch T, Sadler EM (2007) Radio sources in the 6dFGS: local luminosity functions at 1.4 GHz for star-forming galaxies and radio-loud AGN. *MNRAS* 375:931–950. <https://doi.org/10.1111/j.1365-2966.2006.11353.x>. arXiv:astro-ph/0612018
- Mbarek R, Caprioli D (2021) Espresso and stochastic acceleration of ultra-high-energy cosmic rays in relativistic jets. *ApJ* 921(1):85. <https://doi.org/10.3847/1538-4357/ac1da8>. arXiv:2105.05262 [astro-ph.HE]
- McConnell NJ, Ma CP (2013) Revisiting the scaling relations of black hole masses and host galaxy properties. *ApJ* 764(2):184. <https://doi.org/10.1088/0004-637X/764/2/184>. arXiv:1211.2816 [astro-ph.CO]
- McKinney JC (2006) General relativistic magnetohydrodynamic simulations of the jet formation and large-scale propagation from black hole accretion systems. *MNRAS* 368(4):1561–1582. <https://doi.org/10.1111/j.1365-2966.2006.10256.x>. arXiv:astro-ph/0603045
- McKinney JC, Gammie CF (2004) A measurement of the electromagnetic luminosity of a Kerr black hole. *ApJ* 611(2):977–995. <https://doi.org/10.1086/422244>. arXiv:astro-ph/0404512
- McKinney JC, Tchekhovskoy A, Blandford RD (2012) General relativistic magnetohydrodynamic simulations of magnetically choked accretion flows around black holes. *MNRAS* 423(4):3083–3117. <https://doi.org/10.1111/j.1365-2966.2012.21074.x>. arXiv:1201.4163 [astro-ph.HE]
- McNamara BR, Nulsen PEJ (2007) Heating hot atmospheres with active galactic nuclei. *ARA&A* 45 (1):117–175. <https://doi.org/10.1146/annurev.astro.45.051806.110625>. arXiv:0709.2152 [astro-ph]
- McNamara BR, Nulsen PEJ (2012) Mechanical feedback from active galactic nuclei in galaxies, groups and clusters. *New J Phys* 14(5):055023. <https://doi.org/10.1088/1367-2630/14/5/055023>. arXiv:1204.0006 [astro-ph.CO]
- Meier DL (1999) A magnetically switched, rotating black hole model for the production of extragalactic radio jets and the Fanaroff and Riley class division. *ApJ* 522(2):753–766. <https://doi.org/10.1086/307671>. arXiv:astro-ph/9810352
- Meier DL (2001) The association of jet production with geometrically thick accretion flows and black hole rotation. *ApJ* 548:L9–L12. <https://doi.org/10.1086/318921>. arXiv:astro-ph/0010231
- Meier DL, Koide S, Uchida Y (2001) Magnetohydrodynamic production of relativistic jets. *Science* 291 (5501):84–92. <https://doi.org/10.1126/science.291.5501.84>
- Merten L, Bougelilba M, Reimer A et al (2021) Scrutinizing FR 0 radio galaxies as ultra-high-energy cosmic ray source candidates. *Astropart Phys* 128:102564. <https://doi.org/10.1016/j.astropartphys.2021.102564>. arXiv:2102.01087 [astro-ph.HE]

- Merten L, Boughelilba M, Reimer A et al (2022) FR-0 jetted active galaxies: extending the zoo of candidate sites for UHECR acceleration. In: 37th International cosmic ray conference, 12–23 July 2021. Berlin, p 986. [arXiv:2107.13278](https://arxiv.org/abs/2107.13278) [astro-ph.HE]
- Mezcua M, Prieto MA (2014) Evidence of parsec-scale jets in low-luminosity active galactic nuclei. *ApJ* 787(1):62. <https://doi.org/10.1088/0004-637X/787/1/62>. [arXiv:1403.6675](https://arxiv.org/abs/1403.6675) [astro-ph.GA]
- Mikhailov A, Sotnikova Y (2021a) The relationship between FR0 radio galaxies and gigahertz-peaked spectrum sources. *Astron Nachr* 342(1130):1130–1134. <https://doi.org/10.1002/asna.20210050>. [arXiv:2111.06141](https://arxiv.org/abs/2111.06141) [astro-ph.GA]
- Mikhailov AG, Sotnikova YV (2021b) Radio properties of FR0 galaxies according to multifrequency measurements with RATAN-600. *Astron Rep* 65(4):233–245. <https://doi.org/10.1134/S1063772921040028>
- Miley G (1980) The structure of extended extragalactic radio sources. *ARA&A* 18:165–218. <https://doi.org/10.1146/annurev.aa.18.090180.001121>
- Mingo B, Hardcastle MJ, Croston JH et al (2014) An X-ray survey of the 2 Jy sample-I. Is there an accretion mode dichotomy in radio-loud AGN? *MNRAS* 440(1):269–297. <https://doi.org/10.1093/mnras/stu263>. [arXiv:1402.1770](https://arxiv.org/abs/1402.1770) [astro-ph.GA]
- Mingo B, Croston JH, Hardcastle MJ et al (2019) Revisiting the Fanaroff–Riley dichotomy and radio-galaxy morphology with the LOFAR Two-Metre Sky Survey (LoTSS). *MNRAS* 488(2):2701–2721. <https://doi.org/10.1093/mnras/stz1901>. [arXiv:1907.03726](https://arxiv.org/abs/1907.03726) [astro-ph.GA]
- Mingo B, Croston JH, Best PN et al (2022) Accretion mode versus radio morphology in the LOFAR Deep Fields. *MNRAS* 511(3):3250–3271. <https://doi.org/10.1093/mnras/stac140>. [arXiv:2201.04433](https://arxiv.org/abs/2201.04433) [astro-ph.GA]
- Miraghaei H, Best PN (2017) The nuclear properties and extended morphologies of powerful radio galaxies: the roles of host galaxy and environment. *MNRAS* 466(4):4346–4363. <https://doi.org/10.1093/mnras/stx007>. [arXiv:1701.00919](https://arxiv.org/abs/1701.00919) [astro-ph.GA]
- Morabito LK, Jackson NJ, Mooney S et al (2022a) Sub-arcsecond imaging with the International LOFAR Telescope. I. Foundational calibration strategy and pipeline. *A&A* 658:A1. <https://doi.org/10.1051/0004-6361/202140649>. [arXiv:2108.07283](https://arxiv.org/abs/2108.07283) [astro-ph.IM]
- Morabito LK, Sweijsen F, Radcliffe JF et al (2022b) Identifying active galactic nuclei via brightness temperature with sub-arcsecond International LOFAR Telescope observations. *MNRAS*. <https://doi.org/10.1093/mnras/stac2129>. [arXiv:2207.13096](https://arxiv.org/abs/2207.13096) [astro-ph.GA]
- Morganti R (2017) The many routes to AGN feedback. *Front Astron Space Sci* 4:42. <https://doi.org/10.3389/fspas.2017.00042>. [arXiv:1712.05301](https://arxiv.org/abs/1712.05301) [astro-ph.GA]
- Morganti R, Oosterloo TA, Reynolds JE, Tadhunter CN, Migenes V (1997) A study of cores in a complete sample of radio sources. *MNRAS* 284(3):541–551. <https://doi.org/10.1093/mnras/284.3.541>
- Morganti R, Schulz R, Nyland K et al (2018) The parsec-scale structure of jet-driven H I outflows in radio galaxies. In: *Astronomy in focus XXX*, vol A30, pp 74–77. <https://doi.org/10.1017/S1743921319003491>. [arXiv:1901.01446](https://arxiv.org/abs/1901.01446) [astro-ph.GA]
- Morganti R, Jurlin N, Oosterloo T et al (2021a) Combining LOFAR and Apertif data for understanding the life cycle of radio galaxies. *Galaxies* 9(4):88. <https://doi.org/10.3390/galaxies9040088>. [arXiv:2111.04776](https://arxiv.org/abs/2111.04776) [astro-ph.GA]
- Morganti R, Oosterloo T, Murthy S, Tadhunter C (2021b) The impact of young radio jets traced by cold molecular gas. *Astron Nachr* 342(9–10):1135–1139. <https://doi.org/10.1002/asna.20210037>. [arXiv:2201.04157](https://arxiv.org/abs/2201.04157) [astro-ph.GA]
- Mukherjee D, Bicknell GV, Sutherland R, Wagner A (2016) Relativistic jet feedback in high-redshift galaxies-I. Dynamics. *MNRAS* 461(1):967–983. <https://doi.org/10.1093/mnras/stw1368>. [arXiv:1606.01143](https://arxiv.org/abs/1606.01143) [astro-ph.HE]
- Mukherjee D, Bicknell GV, Wagner AY, Sutherland RS, Silk J (2018) Relativistic jet feedback-III. Feedback on gas discs. *MNRAS* 479(4):5544–5566. <https://doi.org/10.1093/mnras/sty1776>. [arXiv:1803.08305](https://arxiv.org/abs/1803.08305) [astro-ph.HE]
- Müller-Sánchez F, Prieto MA, Mezcua M et al (2013) The central molecular gas structure in LINERs with Low-luminosity active galactic nuclei: evidence for gradual disappearance of the torus. *ApJ* 763(1):L1. <https://doi.org/10.1088/2041-8205/763/1/L1>. [arXiv:1212.1162](https://arxiv.org/abs/1212.1162) [astro-ph.CO]
- Murthy S, Morganti R, Wagner AY et al (2022) Cold gas removal from the centre of a galaxy by a low-luminosity jet. *Nat Astron* 6:488–495. <https://doi.org/10.1038/s41550-021-01596-6>. [arXiv:2202.05222](https://arxiv.org/abs/2202.05222) [astro-ph.GA]
- Nagar NM, Falcke H, Wilson AS, Ho LC (2000) Radio sources in low-luminosity active galactic nuclei. I. VLA detections of compact, flat-spectrum cores. *ApJ* 542:186–196. <https://doi.org/10.1086/309524>

- Nagar NM, Falcke H, Wilson AS, Ho LC (2002a) ‘Radio-loud’ low luminosity AGN. *New Astron Rev* 46 (2–7):225–229. [https://doi.org/10.1016/S1387-6473\(01\)00185-3](https://doi.org/10.1016/S1387-6473(01)00185-3)
- Nagar NM, Falcke H, Wilson AS, Ulvestad JS (2002b) Radio sources in low-luminosity active galactic nuclei. III. “AGNs” in a distance-limited sample of “LLAGNs”. *A&A* 392:53–82. <https://doi.org/10.1051/0004-6361:20020874>. [arXiv:astro-ph/0207176](https://arxiv.org/abs/astro-ph/0207176)
- Nagar NM, Falcke H, Wilson AS (2005) Radio sources in low-luminosity active galactic nuclei. IV. Radio luminosity function, importance of jet power, and radio properties of the complete Palomar sample. *A&A* 435:521–543. <https://doi.org/10.1051/0004-6361:20042277>. [arXiv:astro-ph/0502551](https://arxiv.org/abs/astro-ph/0502551)
- Nakamura M, Uchida Y, Hirose S (2001) Production of wiggled structure of AGN radio jets in the sweeping magnetic twist mechanism. *New Astron* 6(2):61–78. [https://doi.org/10.1016/S1384-1076\(01\)00041-0](https://doi.org/10.1016/S1384-1076(01)00041-0)
- Narayan R, McClintock JE (2012) Observational evidence for a correlation between jet power and black hole spin. *MNRAS* 419(1):L69–L73. <https://doi.org/10.1111/j.1745-3933.2011.01181.x>. [arXiv:1112.0569](https://arxiv.org/abs/1112.0569) [astro-ph.HE]
- Narayan R, Yi I (1994) Advection-dominated accretion: a self-similar solution. *ApJ* 428:L13–L16. <https://doi.org/10.1086/187381>. [arXiv:astro-ph/9403052](https://arxiv.org/abs/astro-ph/9403052)
- Narayan R, Yi I (1995) Advection-dominated accretion: self-similarity and bipolar outflows. *ApJ* 444:231–243
- Narayan R, Igumenshchev IV, Abramowicz MA (2000) Self-similar accretion flows with convection. *ApJ* 539:798–808
- Narayan R, Igumenshchev IV, Abramowicz MA (2003) Magnetically arrested disk: an energetically efficient accretion flow. *PASJ* 55:L69–L72. <https://doi.org/10.1093/pasj/55.6.L69>. [arXiv:astro-ph/0305029](https://arxiv.org/abs/astro-ph/0305029)
- Narayan R, Sądowski A, Penna RF, Kulkarni AK (2012) GRMHD simulations of magnetized advection-dominated accretion on a non-spinning black hole: role of outflows. *MNRAS* 426(4):3241–3259. <https://doi.org/10.1111/j.1365-2966.2012.22002.x>. [arXiv:1206.1213](https://arxiv.org/abs/1206.1213) [astro-ph.HE]
- Netzer H (2015) Revisiting the unified model of active galactic nuclei. *ARA&A* 53:365–408. <https://doi.org/10.1146/annurev-astro-082214-122302>. [arXiv:1505.00811](https://arxiv.org/abs/1505.00811) [astro-ph.GA]
- Norris RP, Hopkins AM, Afonso J et al (2011) EMU: evolutionary map of the universe. *PASA* 28(3):215–248. <https://doi.org/10.1071/AS11021>. [arXiv:1106.3219](https://arxiv.org/abs/1106.3219) [astro-ph.CO]
- Nyland K, Alatalo K, Wrobel JM et al (2013) Detection of a high brightness temperature radio core in the active-galactic-nucleus-driven molecular outflow candidate NGC 1266. *ApJ* 779(2):173. <https://doi.org/10.1088/0004-637X/779/2/173>. [arXiv:1310.7588](https://arxiv.org/abs/1310.7588) [astro-ph.CO]
- Nyland K, Young LM, Wrobel JM et al (2016) The ATLAS<sup>3D</sup> project-XXXI. Nuclear radio emission in nearby early-type galaxies. *MNRAS* 458:2221–2268. <https://doi.org/10.1093/mnras/stw391>. [arXiv:1602.05579](https://arxiv.org/abs/1602.05579)
- Nyland K, Harwood JJ, Mukherjee D et al (2018a) Revolutionizing our understanding of AGN feedback and its importance to galaxy evolution in the era of the next generation very large array. *ApJ* 859 (1):23. <https://doi.org/10.3847/1538-4357/aab3d1>. [arXiv:1803.02357](https://arxiv.org/abs/1803.02357) [astro-ph.GA]
- Nyland K, Mukherjee D, Lacy M et al (2018b) Science with an ngVLA: radio Jet-ISM feedback on sub-galactic scales. In: Murphy EJ (ed) *The ASP Monograph Series, “Science with a Next-Generation VLA”*, San Francisco. [arXiv e-prints arXiv:1810.07526](https://arxiv.org/abs/1810.07526) [astro-ph.GA]
- Nyland K, Dong DZ, Patil P et al (2020) Quasars that have transitioned from radio-quiet to radio-loud on decadal timescales revealed by VLASS and FIRST. *ApJ* 905(1):74. <https://doi.org/10.3847/1538-4357/abc341>. [arXiv:2011.08872](https://arxiv.org/abs/2011.08872) [astro-ph.GA]
- O’Dea CP (1998) The compact steep-spectrum and gigahertz peaked-spectrum radio sources. *PASP* 110 (747):493–532. <https://doi.org/10.1086/316162>
- O’Dea CP, Baum SA (1997) Constraints on radio source evolution from the compact steep spectrum and GHz peaked spectrum radio sources. *AJ* 113:148–161. <https://doi.org/10.1086/118241>
- O’Dea CP, Saikia DJ (2021) Compact steep-spectrum and peaked-spectrum radio sources. *A&A Rev* 29 (1):3. <https://doi.org/10.1007/s00159-021-00131-w>. [arXiv:2009.02750](https://arxiv.org/abs/2009.02750) [astro-ph.GA]
- O’Dea CP, Daly RA, Kharb P, Freeman KA, Baum SA (2009) Physical properties of very powerful FR II radio galaxies. *A&A* 494(2):471–488. <https://doi.org/10.1051/0004-6361:200809416>. [arXiv:0810.1213](https://arxiv.org/abs/0810.1213) [astro-ph]
- O’Dell SL (1978) The continuum radiation of compact extragalactic objects. In: Wolfe AM (ed) *BL Lac objects. In: Pittsburgh Conference on BL Lac Objects, Pittsburgh, April 24–26, 1978, Proceedings*, pp 312–325 (A79-30026 11-90)

- Ohsuga K, Mineshige S, Mori M, Kato Y (2009) Global radiation-magnetohydrodynamic simulations of black-hole accretion flow and outflow: unified model of three states. *PASJ* 61(3):L7–L11. <https://doi.org/10.1093/pasj/61.3.L7>. arXiv:0903.5364 [astro-ph.HE]
- Orienti M (2016) Radio properties of compact steep spectrum and GHz-peaked spectrum radio sources. *Astron Nachr* 337(1–2):9. <https://doi.org/10.1002/asna.201512257>. arXiv:1511.00436 [astro-ph.GA]
- Orienti M, Dallacasa D, Stanghellini C (2007) Constraining the nature of high frequency peakers. The spectral variability. *A&A* 475(3):813–820. <https://doi.org/10.1051/0004-6361:20078105>. arXiv:0708.3979 [astro-ph]
- Orienti M, Murgia M, Dallacasa D (2010) The last breath of the young gigahertz-peaked spectrum radio source PKS1518+047. *MNRAS* 402:1892–1898. <https://doi.org/10.1111/j.1365-2966.2009.16016.x>. arXiv:0911.1723
- O’Sullivan SP, Gaensler BM, Lara-López MA et al (2015) The magnetic field and polarization properties of radio galaxies in different accretion states. *ApJ* 806(1):83. <https://doi.org/10.1088/0004-637X/806/1/83>. arXiv:1504.06679 [astro-ph.GA]
- Padovani P (2016) The faint radio sky: radio astronomy becomes mainstream. *A&A Rev* 24(1):13. <https://doi.org/10.1007/s00159-016-0098-6>. arXiv:1609.00499 [astro-ph.GA]
- Padovani P, Bonzini M, Kellermann KI et al (2015) Radio-faint AGN: a tale of two populations. *MNRAS* 452(2):1263–1279. <https://doi.org/10.1093/mnras/stv1375>. arXiv:1506.06554 [astro-ph.GA]
- Padovani P, Alexander DM, Assef RJ et al (2017) Active galactic nuclei: what’s in a name? *A&A Rev* 25(1):2. <https://doi.org/10.1007/s00159-017-0102-9>. arXiv:1707.07134 [astro-ph.GA]
- Paliya VS (2021) A new gamma-ray-emitting population of FR0 radio galaxies. *ApJ* 918(2):L39. <https://doi.org/10.3847/2041-8213/ac2143>. arXiv:2108.11701 [astro-ph.HE]
- Panessa F, Baldi RD, Laor A et al (2019) The origin of radio emission from radio-quiet active galactic nuclei. *Nat Astron* 3:387–396. <https://doi.org/10.1038/s41550-019-0765-4>. arXiv:1902.05917 [astro-ph.GA]
- Parma P, Fanti C, Fanti R, Morganti R, de Ruiter HR (1987) VLA observations of low-luminosity radio galaxies. VI-discussion of radio jets. *A&A* 181:244–264
- Perucho M, Martí JM, Laing RA, Hardee PE (2014) On the deceleration of Fanaroff–Riley class I jets: mass loading by stellar winds. *MNRAS* 441(2):1488–1503. <https://doi.org/10.1093/mnras/stu676>. arXiv:1404.1209 [astro-ph.HE]
- Phillips RB, Mutel RL (1982) On symmetric structure in compact radio sources. *A&A* 106:21–24
- Pierce JCS, Tadhunter CN, Ramos Almeida C, Bessiere PS, Rose M (2019) Do AGN triggering mechanisms vary with radio power?—I. Optical morphologies of radio-intermediate HERGs. *MNRAS* 487(4):5490–5507. <https://doi.org/10.1093/mnras/stz1253>. arXiv:1905.01315 [astro-ph.GA]
- Pierce JCS, Tadhunter CN, Morganti R (2020) The radio properties of high-excitation radio galaxies with intermediate radio powers. *MNRAS* 494(2):2053–2067. <https://doi.org/10.1093/mnras/staa531>. arXiv:2002.07820 [astro-ph.GA]
- Prandoni I, Seymour N (2014) Proceedings of ‘Advancing Astrophysics with the SKA’ (AASKA14)-continuum science’, chapters presented at the Conference ‘Advancing Astrophysics with the SKA’ (AASKA14), Giardini Naxos, June 9–13. arXiv e-prints arXiv:1412.6942 [astro-ph.GA]
- Prandoni I, Seymour N (2015) Revealing the physics and evolution of galaxies and galaxy clusters with SKA continuum surveys. In: *Advancing astrophysics with the square kilometre array (AASKA14)*, p 67. <https://doi.org/10.22323/1.215.0067>. arXiv:1412.6512 [astro-ph.IM]
- Prestage RM, Peacock JA (1988) The cluster environments of powerful radio galaxies. *MNRAS* 230:131–160. <https://doi.org/10.1093/mnras/230.1.131>
- Pringle JE (1981) Accretion discs in astrophysics. *ARA&A* 19:137–162. <https://doi.org/10.1146/annurev.aa.19.090181.001033>
- Rafferty DA, McNamara BR, Nulsen PEJ, Wise MW (2006) The feedback-regulated growth of black holes and bulges through gas accretion and starbursts in cluster central dominant galaxies. *ApJ* 652(1):216–231. <https://doi.org/10.1086/507672>. arXiv:astro-ph/0605323
- Rani B (2019) Radio galaxies—the TeV challenge. *Galaxies* 7(1):23. <https://doi.org/10.3390/galaxies7010023>. arXiv:1811.00567 [astro-ph.HE]
- Rawlings S, Saunders R (1991) Evidence for a common central-engine mechanism in all extragalactic radio sources. *Nature* 349:138–140
- Readhead ACS (1995) Evolution of powerful extragalactic radio sources. *PNAS* 92(25):11447–11450. <https://doi.org/10.1073/pnas.92.25.11447>
- Readhead ACS, Xu W, Pearson TJ, Wilkinson PN, Polatidis AG (1994) Compact symmetric objects. In: Zensus JA, Kellermann KI (eds) *Compact extragalactic radio sources*. NRAO, Green Bank, p 17

- Reynolds CS (2014) Measuring black hole spin using X-ray reflection spectroscopy. *Space Sci Rev* 183(1–4):277–294. <https://doi.org/10.1007/s11214-013-0006-6>. arXiv:1302.3260 [astro-ph.HE]
- Rieger F, Levinson A (2018) Radio galaxies at VHE energies. *Galaxies* 6(4):116. <https://doi.org/10.3390/galaxies6040116>. arXiv:1810.05409 [astro-ph.HE]
- Riggi S, Umam G, Tringilio C et al (2021) Evolutionary map of the Universe (EMU): compact radio sources in the SCORPIO field towards the galactic plane. *MNRAS* 502(1):60–79. <https://doi.org/10.1093/mnras/stab028>. arXiv:2101.03843 [astro-ph.GA]
- Rogstad DH, Ekers RD (1969) Radio sources and elliptical galaxies. *ApJ* 157:481. <https://doi.org/10.1086/150089>
- Rossi P, Bodo G, Massaglia S, Capetti A (2020) The different flavors of extragalactic jets: the role of relativistic flow deceleration. *A&A* 642:A69. <https://doi.org/10.1051/0004-6361/202038725>. arXiv:2007.11423 [astro-ph.HE]
- Roy N, Moravec E, Bundy K et al (2021) Radio morphology of red geysers. *ApJ* 922(2):230. <https://doi.org/10.3847/1538-4357/ac24a0>. arXiv:2109.02609 [astro-ph.GA]
- Rulten C (2022) Radio galaxies at TeV energies. *Galaxies* 10(3):61. <https://doi.org/10.3390/galaxies10030061>
- Sabater J, Best PN, Hardcastle MJ et al (2019) The LoTSS view of radio AGN in the local Universe. The most massive galaxies are always switched on. *A&A* 622:A17. <https://doi.org/10.1051/0004-6361/201833883>. arXiv:1811.05528 [astro-ph.GA]
- Sadler EM (1984) Radio and optical observations of a complete sample of E and SO galaxies. III. A radio continuum survey at 2.7 and 5.0 GHz. *A J*. <https://doi.org/10.1086/113483>
- Sadler EM (2016) GPS/CSS radio sources and their relation to other AGN. *Astron Nachr* 337:105. <https://doi.org/10.1002/asna.201512274>. arXiv:1512.01851
- Sadler EM, Ekers RD, Mahony EK, Mauch T, Murphy T (2014) The local radio-galaxy population at 20 GHz. *MNRAS* 438:796–824. <https://doi.org/10.1093/mnras/stt2239>. arXiv:1304.0268
- Saikia DJ (2022) Jets in radio galaxies and quasars: an observational perspective. *J Astrophys Astron* 43(2):97. <https://doi.org/10.1007/s12036-022-09863-2>. arXiv:2206.05803 [astro-ph.GA]
- Saikia P, Körding E, Coppejans DL et al (2018) 15-GHz radio emission from nearby low-luminosity active galactic nuclei. *A&A* 616:A152. <https://doi.org/10.1051/0004-6361/201833233>. arXiv:1805.06696 [astro-ph.HE]
- Schaller M, Borrow J, Draper PW et al (2023) Swift: a modern highly-parallel gravity and smoothed particle hydrodynamics solver for astrophysical and cosmological applications. arXiv e-prints. <https://doi.org/10.48550/arXiv.2305.13380>. arXiv:2305.13380 [astro-ph.IM]
- Schawinski K, Lintott C, Thomas D et al (2009) Galaxy Zoo: a sample of blue early-type galaxies at low redshift. *MNRAS* 396:818–829. <https://doi.org/10.1111/j.1365-2966.2009.14793.x>. arXiv:0903.3415
- Schaye J, Crain RA, Bower RG et al (2015) The EAGLE project: simulating the evolution and assembly of galaxies and their environments. *MNRAS* 446(1):521–554. <https://doi.org/10.1093/mnras/stu2058>. arXiv:1407.7040 [astro-ph.GA]
- Scheuer PAG (1974) Models of extragalactic radio sources with a continuous energy supply from a central object. *MNRAS* 166:513–528. <https://doi.org/10.1093/mnras/166.3.513>
- Schmidt M (1963) 3C 273: a star-like object with large red-shift. *Nature* 197(4872):1040. <https://doi.org/10.1038/1971040a0>
- Schmidt M (1968) Space distribution and luminosity functions of quasi-stellar radio sources. *ApJ* 151:393. <https://doi.org/10.1086/149446>
- Shabala SS, Ash S, Alexander P, Riley JM (2008) The duty cycle of local radio galaxies. *MNRAS* 388:625–637. <https://doi.org/10.1111/j.1365-2966.2008.13459.x>. arXiv:0805.4152
- Shabala SS, Deller A, Kaviraj S et al (2017) Delayed triggering of radio active galactic nuclei in gas-rich minor mergers in the local Universe. *MNRAS* 464(4):4706–4720. <https://doi.org/10.1093/mnras/stw2536>. arXiv:1608.04178 [astro-ph.GA]
- Shabala SS, Jurlin N, Morganti R et al (2020) The duty cycle of radio galaxies revealed by LOFAR: remnant and restarted radio source populations in the Lockman Hole. *MNRAS* 496(2):1706–1717. <https://doi.org/10.1093/mnras/staa1172>. arXiv:2004.08979 [astro-ph.GA]
- Shakura NI, Sunyaev RA (1973) Black holes in binary systems. Observational appearance. *A&A* 24:337–355
- Shang Z, Brotherton MS, Wills BJ et al (2011) The next generation Atlas of quasar spectral energy distributions from radio to X-rays. *ApJS* 196(1):2. <https://doi.org/10.1088/0067-0049/196/1/2>. arXiv:1107.1855 [astro-ph.CO]

- Shankar F (2009) The demography of supermassive black holes: growing monsters at the heart of galaxies. *New Astron Rev* 53(4–6):57–77. <https://doi.org/10.1016/j.newar.2009.07.006>. arXiv:0907.5213 [astro-ph.CO]
- Shimwell TW, Röttgering HJA, Best PN et al (2017) The LOFAR Two-metre Sky Survey. I. Survey description and preliminary data release. *A&A* 598:A104. <https://doi.org/10.1051/0004-6361/201692313>. arXiv:1611.02700 [astro-ph.IM]
- Shimwell TW, Tasse C, Hardcastle MJ et al (2019) The LOFAR Two-metre Sky Survey. II. First data release. *A&A* 622:A1. <https://doi.org/10.1051/0004-6361/201833559>. arXiv:1811.07926
- Shlosman I (2013) Cosmological evolution of galaxies. In: Falcón-Barroso J, Knapen JH (eds) *Secular evolution of galaxies*. Cambridge University Press, Cambridge, p 555
- Sikora M, Begelman MC (2013) Magnetic flux paradigm for radio loudness of active galactic nuclei. *ApJ* 764(2):L24. <https://doi.org/10.1088/2041-8205/764/2/L24>. arXiv:1301.5638 [astro-ph.HE]
- Sikora M, Stawarz Ł, Lasota JP (2007) Radio loudness of active galactic nuclei: observational facts and theoretical implications. *ApJ* 658:815–828. <https://doi.org/10.1086/511972>. arXiv:astro-ph/0604095
- Singh V, Ishwara-Chandra CH, Sievers J et al (2015a) Discovery of rare double-lobe radio galaxies hosted in spiral galaxies. *MNRAS* 454(2):1556–1572. <https://doi.org/10.1093/mnras/stv2071>. arXiv:1509.01559 [astro-ph.GA]
- Singh V, Ishwara-Chandra CH, Wadadekar Y, Beelen A, Kharb P (2015b) Kiloparsec-scale radio emission in Seyfert and LINER galaxies. *MNRAS* 446(1):599–612. <https://doi.org/10.1093/mnras/stu2124>. arXiv:1410.2720 [astro-ph.GA]
- Singh CB, Garofalo D, Kennedy K (2019) The generalized hardness-intensity diagram for black hole and neutron star X-ray binaries. *ApJ* 887(2):164. <https://doi.org/10.3847/1538-4357/ab4656>. arXiv:1909.08932 [astro-ph.HE]
- Sirothia SK, Dennefeld M, Saikia DJ et al (2009) 325-MHz observations of the ELAIS-N1 field using the Giant Metrewave Radio Telescope. *MNRAS* 395(1):269–281. <https://doi.org/10.1111/j.1365-2966.2009.14317.x>. arXiv:0812.0813 [astro-ph]
- Slee OB, Sadler EM, Reynolds JE, Ekers RD (1994) Parsec-scale radio cores in early type galaxies. *MNRAS* 269:928. <https://doi.org/10.1093/mnras/269.4.928>
- Slob MM, Callingham JR, Röttgering HJA et al (2022) Extragalactic peaked-spectrum radio sources at low frequencies are young radio galaxies. *A&A* 668:A186. <https://doi.org/10.1051/0004-6361/202244651>. arXiv:2210.16570 [astro-ph.GA]
- Smethurst RJ, Simmons BD, Lintott CJ, Shanahan J (2019) Secularly powered outflows from AGNs: the dominance of non-merger driven supermassive black hole growth. *MNRAS* 489(3):4016–4031. <https://doi.org/10.1093/mnras/stz2443>. arXiv:1909.01355 [astro-ph.GA]
- Smith EP, Heckman TM, Bothun GD, Romanishin W, Balick B (1986) On the nature of QSO host galaxies. *ApJ* 306:64. <https://doi.org/10.1086/164321>
- Snellen IAG, Schilizzi RT, de Bruyn AG et al (1998) A new sample of faint Gigahertz Peaked Spectrum radio sources. *A&AS* 131:435–449. <https://doi.org/10.1051/aas:1998281>. arXiv:astro-ph/9803140
- Snellen IAG, Schilizzi RT, Miley GK et al (2000) On the evolution of young radio-loud AGN. *MNRAS* 319(2):445–456. <https://doi.org/10.1046/j.1365-8711.2000.03935.x>. arXiv:astro-ph/0002130
- Sol H, Pelletier G, Asseo E (1989) Two-flow model for extragalactic radio jets. *MNRAS* 237:411–429. <https://doi.org/10.1093/mnras/237.2.411>
- Spencer RE, McDowell JC, Charlesworth M et al (1989) MERLIN and VLA observations of compact steep-spectrum radio sources. *MNRAS* 240:657–687. <https://doi.org/10.1093/mnras/240.3.657>
- Spinoglio L, Fernández-Ontiveros JA (2021) AGN types and unification model. In: Pović M, Marziani P, Masegosa J et al (eds) *Nuclear activity in galaxies across cosmic time*. IAU symposium, vol 356, pp 29–43. <https://doi.org/10.1017/S1743921320002549>. arXiv:1911.12176 [astro-ph.GA]
- Stanghellini C, O’Dea CP, Dallacasa D et al (1998) A complete sample of GHz-peaked-spectrum radio sources and its radio properties. *A&AS* 131:303–315. <https://doi.org/10.1051/aas:1998270>. arXiv:astro-ph/9803222
- Stecker FW, Shrader CR, Malkan MA (2019) The extragalactic gamma-ray background from core-dominated radio galaxies. *ApJ* 879(2):68. <https://doi.org/10.3847/1538-4357/ab23ee>. arXiv:1903.06544 [astro-ph.GA]
- Stratava I, Ivezić Ž, Knapp GR et al (2001) Color separation of galaxy types in the Sloan Digital Sky Survey imaging data. *AJ* 122:1861–1874. <https://doi.org/10.1086/323301>. arXiv:astro-ph/0107201
- Sutherland RS, Bicknell GV (2007) Interaction of jets with the ISM of radio galaxies. *Ap & SS* 311(1–3):293–303. <https://doi.org/10.1007/s10509-007-9580-y>. arXiv:0707.3669 [astro-ph]

- Tadhunter C (2016a) Radio AGN in the local universe: unification, triggering and evolution. *A&A Rev* 24 (1):10. <https://doi.org/10.1007/s00159-016-0094-x>. arXiv:1605.08773 [astro-ph.GA]
- Tadhunter C (2016b) The impact of compact radio sources on their host galaxies: observations. *Astron Nachr* 337(1–2):159. <https://doi.org/10.1002/asna.201512286>
- Tadhunter C, Morganti R, Santoro F, Bernhard E (2021) Compact radio sources: triggering and feedback. *Astron Nachr* 342(1200):1200–1206. <https://doi.org/10.1002/asna.20210048>
- Talbot RY, Sijacki D, Bourne MA (2022) Blandford–Znajek jets in galaxy formation simulations: exploring the diversity of outflows produced by spin-driven AGN jets in Seyfert galaxies. *MNRAS* 514(3):4535–4559. <https://doi.org/10.1093/mnras/stac1566>. arXiv:2111.01801 [astro-ph.GA]
- Tanner R, Weaver KA (2022) Simulations of AGN-driven galactic outflow morphology and content. *AJ* 163(3):134. <https://doi.org/10.3847/1538-3881/ac4d23>. arXiv:2201.08360 [astro-ph.GA]
- Tavecchio F, Righi C, Capetti A, Grandi P, Ghisellini G (2018) High-energy neutrinos from FR0 radio galaxies? *MNRAS* 475(4):5529–5534. <https://doi.org/10.1093/mnras/sty251>. arXiv:1711.03757 [astro-ph.HE]
- Tchekhovskoy A, Narayan R, McKinney JC (2010) Black hole spin and the radio loud/quiet dichotomy of active galactic nuclei. *ApJ* 711:50–63. <https://doi.org/10.1088/0004-637X/711/1/50>. arXiv:0911.2228 [astro-ph.HE]
- Tchekhovskoy A, Narayan R, McKinney JC (2011) Efficient generation of jets from magnetically arrested accretion on a rapidly spinning black hole. *MNRAS* 418:L79–L83. <https://doi.org/10.1111/j.1745-3933.2011.01147.x>. arXiv:1108.0412 [astro-ph.HE]
- Terashima Y, Wilson AS (2003) Chandra snapshot observations of low-luminosity active galactic nuclei with a compact radio source. *ApJ* 583(1):145–158. <https://doi.org/10.1086/345339>. arXiv:astro-ph/0209607
- Thorne KS, Price RH, MacDonald DA (1986) Black holes: the membrane paradigm (book review). *Science* 234:224. <https://doi.org/10.1126/science.234.4778.882>
- Torresi E (2020) Gamma-ray emission in radio galaxies, from MeV to TeV. In: Asada K, de Gouveia Dal Pino E, Giroletti M, Nagai H, Nemmen R (eds) *Perseus in sicily: from black hole to cluster outskirts*. IAU symposium, vol 342, pp 158–166. <https://doi.org/10.1017/S1743921318007895>. arXiv:1809.08074 [astro-ph.HE]
- Torresi E, Grandi P, Capetti A, Baldi RD, Giovannini G (2018) X-ray study of a sample of FR0 radio galaxies: unveiling the nature of the central engine. *MNRAS* 476(4):5535–5547. <https://doi.org/10.1093/mnras/sty520>. arXiv:1802.08581 [astro-ph.HE]
- Torresi E, Balmaverde B, Liuzzo E et al (2022) Exploring the radio morphology-accretion mode link in radio galaxies at high energies. *Mem Soc Astron Ital* 93(2–3):81
- Tremaine S, Gebhardt K, Bender R et al (2002) The slope of the black hole mass versus velocity dispersion correlation. *ApJ* 574:740–753
- Trinchieri G, Marino A, Mazzei P, Rampazzo R, Wolter A (2012) Hot gas in groups: NGC 5328 and the intriguing case of NGC 4756 with XMM-Newton. *A&A* 545:A140. <https://doi.org/10.1051/0004-6361/201219775>. arXiv:1208.1408 [astro-ph.CO]
- Ubertosi F, Gitti M, Torresi E, Brighenti F, Grandi P (2021a) A Chandra study of Abell 795—a sloshing cluster with an FR0 radio galaxy at its centre. *MNRAS* 503(3):4627–4645. <https://doi.org/10.1093/mnras/stab819>. arXiv:2103.08682 [astro-ph.GA]
- Ubertosi F, Gitti M, Torresi E, Brighenti F, Grandi P (2021b) The central FR0 in the sloshing cluster Abell 795: indications of mechanical feedback from Chandra data. *Astron Nachr* 342(1207):1207–1211. <https://doi.org/10.1002/asna.202100555>. arXiv:2111.02160 [astro-ph.GA]
- Ulvestad JS, Ho LC (2001a) Statistical properties of radio emission from the Palomar Seyfert galaxies. *ApJ* 558:561–577. <https://doi.org/10.1086/322307>. arXiv:astro-ph/0105373
- Ulvestad JS, Ho LC (2001b) The origin of radio emission in low-luminosity active galactic nuclei: jets, accretion flows, or both? *ApJ* 562:L133–L136. <https://doi.org/10.1086/338254>. arXiv:astro-ph/0110535
- Ulvestad JS, Wrobel JM, Roy AL et al (1999) Subrelativistic radio jets and parsec-scale absorption in two Seyfert galaxies. *ApJ* 517(2):L81–L84. <https://doi.org/10.1086/312040>. arXiv:astro-ph/9903378
- Urry CM, Padovani P (1995) Unified schemes for radio-loud active galactic nuclei. *PASP* 107:803. <https://doi.org/10.1086/133630>. arXiv:astro-ph/9506063
- van Breugel W, Miley G, Heckman T (1984) Studies of kiloparsec-scale, steep-spectrum radio cores. I. VLA maps. *AJ* 89:5–22. <https://doi.org/10.1086/113480>
- van der Wolk G, Barthel PD, Peletier RF, Pel JW (2010) Dust tori in radio galaxies. *A&A* 511:A64. <https://doi.org/10.1051/0004-6361/200912435>. arXiv:0911.3734 [astro-ph.GA]

- Vardoulaki E, Jiménez Andrade EF, Delvecchio I et al (2021) FR-type radio sources at 3 GHz VLA-COSMOS: relation to physical properties and large-scale environment. *A&A* 648:A102. <https://doi.org/10.1051/0004-6361/202039488>. [arXiv:2009.10721](https://arxiv.org/abs/2009.10721) [astro-ph.GA]
- Vattakunnel S, Trussoni E, Capetti A, Baldi RD (2010) Accretion and nuclear activity in Virgo early-type galaxies. *A&A* 522:A89. <https://doi.org/10.1051/0004-6361/201014611>. [arXiv:1007.3845](https://arxiv.org/abs/1007.3845) [astro-ph.CO]
- Venturi T, Castaldini C, Cotton WD et al (1995) VLBI observations of a complete sample of radio galaxies. VI. The two FR I radio galaxies B2 0836+29 and 3C 465. *ApJ* 454:735. <https://doi.org/10.1086/176525>
- Venturi G, Cresci G, Marconi A et al (2021) MAGNUM survey: compact jets causing large turmoil in galaxies. Enhanced line widths perpendicular to radio jets as tracers of jet-ISM interaction. *A&A* 648:A17. <https://doi.org/10.1051/0004-6361/202039869>. [arXiv:2011.04677](https://arxiv.org/abs/2011.04677) [astro-ph.GA]
- Verdoes Kleijn GA, Baum SA, de Zeeuw PT, O'Dea CP (2002) Core radio and optical emission in the nuclei of nearby FR I radio galaxies. *AJ* 123(3):1334–1356. <https://doi.org/10.1086/339177>. [arXiv:astro-ph/0112356](https://arxiv.org/abs/astro-ph/0112356)
- Vogelsberger M, Genel S, Springel V et al (2014) Introducing the Illustris Project: simulating the coevolution of dark and visible matter in the Universe. *MNRAS* 444(2):1518–1547. <https://doi.org/10.1093/mnras/stu1536>. [arXiv:1405.2921](https://arxiv.org/abs/1405.2921) [astro-ph.CO]
- Wagner AY, Bicknell GV (2011) Relativistic jet feedback in evolving galaxies. *ApJ* 728(1):29. <https://doi.org/10.1088/0004-637X/728/1/29>. [arXiv:1012.1092](https://arxiv.org/abs/1012.1092) [astro-ph.CO]
- Wang A, An T, Guo S et al (2023) Interactions between the jet and disk wind in nearby radio-intermediate Quasar III Zw 2. *ApJ* 944(2):187. <https://doi.org/10.3847/1538-4357/acaf02>. [arXiv:2212.13735](https://arxiv.org/abs/2212.13735) [astro-ph.HE]
- Webster B, Croston JH, Harwood JJ et al (2021a) Investigating the spectra and physical nature of galaxy scale jets. *MNRAS* 508(4):5972–5990. <https://doi.org/10.1093/mnras/stab2939>. [arXiv:2110.04018](https://arxiv.org/abs/2110.04018) [astro-ph.GA]
- Webster B, Croston JH, Mingo B et al (2021b) A population of galaxy-scale jets discovered using LOFAR. *MNRAS* 500(4):4921–4936. <https://doi.org/10.1093/mnras/staa3437>. [arXiv:2011.01015](https://arxiv.org/abs/2011.01015) [astro-ph.GA]
- Whittam IH, Riley JM, Green DA, Jarvis MJ (2016) The faint source population at 15.7 GHz—III. A high-frequency study of HERGs and LERGs. *MNRAS* 462:2122–2137. <https://doi.org/10.1093/mnras/stw1725>. [arXiv:1607.03709](https://arxiv.org/abs/1607.03709)
- Whittam IH, Prescott M, McAlpine K, Jarvis MJ, Heywood I (2018) The stripe 82 1–2 GHz Very Large Array Snapshot Survey: host galaxy properties and accretion rates of radio galaxies. *MNRAS* 480(1):358–370. <https://doi.org/10.1093/mnras/sty1787>. [arXiv:1806.10143](https://arxiv.org/abs/1806.10143) [astro-ph.GA]
- Whittam IH, Green DA, Jarvis MJ, Riley JM (2020) The faint radio source population at 15.7 GHz—IV. The dominance of core emission in faint radio galaxies. *MNRAS* 493(2):2841–2853. <https://doi.org/10.1093/mnras/staa306>. [arXiv:2001.10961](https://arxiv.org/abs/2001.10961) [astro-ph.GA]
- Whittam IH, Jarvis MJ, Hale CL et al (2022) MIGHTEE: the nature of the radio-loud AGN population. *MNRAS*. <https://doi.org/10.1093/mnras/stac2140>. [arXiv:2207.12379](https://arxiv.org/abs/2207.12379) [astro-ph.GA]
- Wilkinson PN, Tzioumis AK, Benson JM et al (1991) A disrupted radio jet inside the host galaxy of the quasar 3C48. *Nature* 352(6333):313–315. <https://doi.org/10.1038/352313a0>
- Williams DRA, Pahari M, Baldi RD et al (2022) LeMMINGS—IV. The X-ray properties of a statistically complete sample of the nuclei in active and inactive galaxies from the Palomar sample. *MNRAS* 510(4):4909–4928. <https://doi.org/10.1093/mnras/stab3310>. [arXiv:2111.09077](https://arxiv.org/abs/2111.09077) [astro-ph.HE]
- Williams DRA, Baldi RD, Beswick RJ et al (2023) The LeMMINGS survey: probing sub-kpc radio structures of nearby galaxies with e-MERLIN. In: Proceedings of 15th European VLBI network mini-symposium and users' meeting—PoS(EVN2022). PoS, vol 428, p 046. <https://doi.org/10.22323/1.428.0046>. [arXiv:2303.08647](https://arxiv.org/abs/2303.08647) [astro-ph.GA]
- Willott CJ, Rawlings S, Blundell KM, Lacy M (1999) The emission line-radio correlation for radio sources using the 7C Redshift Survey. *MNRAS* 309:1017–1033. <https://doi.org/10.1046/j.1365-8711.1999.02907.x>. [arXiv:astro-ph/9905388](https://arxiv.org/abs/astro-ph/9905388)
- Wójtowicz A, Stawarz Ł, Cheung CC, Werner N, Rudka D (2023) Radio emission of nearby early-type galaxies in the low and very low radio luminosity range. *ApJ* 944(2):195. <https://doi.org/10.3847/1538-4357/acb498>. [arXiv:2209.14638](https://arxiv.org/abs/2209.14638) [astro-ph.GA]
- Wright EL, Eisenhardt PRM, Mainzer AK et al (2010) The Wide-field Infrared Survey Explorer (WISE): mission description and initial on-orbit performance. *AJ* 140(6):1868–1881. <https://doi.org/10.1088/0004-6256/140/6/1868>. [arXiv:1008.0031](https://arxiv.org/abs/1008.0031) [astro-ph.IM]

- Wrobel JM (2000) Photometric variability and astrometric stability of the radio continuum nucleus in the Seyfert Galaxy NGC 5548. *ApJ* 531:716–726. <https://doi.org/10.1086/308519>. [arXiv:astro-ph/9910427](#)
- Wrobel JM, Heeschen DS (1991) Radio-continuum sources in nearby and bright E/S0 galaxies—active nuclei versus star formation. *AJ* 101:148–169
- Wu F, An T, Baan WA et al (2013) Kinematics of the compact symmetric object OQ 208 revisited. *A&A* 550:A113. <https://doi.org/10.1051/0004-6361/201219700>. [arXiv:1211.4287](#) [astro-ph.CO]
- Xu C, Baum SA, O’Dea CP, Wrobel JM, Condon JJ (2000) VLBA observations of a sample of nearby FR I radio galaxies. *AJ* 120:2950–2964
- York DG, Adelman J, Anderson JE Jr et al (2000) The Sloan Digital Sky Survey: technical summary. *AJ* 120:1579–1587. <https://doi.org/10.1086/301513>. [arXiv:astro-ph/0006396](#)
- Younes G, Porquet D, Sabra B, Reeves JN, Grosso N (2012) Study of LINER sources with broad H $\alpha$  emission. Spectral energy distribution and multiwavelength correlations. *A&A* 539:A104. <https://doi.org/10.1051/0004-6361/201118299>. [arXiv:1201.5660](#) [astro-ph.CO]
- Yuan F, Narayan R (2014) Hot accretion flows around black holes. *ARA&A* 52:529–588. <https://doi.org/10.1146/annurev-astro-082812-141003>. [arXiv:1401.0586](#) [astro-ph.HE]
- Zajaček M, Busch G, Valencia-S M et al (2019) Radio spectral index distribution of SDSS-FIRST sources across optical diagnostic diagrams. *A&A* 630:A83. <https://doi.org/10.1051/0004-6361/201833388>. [arXiv:1906.08877](#) [astro-ph.GA]
- Zamaninasab M, Clausen-Brown E, Savolainen T, Tchekhovskoy A (2014) Dynamically important magnetic fields near accreting supermassive black holes. *Nature* 510(7503):126–128. <https://doi.org/10.1038/nature13399>
- Zanni C, Ferrari A, Rosner R, Bodo G, Massaglia S (2007) MHD simulations of jet acceleration from Keplerian accretion disks. The effects of disk resistivity. *A&A* 469(3):811–828. <https://doi.org/10.1051/0004-6361:20066400>. [arXiv:astro-ph/0703064](#)
- Zheng XC, Röttgering HJA, Best PN et al (2020) Link between radio-loud AGNs and host-galaxy shape. *A&A* 644:A12. <https://doi.org/10.1051/0004-6361/202038646>. [arXiv:2010.07851](#) [astro-ph.GA]
- Zirbel EL (1997) The megaparsec environments of radio galaxies. *ApJ* 476:489
- Zuther J, Fischer S, Eckart A (2012) Compact radio emission from  $z \sim 0.2$  X-ray bright AGN. *A&A* 543:A57. <https://doi.org/10.1051/0004-6361/201118200>. [arXiv:1204.3162](#) [astro-ph.CO]

**Publisher's Note** Springer Nature remains neutral with regard to jurisdictional claims in published maps and institutional affiliations.